Self-Organization and Functionalization of Ionic Liquids

（イオン性液体の組織化と機能化）

Masafumi Yoshio

2005

Department of Chemistry and Biotechnology
School of Engineering
The University of Tokyo

Table of Contents

Chapter 1

General Introduction

1.1. Ionic Liquids

Ionic liquids are salts with melting temperatures below 100 °C.[1] Typical examples of the salts are shown in Figure 1–1. These salts containing perfluorinated anions show high thermal stability, non-volatility, non-flammability, high polarity, low viscosity, high ionic conductivity, and wide electrochemical window (the range between the anodic and cathodic decomposition potentials). Alternating the combination of cation and anion used or modifying the nature of one or more alkyl chains on the cations allow a large number of variations within this general framework, providing the possibility to fine tune the properties for specific applications.

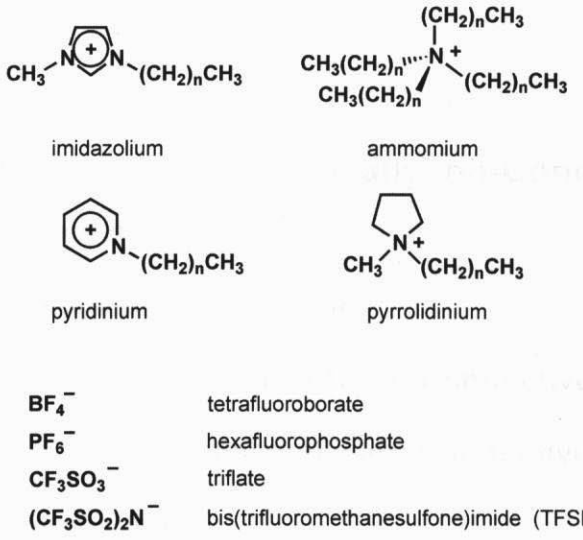

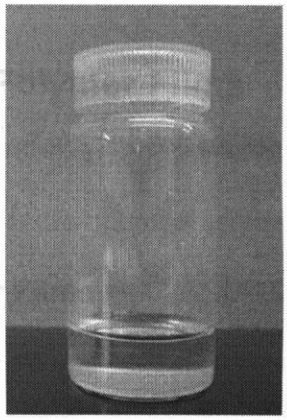

Figure 1–1. Molecular structures of several cations and anions commonly employed in the synthesis of ionic liquids and a photograph of 1-ethyl-3-methylimidazolium tetrafluoroborate.

Several comprehensive reviews and books have been published recently on ionic liquids[2] and their use in organic chemistry,[3] polymer synthesis,[4] inorganic chemistry,[5] and electrochemistry.[6]

1.1.1. Brief History of Ionic Liquids

The development of ionic liquids goes back to 1914. The first ionic liquid is ethylammonium nitrate,[7] which has a melting point of 14 °C. In the late 1940s, *N*-alkylpyridinium chloroaluminates were studied as electrolytes for electroplating aluminium.[8] However, these systems were not studied further until the groups of Osteryoung and Wilkes rediscovered them in the late 1970s.[9] The first examples of ionic liquids based on *N,N*-dialkylimidazolium cations were reported in the early 1980s by Wilkes et al.[10] They contain chloroaluminate anions ($AlCl_4^-$ or $Al_2Cl_7^-$) and were also used as electrolytes for electroplating of metals. It was reported that the Lewis acidity of the ionic liquids can be controlled by changing the mixing ratio (Figure 1–2). Moreover, the acidic ionic liquids proved to be effective catalysts and solvents for Friedel-Crafts acylations.[11] However, their use as reaction media and catalysts for organic synthesis was limited because these ionic liquids are moisture-sensitive as aluminium tetrachloride hydrolyzes to form HCl in the presence of water.

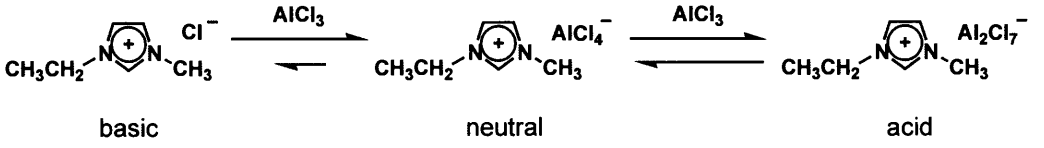

Figure 1–2. Control of the acidity of ionic liquids by varying the ratio of imidazolium chloride and $AlCl_3$.

The first fluid, air- and water-stable ionic liquid, 1-ethyl-3-methylimidazolium tetrafluoroborate was reported by Wilkes et al. in 1992.[12] The discovery gave an impetus for a dramatic increase in activity in the area of ionic liquids. The corresponding hexafluorophosphate followed shortly thereafter.[13] Subsequently, *N,N*-dialkylimidazolium salts containing a wide variety of fluorinated anions, *e.g.* $(CF_3SO_2)_2N^-$, $(CF_3CF_2SO_2)_2N^-$, and $(CF_3SO_2)_3C^-$ were prepared.[14] These ionic liquids are immiscible with water and can be easily

purified by washing with water.[15] Chemically inertness and the more facile handling capability of such ionic liquids should greatly enhance the range of possible applications.

1.1.2. Applications of Ionic Liquids

Ionic liquids have been extensively studied taking advantage of their unusual characters such as non-volatility and high ionic conductivity in the fields of organic chemistry and electrochemistry. Principal applications of ionic liquids can be divided into two categories: (1) as neoteric solvents for organic and inorganic syntheses and extractions, (2) as electrolytes for electrochemical devices. However, the potential of ionic liquids is considerably greater. This section will outline the principal applications.

Solvents and Catalysts. Ionic liquids are able to solvate a wide range of species including organic, inorganic, and organometallic compounds. Ionic liquids were employed as reusable reaction media for many reactions such as Friedel-Crafts reactions,[16] Diels-Alder reactions,[17] palladium catalyzed cross-coupling reactions,[18] enzyme-catalyzed reactions,[19] olefin metathesis[20] and so on. Ionic liquids had also been shown to be good solvents for radical polymerizations.[21] Relatively high solvent viscosity and support for long radical lifetimes have been suggested as factors enabling the formation of polymers with high molecular weights and controllable characteristics. Ionic liquids can be used to dissolve cellulose, which is insoluble in water and common organic solvents due to its strong intermolecular hydrogen-bonding network.[22] Interestingly, it was reported that the viscous solutions of cellulose dissolved in 1-butyl-3-methylimidazolium chloride shows liquid crystalline behavior.

Ion-Conductive Materials. Ionic liquids have been investigated as electrolyte materials for lithium batteries,[23] solar cells,[24] fuel cells,[25] capacitors,[26] organic light-emitting diodes,[27] actuators (artificial muscles)[28] and metal electrodeposition[29] because many ionic liquids show high ionic conductivity above 10^{-2} S cm^{-1} at room temperature. Recently, specific ionic liquids were designed to conduct specific ions such as lithium, iodide, triiodide and proton. Ohno and coworkers designed zwitterionic-type imidazolium ionic liquids (Figure 1–3a), in which the component ions of ionic liquids cannot migrate, promoting the lithium ion as the only one able to move.[30] Boron-based anion trapping ionic liquids were designed as a cation conductor (Figure 1–3b).[31] Polymer materials based on ionic liquids were developed as a new family of solid electrolytes and gel electrolytes. Polymerizable ionic liquids having vinyl or acrylate groups (Figure 1–3c) were polymerized to prepare flexible polymer films.[32] Ion gels were prepared by chemical cross-linking of acrylate monomers in conventional ionic liquids.[33] DNA-based materials forming ionic liquids or ion-conductive pathways were also studied as a new type of ion conductors.[34]

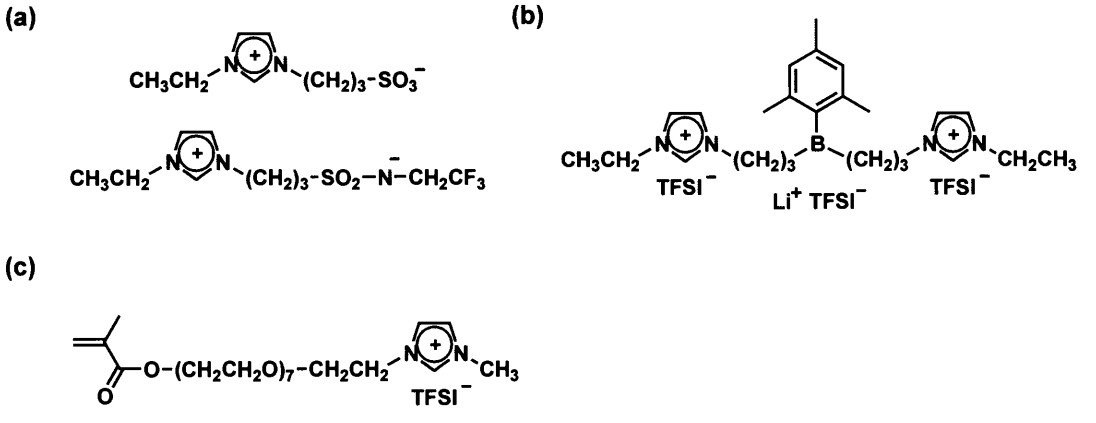

Figure 1–3. Specific ionic liquids: (a) zwitterionic-type imidazolium salts; (b) imidazolium salt bearing an anion receptor; (c) polymerizable imidazolium salt.

Other Applications. Ionic liquids have potential applications as lubricants[35] for steel/steel contact and plasticizers[36] to produce plasticized polymer materials. In addition, the advantages of ionic liquids in inorganic synthetic procedures have been gradually realized and received attention. Metallic nanoparticles such as palladium, gold, and platinum were prepared by using thiol-functionalized ionic liquids.[37] Hollow titania microspheres were also prepared by the sol-gel reaction in ionic liquids, which act not only as the solvent but also as stabilizers for the microspheres.[38]

1.1.3 Molecular Assemblies Based on Ionic Liquids

The formation of molecular self-assemblies containing ionic liquids has attracted much attention because of their potential application as novel functional materials. Very recently, liquid crystals, physical gels by low-molecular weight gelators, and composite materials have been developed as new types of self-assembled soft materials.

Formation of Liquid Crystalline Phases in Ionic Liquids. The formation of lyotropic liquid crystals (see section 1.2) in a molten salt was first reported in 1983.[39] A 1:1 mixture by weight of distearoylphosphotidylcholine and *N*-ethylammonium nitrate formed two lamellar phases (L_α and L_β). The formation of lamellar assemblies can be also induced by the addition of a small amount of water to 1-decyl-3-methylimidazolium bromide that is a room temperature ionic liquid.[40] A lyotropic liquid crystalline gel consisting of the imidazolium salt and water (16 wt %) was prepared. Addition of water to the ionic liquid induced the formation of a lamellar structure stabilized by hydrogen bonding between the imidazolium ring (in particular, the proton on C2) and Br^-, and Br^- and water, while a dried ionic liquid including less than 1.6 wt % of water showed no liquid crystalline phases. Also, lyotropic liquid crystals

based on poly(ethylene oxide)–poly(propylene oxide) block copolymer[41] and a triphenylene derivative bearing imidazolium moieties[42] have recently been reported.

Liquid Crystalline Ionic Liquids. Ionic liquid crystals bearing an ammonium and pyridinium salts moiety were reported to show stable thermotropic liquid crystalline behavior. Seddon, Bruce and coworkers showed that some imidazolium and pyridinium salts exhibit low melting points and liquid crystalline behavior. Ionic liquid crystals with lower temperature mesophase ranges are called liquid crystalline ionic liquids.[43] A large variety of thermotropic liquid crystalline ionic liquids exhibiting anisotropic fluid states were prepared. In particular, the ionic liquid crystals based on imidazolium salts **1**,[44–48] **2**,[49] **3**,[50] **4**[51] and pyridinium salts **5**[44] containing weakly coordinating perfluorinated anions, such as BF_4^- and PF_6^- are representative liquid crystalline ionic liquids due to their thermal and electrochemical stabilities (Figure 1–4). Liquid crystalline ionic liquids having a benzimidazolium unit **6** were also prepared.[52] For these materials, liquid crystalline phases are induced by microphase-segregation of ionic moieties and long alkyl or perfluoroalkyl chains. The influence of the anion type and chain length on the liquid crystalline phases has been systematically studied for 1-alkyl-3-methylimidazolium salts.

Metal-based ionic liquid crystals containing a tetrahedral tetrahalometalate ion (MX_4^{2-}; X = Cl, Br, I; M = Co, Ni, Cu, Pd, etc.) **7**,[53] **8**[54] were studied (Figure 1–4). These metal-based materials can exhibit properties as metal complexes such as chromism, magnetism, polarizability, redox behavior, and catalysis.

Bipyridinium cation **9**,[55] phosphonium,[56] guanidinium,[57] and vinamidinium[58] cations were used to form thermotropic ionic liquid crystals. For example, the mixture of diheptyl and dioctyl viologens (20:80 by wt %) with TFSI anion forms a smectic A phase between 22 and

132 °C. It was reported that the viologens show fluorescence in both non-polar and polar organic solvents, which can be useful for the development of biological and chemical sensors. Combining self-organization and ionic liquids may open a new avenue in the field of material science and supramolecular chemistry.[59]

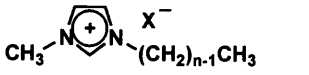

$X^- = Cl^-, Br^-, BF_4^-, PF_6^-, CF_3SO_3^-$
n = 12, 14, 16, 18

1

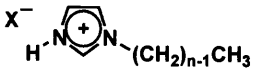

$X^- = Cl^-, NO_3^-, BF_4^-$
n = 10, 12, 14, 16, 18

2

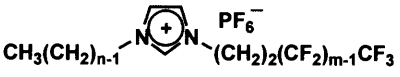

n = 1, m = 6, 8
n = 4, m = 6, 8

3

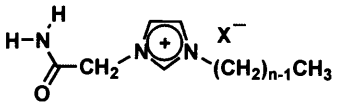

$X^- = Br^-, BF_4^-, PF_6^-$
n = 10, 12, 14, 16, 18

4

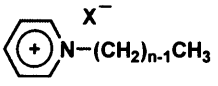

$X^- = Cl^-, PF_6^-$
n = 12, 14, 16, 18

5

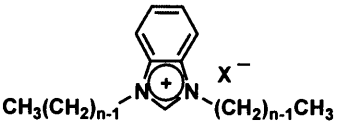

$X^- = Cl^-, Br^-$
n = 12, 14, 16, 18

6

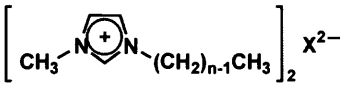

X^{2-} = $[MCl_4]^{2-}$ (M: Co, Ni, Cu, Pd)
n = 12, 14, 16, 18

7

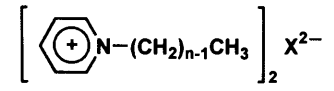

X^{2-} = $[MCl_4]^{2-}$, $[MBr_4]^{2-}$, $[MI_4]^{2-}$
(M: Co, Ni, Cu, Pd)
n = 12, 14, 16, 18

8

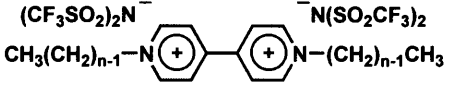

n = 7, 8

9

Figure 1–4. Molecular structures of liquid crystalline ionic liquids.

Physical Gels. Physical gelation of ionic liquids was accompanied by the formation of bilayer structures of glycolipids and a cationic amphiphile in ionic liquids.[60,61] In order to tune the fluidity of ionic liquids for application in electrochemical devices, ionic liquids were also physically gelled by low-molecular weight organogelators based on cholesterol and amino acid.[62,63] Moreover, gelation of ionic liquids was induced by physical cross-linking of single-walled carbon nanotubes, which was mediated by the local molecular ordering of ionic liquids around the nanotubes.[64]

1.2. Liquid Crystals

Liquid crystals are anisotropically ordered and mobile materials and have been successful in the field of electrooptic devices and high-strength fibers.[65,66] Liquid crystals are classified as being either thermotropic or lyotropic depending on whether their self-organization occurs only on heating of the pure compounds (thermotropic liquid crystals) or is induced by isotropic solvents (lyotropic liquid crystals).

Thermotropic liquid crystalline molecules usually consist of anisometric rigid moieties (calamitic or discotic) to which flexible alkyl chains are attached. These anisometric rigid units preferentially arrange parallel to each other, giving rise to nematic phases (N, N_D). Elongation of the alkyl chains leads to segregation of the rigid units and the flexible alkyl chains. In this way, calamitic molecules form smectic phases (S_A, S_B, S_C, etc.) in which the individual molecules are arranged in layers and discotic molecules form columns which aggregate either to columnar nematic (N_C) or two-dimensional ordered columnar phases (D_h, D_r, etc.) (Figure 1–5). Recently, new liquid crystalline molecules with specific shapes (*e.g.* banana-shape,[67–70] shuttlecock-shape,[71] dendrimer,[72–76] Janus-like,[77] ring,[78–80] helix[81–83]) were synthesized and self-assembly of these molecules results in a variety of functional liquid

crystalline structures.

On the other hand, molecules forming lyotropic mesophases usually consist of two chemically distinct regions, *e.g.* a flexible lipophilic chain and a polar (ionic or non-ionic) head group. For example, phospholipids like lecithin, glycolipids,[84] and block molecules consisting of oligo(ethylene oxide) and hydrophobic chains can form mesophases in water (Figure 1–6). Depending on the molecular structure, solvent, concentration of the amphiphile, and temperature, different mesophases (*e.g.* micellar cubic, columnar, lamellar, hexagonal columnar, and bicontinuous cubic) can be observed (Figure 1–6).

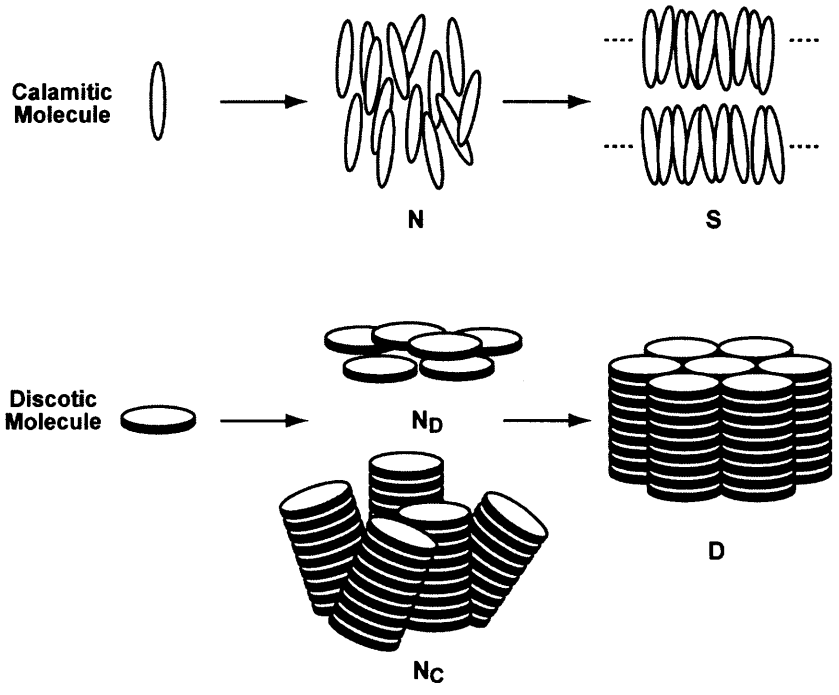

Figure 1–5. Representation of the molecular shape and orientation of the major thermotropic liquid crystalline phases. N: nematic phase; S: smectic phase; N_D: discotic nematic phase; N_C: columnar nematic phase; D: discotic phase.

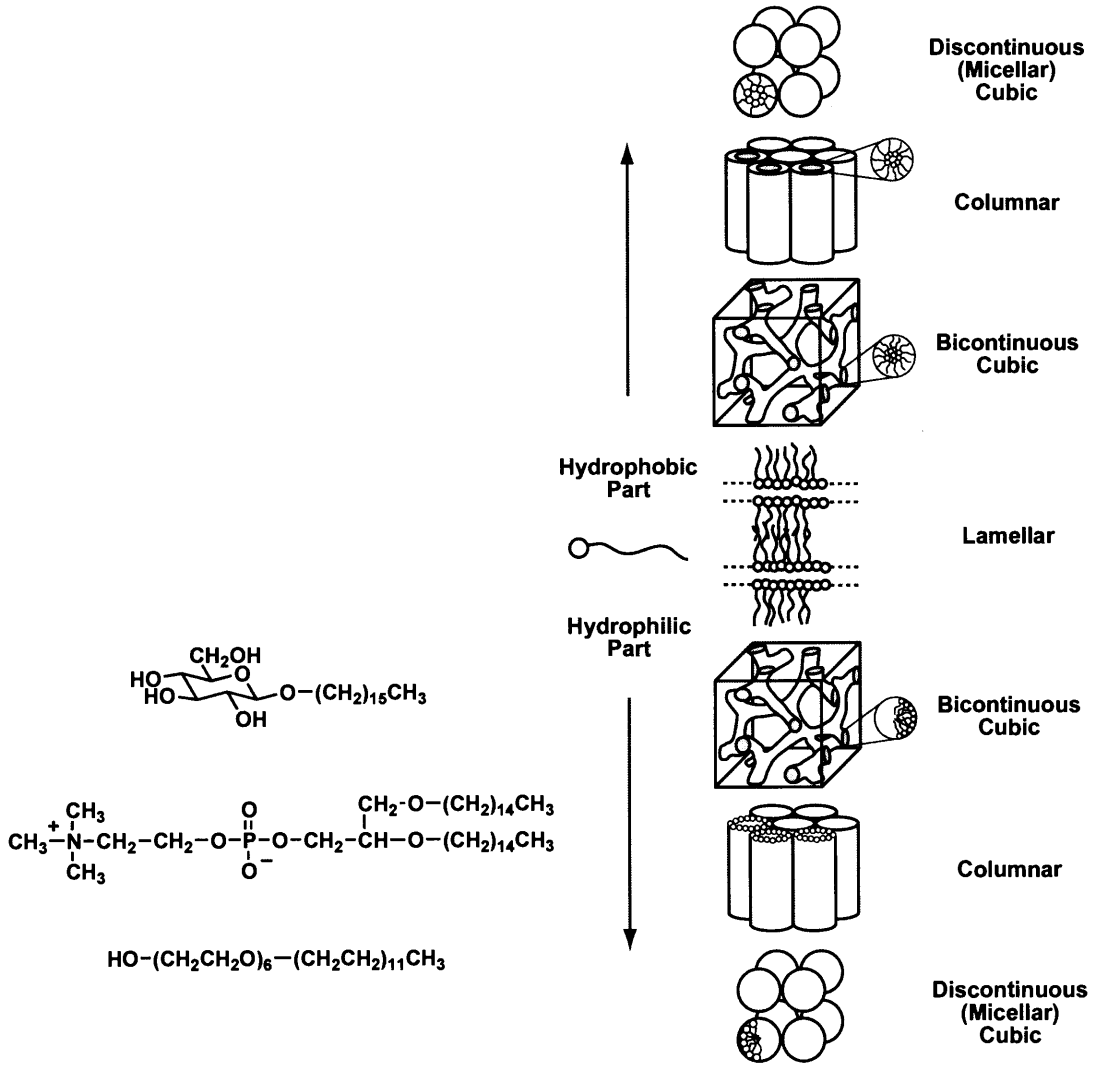

Figure 1–6. Representation of the major lyotropic liquid crystalline phases and examples of amphiphilic molecules.

For the preparation of liquid crystalline molecules, the use of specific molecular interactions such as hydrogen bonding,[85–90] halogen bonding,[91] ionic interactions,[92–95] and charge transfer interactions[96,97] has attracted much attention due to the numerous varieties of complex structures easily accessible. Among these interactions, hydrogen bonding is one of the most frequently used interactions for the design of supramolecular liquid crystals (Figure 1–7a).

Kato and Fréchet first discovered hydrogen-bonded supramolecular liquid crystals

that consist of benzoic acid derivatives and pyridine derivatives.[87] At the same time, Lehn also reported that triple hydrogen-bonded complexes consisting of uracil derivatives and diaminopyridine derivatives show a mesomorphic behavior.[88] Since that time, a variety of hydrogen-bonded liquid crystals have been developed and the research is now in progress.[98]

Phase segregation is another important design strategy for the development of new liquid crystals.[100,101] Although it has been known that phase segregation between aromatic and aliphatic parts results in the formation of smectic phases for calamitic liquid crystals, it was recognized currently that design of various shapes of molecules based on this strategy is useful to create self-assembled complex structures (Figure 1–7b).[102–105] The findings on the morphologies of block copolymers have stimulated the molecular design of liquid crystals from the viewpoint of phase segregation.

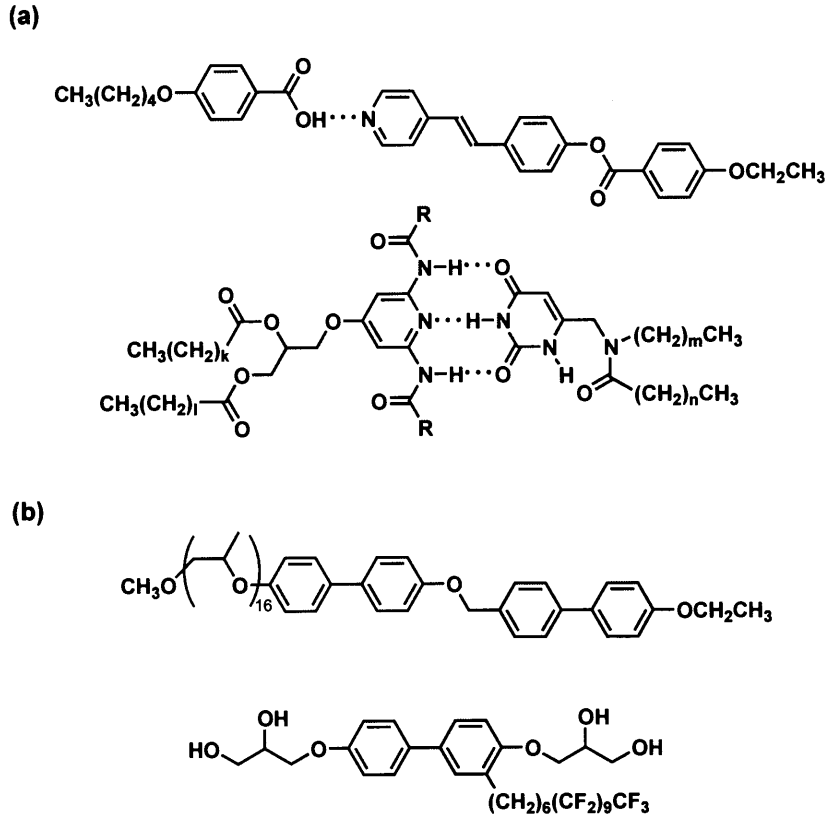

Figure 1–7. Specific liquid crystals: (a) supramolecular hydrogen-bonded liquid crystals; (b) microphase-segregated liquid crystals.

1.3. Ion-Conductive Liquid Crystals

Liquid crystals are expected to serve as anisotropic conductors due to their self-organized structures. Recently, transportation of charges[106–114] and ions[115–126] in liquid crystals has attracted much attention. As the boundaries present in randomly oriented polydomains disturb the transportation of charges and ions, the macroscopic orientation of self-organized monodomains plays a key role in the enhancement of conductive properties For this purpose, the design and control of molecular interactions and nanophase-segregated structures in liquid crystals is essential.[100,101]

As for ion conduction, oligo(ethylene oxide)s and crown ethers, which function as ion-conducting moieties, were incorporated into mesogenic rodlike and fanlike molecules (Figure 1–8).

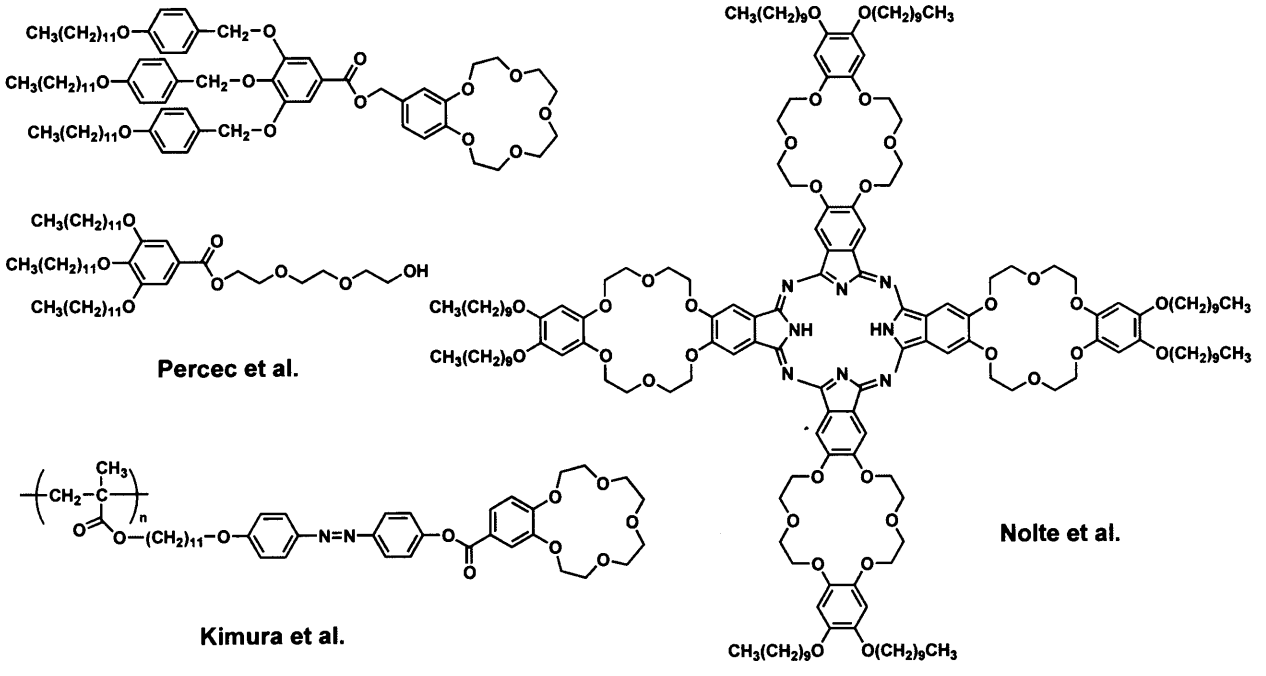

Figure 1–8. Ion-conductive liquid crystalline molecules.

These materials show a columnar or smectic liquid crystallinity. The ionic conductivities of

some of these materials were measured. However, the ionic conductivities of these examples were lower than expected due to the lack of macroscopic orientation. Recently, Kato, Ohno and coworkers have achieved the macroscopic orientation of complexes of smectic liquid crystals containing poly(ethylene oxide) (PEO) moieties with lithium salts (Figure 1–9) and succeeded in measuring a two-dimensional anisotropic ionic conductivity.[115] Lithium salts are incorporated into the PEO layers, which stabilized the smectic mesophases. Highly anisotropic ion conduction along the layer structure was observed for the homeotropically aligned complexes on the surface of the substrates. To enhance the effects of block structures on phase segregation and anisotropic ion conduction, perfluoroalkyl moieties were introduced into the ion-conductive liquid crystals.[115e] The triply layered structures of perfluorocarbon, aromatic mesogen, and PEO moieties led to the thermal stabilization of mesophases and the increase in anisotropy of ionic conductivities.

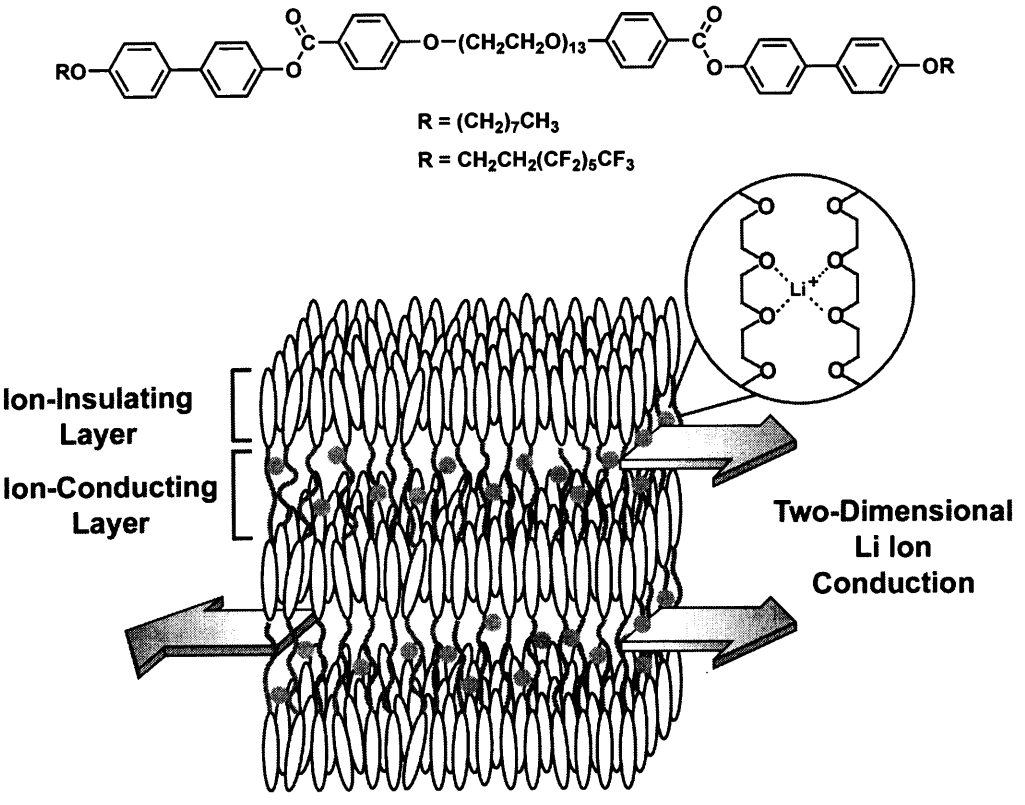

Figure 1–9. Two-dimensionally anisotropic ion-conductive liquid crystals.

For the PEO-based columnar materials, anisotropically one-dimensional ion conduction in a macroscopic monodomain has not yet been measured. These PEO-based anisotropic materials have potential applications as functional electrolytes in lithium ion batteries.

1.4. Objectives and Outline of This Work

The object of this study is to develop new anisotropically ion-conductive materials by self-organization of ionic liquids. As liquid crystals are anisotropic materials that can respond to external stimuli and environmental changes, incorporation of ionic liquids into liquid crystalline nanostructures would lead to new materials conducting ions preferentially along one or two dimensions (Figure 1–10). In addition, the phase transition of the liquid crystalline component could give the possibility to vary the conductivity playing with the external condition. Moreover, to achieve ion-transport along the desired direction would be of great importance in future for the preparation of biomimetic materials such as nerves and cell membranes.

The author intends to prepare three kind of low-dimensional ion conductors based on ionic liquids: (1) liquid crystalline composite materials obtained by self-assembly of ionic liquids and designed mesogenic molecules, (2) ionic liquid crystalline materials, and (3) self-standing nanostructured polymer films. For the composite materials, the liquid crystalline structures and conductivity are expected to be tuned easily by changing the mixing ratio of ionic liquid and mesogenic molecule or by changing the type of ionic liquids. Ionic liquid crystalline materials have merits for applications because of their chemically stable nature and easy of handling without a mixing procedure. These liquid crystalline materials are useful as device materials whose conductivity can be controlled by external stimuli such as temperature, light, and electric and magnetic fields. On the other hand, polymeric films have advantages

for applications because of their self-standing and flexible nature, processability, and lightness. These films can be used to produce portable thin film batteries. In addition, nanostructured films are expected to function as ion-selective membranes, molecular size-selective nanofiltration membranes, and catalytic membranes.[127–130]

In Chapter 2, two- and one-dimensionally anisotropic ion conductors are prepared for the first time by self-assembly of conventional ionic liquids and hydroxyl-functionalized rodlike and taper-shaped mesogenic molecules. Mesophase stabilization and ionic conductivities of these self-organized liquid crystalline composites are examined. Molecular interactions between ionic liquids and hydroxyl groups of mesogenic molecules are investigated by proton NMR titration measurements.

In Chapter 3, self-organized columnar ionic liquid crystals are designed and synthesized by chemical modification of imidazolium salts. The liquid crystalline properties and conductive properties of mixtures containing a lithium salt are examined. Then mesomorphic behavior and ionic conductivities are compared for the columnar ionic liquid crystals containing different anion species.

In Chapter 4, mechanically and thermally stable polymer films with layered and columnar nanostructures are prepared by in situ photopolymerization of polymerizable smectic and columnar ionic liquid crystals having an imidazolium salt moiety. For further improvement of ion-conductive properties, oligo(ethylene oxide) as an ion-conducting moiety is introduced into the smectic monomer as a spacer between the mesogenic moiety and the imidazolium salt moiety. The columnar monomer is polymerized by UV-irradiation at the columnar and isotropic liquid states. The ionic conductivities are compared for these films.

In Chapter 5, a summary of this work is presented.

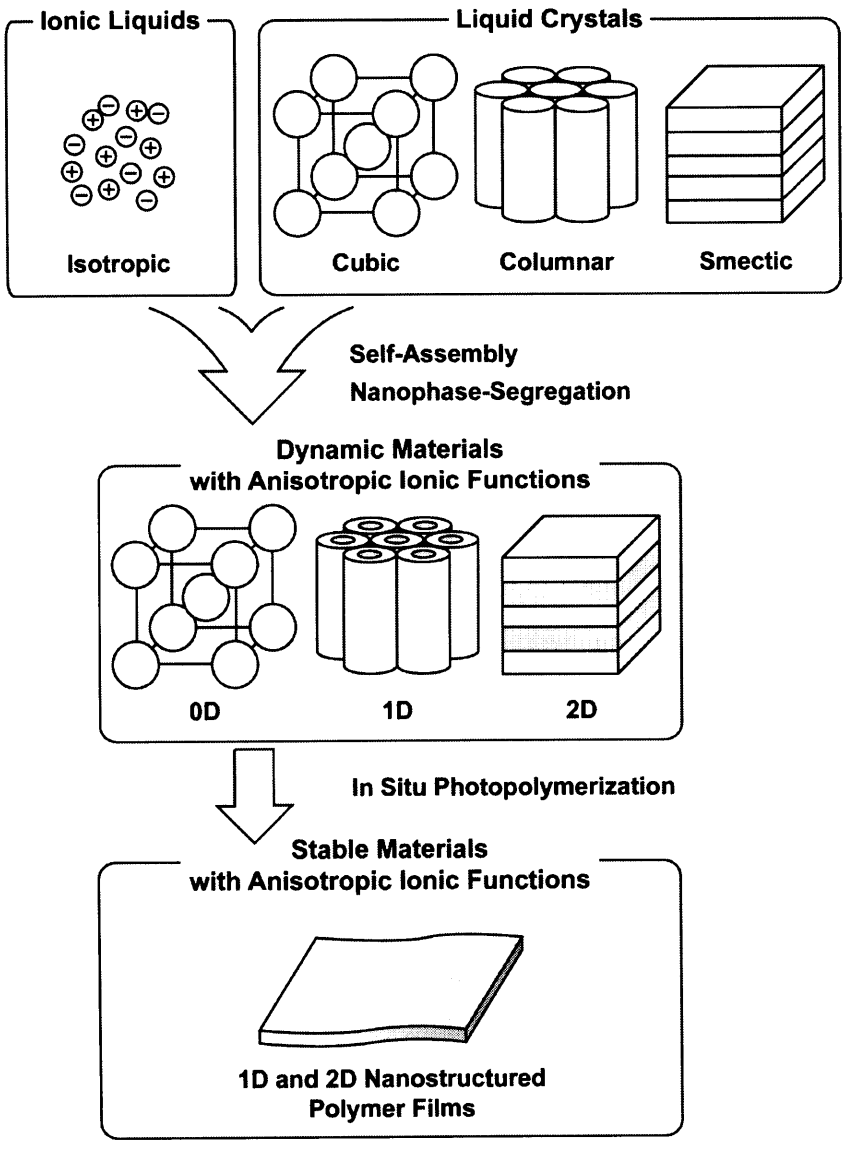

Figure 1–10. Schematic illustration of the design strategies for the development of anisotropic ion-conductive materials based on ionic liquids.

1.5. References

1. R. D. Rogers, K. R. Seddon, *Science* **2003**, *302*, 792.
2. For reviews and books on ionic liquids: (a) R. Hagiwara, Y. Ito, *J. Fluorine Chem.* **2000**, *105*, 221; (b) J. S. Wilkes, *Green. Chem.* **2002**, *4*, 73; (c) S. A. Forsyth, J. M. Pringle, D. R. MacFarlane, *Aust. J. Chem.* **2004**, *57*, 113; (d) H. Ohno, Ed., Ionic Liquids: *The Front and Future of Material Development*, CMC, Tokyo **2003**.
3. For reviews and books on ionic liquids for organic and catalytic reactions: (a) T. Welton, *Chem. Rev.* **1999**, *99*, 2071; (b) P. Wasserscheid, W. Keim, *Angew. Chem. Int. Ed.* **2000**, *39*, 3772; (c) R. Sheldon, *Chem. Commun.* **2001**, 2399; (d) J. Dupont, R. F. de Souza, P. A. Z. Suarez, *Chem. Rev.* **2002**, *102*, 3667; (e) D. Zhao, M. Wu, Y. Kou, E. Min, *Catal. Today* **2002**, *74*, 157; (f) J. H. Davis, Jr., *Chem. Lett.* **2004**, *33*, 1072; (g) C. E. Song, *Chem. Commun.* **2004**, 1033; (h) J. S. Wilkes, *J. Mol. Catal. A: Chem.* **2004**, *214*, 11; (i) R. D. Rogers, K. R. Seddon, Eds., "*Ionic Liquids as Green Solvent: Progress and Prospects*, *ACS Symp. Ser.*, *856*, American Chemical Society, Washington, DC **2003**; (j) R. D. Rogers, K. R. Seddon, Eds., *Ionic Liquids: Industrial Applications for Green Chemistry*, *ACS Symp. Ser.*, *818*, American Chemical Society, Washington, DC **2002**; (k) P. Wasserscheid, T. Welton, Eds., *Ionic Liquids in Synthesis*, Wiley-VCH, Weinheim, Germany **2003**.
4. P. Kubisa, *Prog. Polym. Sci.* **2004**, *29*, 3.
5. M. Antonietti, D. Kuang, B. Smarsly, Y. Zhou, *Angew. Chem. Int. Ed.* **2004**, *43*, 4988.
6. M. C. Buzzeo, R. G. Evans, R. G. Compton, *Chem. Phys. Chem.* **2004**, *5*, 1106.
7. P. Walden, *Bull. Acad. Imper. Sci. (St. Petersburg)* **1914**, 1800.
8. F. H. Hurley, T. P. Wier, *J. Electrochem. Soc.* **1951**, *98*, 203.
9. (a) H. L. Chum, V. R. Kock, L. L. Miller, R. A. Osteryoung, *J. Am. Chem. Soc.* **1975**,

97, 3264; (b) J. Robinson, R. A. Osteryoung, *J. Am. Chem. Soc.* **1979**, *101*, 323.

10. J. S. Wilkes, J. A. Levisky, R. A. Wilson, C. L. Hussey, *Inorg. Chem.* **1982**, *21*, 1263.
11. J. A. Boon, J. A. Levinsky, J. L. Pflug, J. S. Wilkes, *J. Org. Chem.* **1986**, *51*, 480.
12. J. S. Wilkes, M. J. Zaworotko, *J. Chem. Soc., Chem. Commun.* **1992**, 965.
13. J. Fuller, R. T. Carlin, H. C. De Lang, D. Haworth, *J. Chem. Soc., Chem. Commun.* **1994**, 299.
14. (a) P. Bonhôte, A.-P. Dias, N. Papageorgiou, K. Kalyanasundaram, M. Grätzel, *Inorg. Chem.* **1996**, *35*, 1168; (b) V. L. Koch, L. A. Dominey, C. Nanjundiah, M. J. Onderechen, *J. Electrochem. Soc.* **1996**, *143*, 798; (c) J. D. Holbrey, W. M. Reichert, R. D. Rogers, *Dalton Trans.* **2004**, 2267.
15. J. G. Huddleston, A. E. Visser, W. M. Reichert, H. D. Willauer, G. A. Broker, R. D. Rogers, *Green Chem.* **2001**, *3*, 156.
16. (a) P. Wasserscheid, M. Sesing, W. Korth, *Green Chem.* **2002**, *4*, 134; (b) J. Ross, J. Xiao, *Green Chem.* **2002**, *4*, 129.
17. T. Fischer, A. Sethi, T. Welton, J. Woolf, *Tetrahedron Lett.* **1999**, *40*, 793.
18. (a) X. Xie, J. Lu, B. Chen, J. Han, X. She, X. Pan, *Tetrahedron Lett.* **2004**, *45*, 809; (b) R. Rajagopal, D. C. Jarikote, K. V. Srinivasan, *Chem. Commun.* **2002**, 617; (c) J. McNulty, A. Capretta, J. Wilson, J. Dyck, G. Adjabeng, A. Robertson, *Chem. Commun.* **2002**, 1986.
19. (a) R. A. Sheldon, R. M. Lau, M. J. Sorgedrager, F. van Rantwijk, K. R. Seddon, *Green Chem.* **2002**, *4*, 147; (b) J. K. Lee, M.-J. Kim, *J. Org. Chem.* **2002**, *67*, 6845.
20. (a) Q. Yao, Y. Zhang, *Angew. Chem. Int. Ed.* **2003**, *42*, 3395; (b) N. Audic, H. Clavier, M. Mauduit, J.-C. Guillemin, *J. Am. Chem. Soc.* **2003**, *125*, 9249.
21. (a) K. Hong, H. Zhang, J. W. Mays, A. E. Visser, C. S. Brazel, J. D. Holbrey, W. M.

Reichert, R. D. Rogers, *Chem. Commun.* **2002**, 1368; (b) M. G. Benton, C. S. Brazel, *Polym. Int.* **2004**, *53*, 1113; (c) S. Perrier, T. P. Davis, A. J. Carmichael, D. M. Haddleton, *Chem. Commun.* **2002**, 2226.

22. R. P. Swatloski, S. K. Spear, J. D. Holbrey, R. D. Rogers, *J. Am. Chem. Soc.* **2002**, *124*, 4974.

23. (a) D. R. MacFarlane, J. Huang, M. Forsyth, *Nature* **1999**, *402*, 792; (b) D. R. MacFarlane, M. Forsyth, *Adv. Mater.* **2001**, *13*, 957; (c) K. Ito, N. Nishina, H. Ohno, *Electrochim. Acta* **2000**, *45*, 1295; (d) Y. Nakai, K. Ito, H. Ohno, *Solid State Ionics* **1998**, *113–115*, 199; (e) J.-H. Shin, W. A. Henderson, S. Passerini, *Electrochem. Commun.* **2003**, *5*, 1016; (f) H. Sakaebe, H. Matsumoto, *Electrochem. Commun.* **2003**, *5*, 594; (g) Y. Abu-Lebdeh, P.-J. Alarco, M. Armand, *Angew. Chem. Int. Ed.* **2003**, *42*, 4499.

24. (a) P. Wang, S. M. Zakeeruddin, I. Exnar, M. Grätzel, *Chem. Commun.* **2002**, 2972; (b) P. Wang, S. M. Zakeeruddin, J.-E. Moser, R. Humphry-Baker, M. Grätzel, *J. Am. Chem. Soc.* **2004**, *126*, 7164; (c) P. Wang, S. M. Zakeeruddin, R. Humphry-Baker, M. Grätzel, *Chem. Mater.* **2004**, *16*, 2694; (d) H. Matsui, K. Okada, T. Kawashima, T. Ezure, N. Tanabe, R. Kawano, M. Watanabe, *J. Photochem. Photobiol., A* **2004**, *164*, 129.

25. (a) R. F. de Souza, J. C. Padilha, R. S. Gonçalves, J. Dupont, *Electrochem. Commun.* **2003**, *5*, 728; (b) M. A. B. H. Susan, A. Noda, S. Mitsushima, M. Watanabe, *Chem. Commun.* **2003**, 938.

26. M. Ue, M. Takeda, T. Takahashi, M. Takehara, *Electrochem. Solid-State Lett.* **2002**, *5*, A119.

27. C. Yang, Q. Sun, J. Qiao, Y. Li, *J. Phys. Chem. B* **2003**, *107*, 12981.

28. (a) W. Lu, A. G. Fadeev, B, Qi, E. Smela, J. Mazurkiewicz, D. Zhou, G. G. Wallace, D.

R. MacFarlane, S. A. Forsyth, M. Forsyth, *Science* **2002**, *297*, 983; (b) J. Ding, D. Zhou, G. Spinks, G. Wallace, S. Forsyth, M. Forsyth, D. MacFalane, *Chem. Mater.* **2003**, *15*, 2392.

29. I. Mukhopadhyay, W. Freyland, *Langmuir* **2003**, *19*, 1951.

30. (a) M. Yoshizawa, M. Hirao, K. Ito-Akita, H. Ohno, *J. Mater. Chem.* **2001**, *11*, 1057; (b) M. Yoshizawa, A. Narita, H. Ohno, *Aust. J. Chem.* **2004**, *57*, 139.

31. (a) N. Matsumi, M. Miyake, H. Ohno, *Chem. Commun.* **2004**, 2852; (b) T. Mizumo, K. Sakamoto, N. Matsumi, H. Ohno, *Chem. Lett.* **2004**, *33*, 396.

32. (a) M. Yoshizawa, H. Ohno, *Electrochim. Acta* **2001**, *46*, 1723; (b) S. Washiro, M. Yoshizawa, H. Nakajima, H. Ohno, *Polymer* **2004**, *45*, 1577; (c) H. Ohno, *Electrochim. Acta* **2001**, *46*, 1407.

33. (a) A. Noda, M. Watanabe, *Electrochim. Acta* **2000**, *45*, 1265; (a) W. Ogihara, J. Sun, M. Forsyth, D. R. MacFarlane, M. Yoshizawa, H. Ohno, *Electrochim. Acta* **2004**, *49*, 1797; (c) M. A. Klingshirn, S. K. Spear, R. Subramanian, J. D. Holbrey, J. G. Huddleston, R. D. Rogers, *Chem. Mater.* **2004**, *16*, 3091.

34. (a) N. Nishimura, H. Ohno, *J. Mater. Chem.* **2002**, *12*, 2299; (b) H. Nakayama, H. Ohno, Y. Okahata, *Chem. Commun.* **2001**, 2300; (c) A. M. Leone, S. C. Weatherly, M. E. Williams, H. H. Thorp, R. W. Murray, *J. Am. Chem. Soc.* **2001**, *123*, 218.

35. (a) C. Ye, W. Liu, Y. Chen, L. Yu, *Chem. Commun.* **2001**, 2244; (b) H. Wang, Q. Lu, C. Ye, W. Liu, Z. Cui, *Wear* **2004**, *256*, 44.

36. (a) M. P. Scott, C. S. Brazel, M. G. Benton, J. W. Mays, J. D. Holbrey, R. D. Rogers, *Chem. Commun.* **2002**, 1370; (b) M. P. Scott, M. Rahman, C. S. Brazel, *Eur. Polym. J.* **2003**, *39*, 1947.

37. (a) K.-S. Kim, D. Demberelnyamba, H. Lee, *Langmuir* **2004**, *20*, 556; (b) H. Itoh, K.

Naka, Y. Chujo, *J. Am. Chem. Soc.* **2004**, *126*, 3026.

38. T. Nakashima, N. Kimizuka, *J. Am. Chem. Soc.* **2003**, *125*, 6386.

39. D. F. Evans, E. W. Kaler, W. J. Benton, *J. Phys. Chem.* **1983**, *87*, 533.

40. (a) M. A. Firestone, J. A. Dzielawa, P. Zapol, L. A. Curtiss, S. Seifert, M. L. Dietz, *Langmuir* **2002**, *18*, 7258; (b) M. L. Dietz, J. A. Dzielawa, M. P. Jensen, M. A. Firestone, *ACS Symp. Ser.* **2003**, *856*, 526.

41. L. Wang, X. Chen, Y. Chai, J. Hao, Z. Sui, W. Zhuang, Z. Sun, *Chem. Commun.* **2004**, 2840.

42. J. Motoyanagi, T. Fukushima, T. Aida, *Chem. Commun.* **2005**, 101.

43. C. J. Bowlas, D. W. Bruce, K. R. Seddon, *Chem. Commun.* **1996**, 1625.

44. C. M. Gordon, J. D. Holbrey, A. R. Kennedy, K. R. Seddon, *J. Mater. Chem.* **1998**, *8*, 2627.

45. J. D. Holbrey, K. R. Seddon, *J. Chem. Soc., Dalton Trans.* **1999**, 2133.

46. A. E. Bradley, C. Hardacre, J. D. Holbrey, S. Johnston, S. E. J. McMath, M. Nieuwenhuyzen, *Chem. Mater.* **2002**, *14*, 629.

47. C. Hardacre, J. D. Holbrey, S. E. J. McMath, M. Nieuwenhuyzen, *ACS Symp. Ser.* **2002**, *818*, 400.

48. J. De Roche, C. M. Gordon, C. T. Imrie, M. D. Ingram, A. R. Kennedy, F. Lo Celso, A. Triolo, *Chem. Mater.* **2003**, *15*, 3089.

49. C. K. Lee, H. W. Huang, I. J. B. Lin, *Chem. Commun.* **2000**, 1911.

50. T. L. Merrigan, E. D. Bates, S. C. Dorman, J. H. Davis Jr., *Chem. Commun.* **2000**, 2051.

51. K.-M. Lee, Y.-T. Lee, I. J. B. Lin, *J. Mater. Chem.* **2003**, *13*, 1079.

52. K. M. Lee, C. K. Lee, I. J. B. Lin, *Chem. Commun.* **1997**, 899.

53. C. Hardacre, J. D. Holbrey, P. B. McCormac, S. E. J. McMath, M. Nieuwenhuyzen, K.

R. Seddon, *J. Mater. Chem.* **2001**, *11*, 346.

54. (a) F. Neve, A. Crispini, S. Armentano, O. Francescangeli, *Chem. Mater.* **1998**, *10*, 1904; (b) F. Neve, A. Crispini, O. Francescangeli, *Inorg. Chem.* **2000**, *39*, 1187; (c) F. Neve, O. Francescangeli, A. Crispini, J. Charmant, *Chem. Mater.* **2001**, *13*, 2032.

55. P. K. Bhowmik, H. Han, J. J. Cebe, R. A. Burchett, *Liq. Cryst.* **2003**, *30*, 1433.

56. (a) D. J. Abdallah, A. Robertson, H.-F. Hsu, R. G. Weiss, *J. Am. Chem. Soc.* **2000**, *122*, 3053; (b) H. Chen, D. C. Kwait, Z. S. Gönen, B. T. Weslowski, D. J. Abdallah, R. G. Weiss, *Chem. Mater.* **2002**, *14*, 4063; (c) A. Kanazawa, T. Ikeda, J. Abe, *Angew. Chem. Int. Ed.* **2000**, *39*, 612; A. Kanazawa, T. Ikeda, J. Abe, *J. Am. Chem. Soc.* **2001**, *123*, 1748.

57. F. Mathevet, P. Masson, J.-F. Nicoud, A. Skoulios, *Chem. Eur. J.* **2002**, *8*, 2248.

58. C. P. Roll, B. Donnio, D. Guillon, W. Weigand, *J. Mater. Chem.* **2003**, *13*, 1883.

59. D. Wang, J. Wang, D. Moses, G. C. Bazan, A. J. Heeger, *Langmuir* **2001**, *17*, 1262.

60. N. Kimizuka, T. Nakashima, *Langmuir* **2001**, *17*, 6759.

61. T. Nakashima, N. Kimizuka, *Chem. Lett.* **2002**, 1018.

62. A. Ikeda, K. Sonoda, M. Ayabe, S. Tamaru, T. Nakashima, N. Kimizuka, S. Shinkai, *Chem. Lett.* **2001**, 1154.

63. W. Kubo, T. Kitamura, K. Hanabusa, Y. Wada, S. Yanagida, *Chem. Commun.* **2002**, 374.

64. T. Fukushima, A. Kosaka, Y. Ishimura, T. Yamamoto, T. Takigawa, N. Ishii, T. Aida, *Science* **2003**, *300*, 2072.

65. "*Handbook of Liquid Crystals*", D. Demus, J. W. Goodby, G. W. Gray, H.-W. Spiess, V. Vill, Eds., Wiley-VCH, Weinheim **1998**.

66. P. J. Collings, M. Hird, "*Introduction to Liquid Crystals, Chemistry and Physics*",

Taylar & Francis, London **1997**.

67. T. Niori, T. Sekine, J. Watanabe, T. Furukawa, H. Takezoe, *J. Mater. Chem.* **1996**, *6*, 1231.

68. G. Pelzl, S. Diele, W. Weissflog, *Adv. Mater.* **1999**, *11*, 707.

69. (a) G. Dantlgraber, U. Baumeister, S. Diele, H. Kresse, B. Lühmann, H. Lang, C. Tschierske, *J. Am. Chem. Soc.* **2002**, *124*, 14852; (b) G. Dantlgraber, A. Eremin, S. Diele, A. Hauser, H. Kresse, G. Pelzl, C. Tschierske, *Angew. Chem. Int. Ed.* **2002**, *41*, 2408; (c) C. Keith, R. A. Reddy, H. Hahn, H. Lang, C. Tschierske, *Chem. Commun.* **2004**, 1898.

70. (a) C.-D. Keum, A. Kanazawa, T. Ikeda, *Adv. Mater.* **2001**, *13*, 321; (b)A. C. Sentman, D. L. Gin, *Angew. Chem. Int. Ed.* **2003**, *42*, 1815.

71. (a) M. Sawamura, K. Kawai, Y. Matsuo, K. Kanie, T. Kato, E. Nakamura, *Nature* **2002**, *419*, 702; (b) Y. Matsuo, A. Muramatsu, R. Hamasaki, N. Mizoshita, T. Kato, E. Nakamura, *J. Am. Chem. Soc.* **2004**, *126*, 432.

72. (a) V. Percec, C.-H. Ahn, G. Ungar, D. J. P. Yeardley, M. Möller, S. S. Sheiko, *Nature* **1998**, *391*, 161; (b) V. Percec, W.-D. Cho, G. Ungar, *J. Am. Chem. Soc.* **2000**, *122*, 10273; (c) V. Percec, M. Glodde, G. Johansson, V. S. K. Balagurusamy, P. A. Heiney, *Angew. Chem. Int. Ed.* **2003**, *42*, 4338.

75. D. Guillon, R. Deschenaux, *Curr. Opin. Solid State Mater. Sci.* **2002**, *6*, 512.

76. I. M. Saez, J. W. Goodby, *J. Mater. Chem.* **2003**, *13*, 2727.

77. (a) I. M. Saez, J. W. Goodby, *Chem. Commun.*, **2003**, 1726; (b) I, M. Saez, J. W. Goodby, *Chem. Eur. J.* **2003**, *9*, 4869.

78. (a) O. Y. Mindyuk, M. R. Stetzer, P. A. Heiney, J. C. Nelson, J. S. Moore, *Adv. Mater.* **1998**, *10*, 1363; (b) J. Zhang, J. S. Moore, *J. Am. Chem. Soc.* **1994**, *116*, 2655.

79. S. Höger, *Chem. Eur. J.* **2004**, *10*, 1320.

80. (a) S. Höger, V. Enkelmann, K. Bonrad, C. Tschierske, *Angew. Chem. Int. Ed.* **2000**, *39*, 2267; (b) M. Fischer, G. Lieser, A. Rapp, I. Schnell, W. Mamdouh, S. De Feyter, F. C. De Schryver, S. Höger, *J. Am. Chem. Soc.* **2004**, *126*, 214.

81. (a) C. Nuckolls, T. J. Katz, G. Katz, P. J. Collings, L. Castellanos, *J. Am. Chem. Soc.* **1999**, *121*, 79; (b) K. E. S. Phillips, T. J. Katz, S. Jockusch, A. J. Lovinger, N. J. Turro, *J. Am. Chem. Soc.* **2001**, *123*, 11899.

82. H.-J. Kim, W.-C. Zin, M. Lee, *J. Am. Chem. Soc.* **2004**, *126*, 7009.

83. A. Tanatani, M. J. Mio, J. S. Moore, *J. Am. Chem. Soc.* **2001**, *123*, 1792.

84. V. Vill, R. Hashim, *Curr. Opin. Colloid Interface Sci.* **2002**, *7*, 395.

85. T. Kato, *Struct. Bonding* **2000**, *96*, 95.

86. T. Kato, N. Mizoshita, K. Kanie, *Macromol. Rapid Commun.* **2001**, *22*, 797.

87. T. Kato, J. M. J. Fréchet, *J. Am. Chem. Soc.* **1989**, *111*, 8533; (b) T. Kato, J. M. J. Fréchet, *Macromolecules* **1989**, *22*, 3818.

88. M. J. Brienne, J. Gabard, J.-M. Lehn, I. Stibor, *J. Chem. Soc., Chem. Commun.* **1989**, 1868.

89. C. M. Paleos, D. Tsiourvas, *Angew. Chem. Int. Ed. Engl.* **1995**, *34*, 1696.

90. C. M. Paleos, D. Tsiourvas, *Liq. Cryst.* **2001**, *28*, 1127.

91. H. L. Nguyen, P. N. Horton, M. B. Hursthouse, A. C. Legon, D. W. Bruce, *J. Am. Chem. Soc.* **2004**, *126*, 16.

92. (a) S. Ujiie, K. Iimura, *Chem. Lett.* **1990**, 995; (b) S. Ujiie, K. Iimura, *Chem. Lett.* **1991**, 411; (c) S. Ujiie, K. Iimura, *Macromolecules* **1992**, *25*, 3174; (d) S. Ujiie, K. Iimura, *Polym. J.* **1993**, *25*, 347; (e) Y. Haramoto, Y. Akiyama, R. Segawa, S. Ujiie, M. Nanasawa, *J. Mater. Chem.* **1998**, *8*, 275.

93. (a) T. Kunitake, Y. Okahata, M. Shimomura, S. Yasunami, K. Takarabe, *J. Am. Chem. Soc.* **1981**, *103*, 5401; (b) T. Kunitake, *Angew. Chem. Int. Ed. Engl.* **1992**, *31*, 709.

94. Y. Kosaka, T. Kato, T. Uryu, *Liq. Cryst.* **1995**, *18*, 693.

95. A. Kraft, A. Reichert, R. Kleppinger, *Chem. Commun.* **2000**, 1015.

96. (a) H. Ringsdorf, R. Wusterfeld, E. Zerta, M. Ebert, J. H. Wendorff, *Angew. Chem. Int. Ed. Engl.* **1989**, *28*, 914; (b) H. Bengs, M. Ebert, O. Karthaus, B. Kohne, K. Praefcke, H. Ringsdorf, J. H. Wendorff, R. Wustefeld, *Adv. Mater.* **1990**, *2*, 141.

97. (a) P. H. Kouwer, W. F. Jager, W. J. Mijs, S. J. Picken, *Macromolecules* **2001**, *34*, 7582; (b) P. H. Kouwer, O. van den Berg, W. F. Jager, W. J. Mijs, S. J. Picken, *Macromolecules* **2002**, *35*, 2576.

98. (a) T. Kato, H. Kihara, U. Kumar, T. Uryu, J. M. J. Fréchet, *Angew. Chem. Int. Ed. Engl.* **1994**, *33*, 1644; (b) H. Kihara, T. Kato, T. Uryu, J. M. J. Fréchet, *Chem. Mater.* **1996**, *8*, 961; (c) T. Kato, H. Kihara, S. Ujiie, T. Uryu, J. M. J. Fréchet, *Macromolecules* **1996**, *29*, 8734.

99. (a) K. Kanie, M. Nishii, T. Yasuda, T. Taki, S. Ujiie, T. Kato, *J. Mater. Chem.* **2001**, *11*, 2875; (b) T. Kato, T. Matsuoka, M. Nishii, Y. Kamikawa, K. Kanie, T. Nishimura, E. Yashima, S. Ujiie, *Angew. Chem. Int. Ed.* **2004**, *43*, 1969; (b) Y. Kamikawa, M. Nishii, T. Kato, *Chem. Eur. J.* **2004**, *10*, 5942.

100. T. Kato, *Science* **2002**, *295*, 2414.

101. T. Kato, N. Mizoshita, *Curr. Opin. Solid State Mater. Sci.* **2002**, *6*, 579.

102. (a) C. Tschierske, *Curr. Opin. Colloid Interface Sci.* **2002**, *7*, 69; (b) C. Tschierske, *J. Mater. Chem.* **1998**, *8*, 1485; (c) C. Tschierske, *J. Mater. Chem.* **2001**, *11*, 2647; (c) C. Tschierske, *Prog. Polym. Sci.* **1996**, *21*, 775.

103. (a) X. Cheng, M. Prehm, M. K. Das, J. Kain, U. Baumeister, S. Diele, D. Leine, A.

Blume, C. Tschierske, *J. Am. Chem. Soc.* **2003**, *125*, 10977; (b) K. Borisch, C. Tschierske, P. Göring, S. Diele, *Langmuir* **2000**, *16*, 6701; (c) M. Prehm, S. Diele, M. K. Das, C. Tschierske, *J. Am. Chem. Soc.* **2003**, *125*, 614; (d) B. Chen, U. Baumeister, S. Diele, M. K. Das, X. Zeng, G. Ungar, C. Tschierske, *J. Am. Chem. Soc.* **2004**, *126*, 8608; (e) B. Chen, X. B. Zeng, U. Baumeister, S. Diele, G. Ungar, C. Tschierske, *Angew. Chem. Int. Ed.* **2004**, *43*, 4621.

104. J.-H. Ryu, N.-K. Oh, W.-C. Zin, M. Lee, *J. Am. Chem. Soc.* **2004**, *126*, 3551.

105. M. Lee, B.-K. Cho, W.-C. Zin, *Chem. Rev.* **2001**, *101*, 3869.

106. D. Adam, P. Schuhmacher, J. Simmerer, L. Häussking, K. Siemensmeyer, K. H. Etzbach, H. Ringsdorf, D. Haarer, *Nature* **1994**, *371*, 141.

107. N. Boden, R. J. Bushby, J. Clements, B. Movaghar, *J. Mater. Chem.* **1999**, *9*, 2081.

108. R. J. Bushby, O. R. Lozman, *Curr. Opin. Solid State Mater. Sci.* **2002**, *6*, 569.

109. A. M. van de Craats, J. M. Warman, A. Fechtenkötter, J. D. Brand, M. A. Harbison, K. Müllen, *Adv. Mater.* **1999**, *11*, 1469.

110. P. G. Schouten, J. M. Warman, M. P. de Haas, J. F. van der Pol, J. W. Zwikker, *J. Am. Chem. Soc.* **1992**, *114*, 9028.

111. M. Funahashi, J. Hanna, *Phys. Rev. Lett.* **1997**, *78*, 2184.

112. (a) N. Yoshimoto, J. Hanna, *Adv. Mater.* **2002**, *14*, 988; (a) N. Yoshimoto, J. Hanna, *J. Mater. Chem.* **2003**, *13*, 1004.

113. M. O'Neill, S. M. Kelly, *Adv. Mater.* **2003**, *15*, 1135.

114. N. Mizoshita, H. Monobe, M. Inoue, M. Ukon, T. Watanabe, Y. Shimizu, K. Hanabusa, T. Kato, *Chem. Commun.* **2002**, 428.

115. (a) T. Ohtake, K. Ito, N. Nishina, H. Kihara, H. Ohno, T. Kato, *Polym. J.* **1999**, *31*, 1155; (b) T. Ohtake, M. Ogasawara, K. Ito-Akita, N. Nishina, S. Ujiie, H. Ohno, T.

Kato, *Chem. Mater.* **2000**, *12*, 782; (c) T. Ohtake, Y. Takamitsu, K. Ito-Akita, K. Kanie, M. Yoshizawa, T. Mukai, H. Ohno, T. Kato, *Macromolecules* **2000**, *33*, 8109; (d) T. Ohtake, K. Kanie, M. Yoshizawa, T. Mukai, K. Ito-Akita, H. Ohno, T. Kato, *Mol. Cryst. Liq. Cryst.* **2001**, *364*, 589; (e) K. Hoshino, K. Kanie, T. Ohtake, T. Mukai, M. Yoshizawa, S. Ujiie, H. Ohno, T. Kato, *Macromol. Chem. Phys.* **2002**, *203*, 1547.

116. F. B. Dias, S. V. Batty, A. Gupta, G. Ungar, J. P. Voss, P. V. Wright, *Electrochim. Acta* **1998**, *43*, 1217.

117. H. V. St. A. Hubbard, S. A. Sills, G. R. Davies, J. E. MacIntyre, I. M. Ward, *Electrochim. Acta* **1998**, *43*, 1239.

118. C. T. Imrie, M. D. Ingram, G. S. McHattie, *Adv. Mater.* **1999**, *11*, 832.

119. (a) C. F. Van Nostrum, S. J. Picken, A.-J. Schouten, R. J. Nolte, *J. Am. Chem. Soc.* **1995**, *117*, 9957; (b) C. F. Van Nostrum, *Adv. Mater.* **1996**, *8*, 1027.

120. (a) V. Percec, J. Heck, D. Tomazos, G. Ungar, *J. Chem. Soc., Perkin Trans. 2* **1993**, 2381; (b) V. Percec, G. Johansson, J. Heck, G. Ungar, S. V. Batty, *J. Chem. Soc., Perkin Trans. 1* **1993**, 1411.

121. L. Brunsveld, J. A. J. M. Vekemans, H. M. Janssen, E. W. Meijer, *Mol. Crys. Liq. Cryst.* **1999**, *331*, 449.

122. J.-M. Lehn, J. Malthête, A.-M. Levelut, *J. Chem. Soc., Chem. Commun.* **1985**, 1794.

123. T. Hirose, S. Tanaka, Y. Aoki, H. Nohira, *Chem. Lett.* **2000**, 1290.

124. U. Beginn, G. Zipp, M. Möller, *Chem. Eur. J.* **2000**, *6*, 2016.

125. (a) H. Kosonen, S. Valkama, J. Hartikainen, H. Eerikäinen, M. Torkkeli, K. Jokela, R. Serimaa, F. Sundholm, G. ten Brinke, O. Ikkala, *Macromolecules* **2002**, *35*, 10149; (b) R. Mäki-Ontto, K. de Moel, E. Polushkin, G. A. van Ekenstein, G. ten Brinke, O. Ikkala, *Adv. Mater.* **2002**, *14*, 357.

126. H. Tokuhisa, M. Yokoyama, K. Kimura, *J. Mater. Chem.* **1998**, *8*, 889.

127. J. H. Ding, D. L. Gin., *Chem. Mater.* **2000**, *12*, 22.

128. S. A. Miller, J. H. Ding, D. L. Gin, *Curr. Opin. Colloid Inteface Sci.* **1999**, *4*, 338.

129. D. L. Gin, W. Gu, B. A. Pindzola, W.-J. Zhou, *Acc. Chem. Res.* **2001**, *34*, 973.

130. D. L. Gin, W. Gu, *Adv. Mater.* **2001**, *13*, 1407.

Chapter 2

Self-Assembly of Ionic Liquids and Hydroxyl-Functionalized Mesogenic Molecules: Anisotropic Ion Conduction in Layered and Columnar Nanostructures

Abstract: New anisotropic ion-conductive materials have been prepared through self-assembly of conventional imidazolium-based ionic liquids and rod-like or fan-shaped mesogenic molecules having hydroxyl groups. These assemblies form phase-segregated layered and columnar structures on the nanometer scale. The formation of hydrogen bonding between the imidazolium cations and hydroxyl groups plays a key role in the formation of such structures. Anisotropic ionic conductivities along the direction of parallel and perpendicular to the layer and column have been successfully measured for the materials forming oriented monodomains in the liquid crystalline phases.

2.1. Introduction

Liquid crystals have unique properties such as their dynamic and anisotropic nature.[1] These properties can be used for the development of new functional materials that transport ions[2–8] and electrons.[9–12] The intention in the present study is to obtain ionically functional anisotropic materials by self-organization of ionic liquids. Ionic liquids are organic isotropic liquids composed entirely of ions. They have been extensively studied on the utilization of their unusual characters such as nonvolatility and high ionic conductivity in the fields of the organic chemistry[13–15] and electrochemistry.[16–18] For further applications of ionic liquids, the introduction of ordered self-organized structures may be of interest. Amphiphilic ionic liquid derivatives consisting of an ionic head group and long alkyl chains were reported to show mesomorphism.[19–22] However, their ionic activities such as ionic conductivities may be lowered by the introduction of the long alkyl chains. If conventional simpler ionic liquids can form dynamically ordered structures, their specific functions as ionic species will be kept in the self-organized structures.

In this study, the author has developed new liquid crystalline layered and columnar assemblies consisting of ionic liquids and hydroxyl-functionalized mesogenic molecules, which form nanophase-segregated structures. Anisotropic ion conductions of the ionic liquids organized into layer and columnar nanostructures have been achieved for the oriented materials between the electrodes.

2.2. Results and Discussion

2.2.1. Two-Dimensional Ion Conductors

To fabricate two-dimensional ion conductors based on ionic liquids, the author has designed and synthesized rod-like mesogenic compounds **1a** and **1b** having hydroxyl groups at the extremity of the alkyl chains, as shown in Figure 2–1. The effect of the lateral fluoro

substituent is to reduce the melting points of the compounds. As an ionic liquid, 1-ethyl-3-methylimidazolium tetrafluoroborate **2** was chosen due to its higher ionic conductivity and wider electrochemical windows.[18, 23–25]

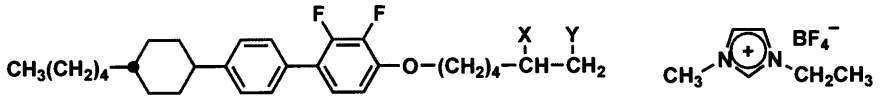

1a: X = OH, Y = OH
1b: X = H, Y = OH
1c: X = H, Y = H

2

Figure 2–1. Molecular structures of mesogenic compounds **1a–c** and ionic liquid **2**.

Liquid Crystalline Properties

The mixing of mesogenic compound **1a** and ionic liquid **2** leads to the formation of layered liquid crystalline phases, while compound **1a** alone gives a columnar phase (Col). Figure 2–2 shows phase diagrams for the mixtures of **1a,b** and **2** as a function of the mole fraction of **2** in the mixtures. Compounds **1a** and **2** are miscible up to the mole fraction of 0.7 for **2** in the mixture. These mixtures exhibit thermally stable smectic phases. For example, an equimolar mixture of **1a** and **2** shows a glass transition at 14 °C and subsequent smectic phases up to 198 °C. Figure 2–3 shows the textures of **1a** in the Col phase at 100 °C and the contact region of **1a** with **2** at the same temperature. Compound **1b** alone shows a smectic A phase (S_A) ranging from 79 to 149 °C and on heating a subsequent nematic (N) phase up to 159 °C. **1b** is miscible with **2** up to the mole fraction of 0.6 for **2** in the mixture. The intermolecular interactions between the hydroxyl groups of **1** and ionic liquid **2** enhance the miscibility and lead to the formation of the smectic phases for the mixtures. In contrast, phase separation is observed for compound **1c** without hydroxyl groups and **2** because of the lack of such strong interactions.

The X-ray diffraction pattern for the equimolar mixture of **1b** and **2** at 100 °C shows

that the layer spacing of the S_A phase is 5.0 nm, while the spacing for compound **1b** alone is 4.6 nm at the same temperature. The incorporation of the ionic liquid layer may extend the layer spacing for the mixture. These types of mesogenic compounds were reported to form layered structures through intermolecular hydrogen bonding by the addition of water and organic solvents.[26–28] In these systems, ionic liquid **2** is used as a functional solvent instead of common inactive solvents.

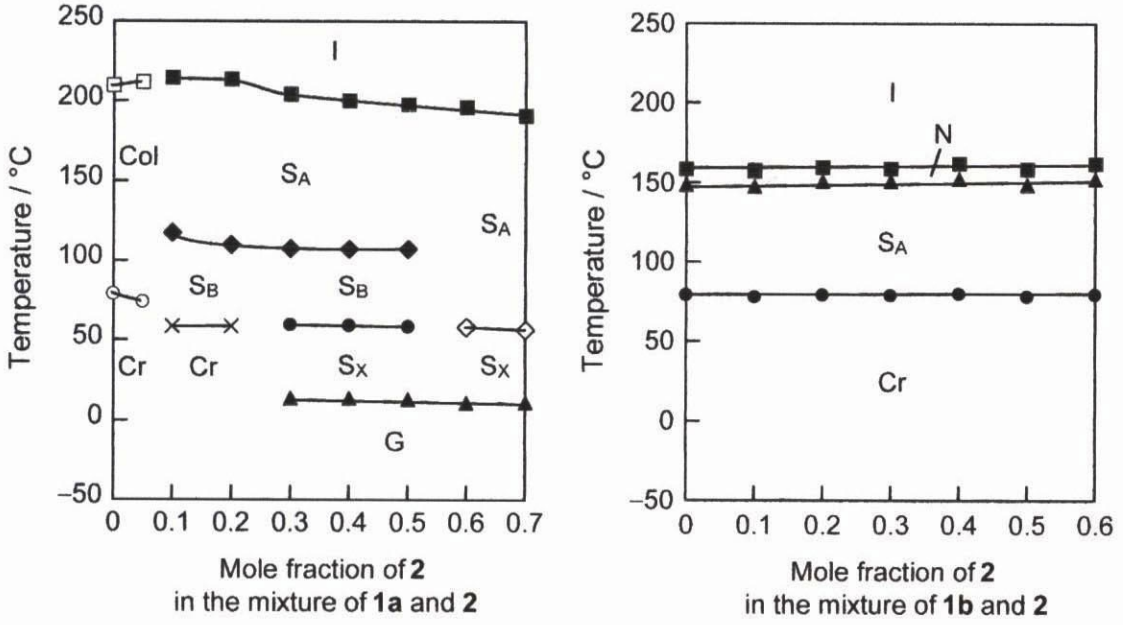

Figure 2–2. Phase transition behavior for a mixture of **1a** and **2** (left) and a mixture of **1b** and **2** (right) determined by DSC on the second heating. Cr: crystalline, S_A: smectic A, S_B: smectic B, S_X: unidentified smectic, Col: columnar, G: glassy, N: nematic.

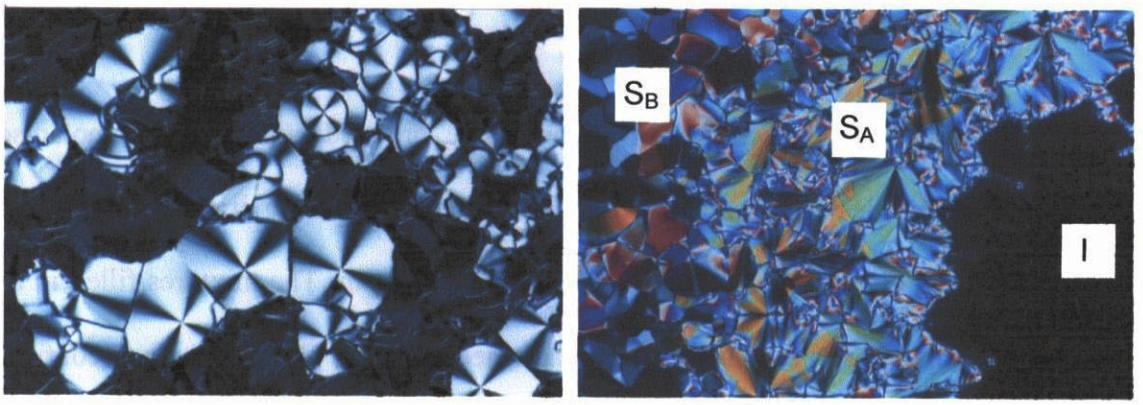

Figure 2–3. Polarized light optical photomicrographs of the texture of **1a** in the Col phase at 100 °C (left) and the contact region of **1a** with **2** (right-hand side) at 100 °C (right).

Anisotropic Ionic Conductivities

The anisotropic ionic conductivities of the equimolar mixtures of **1** and **2** have been successfully measured for the samples forming oriented monodomains in the cells of A and B, as shown in Figure 2–4.

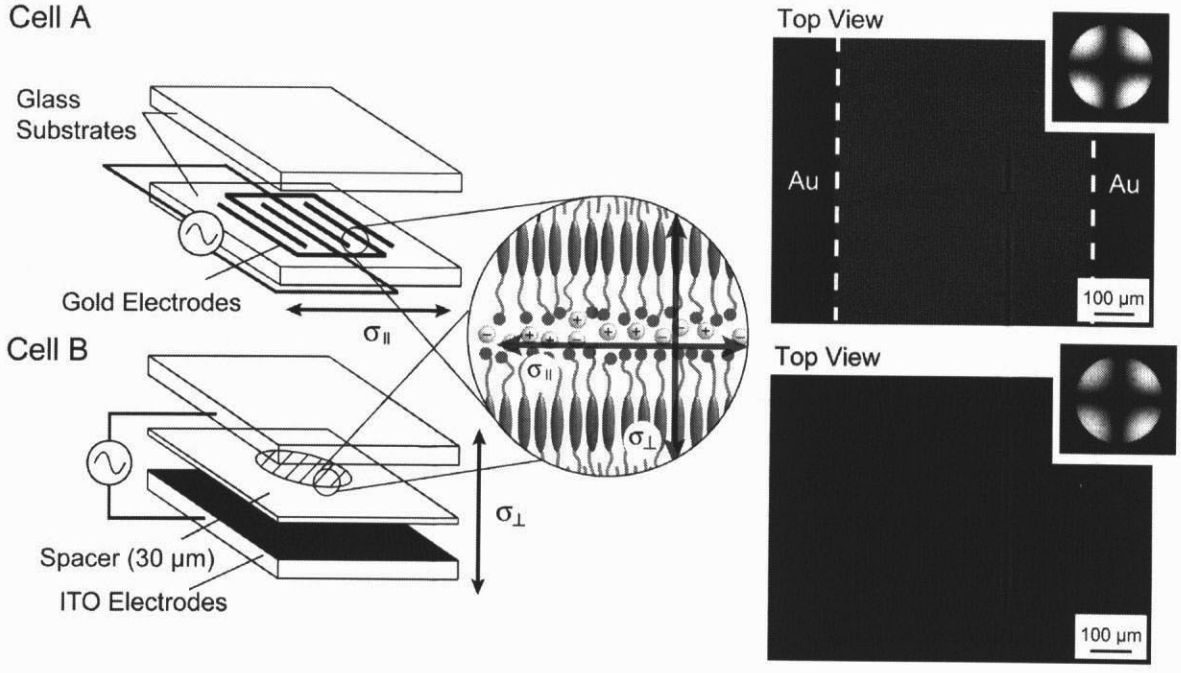

Figure 2–4. Schematic illustrations of the Cell A and B for the anisotropic ion-conductive measurements (left). The samples forming the smectic liquid crystalline phases are filled between electrodes. The samples composed of equimolar amounts of an ionic liquid and mesogenic compounds form homeotropically aligned monodomains in the cells (center). The orthoscopic and conoscopic images at 120 °C for the mixture of **1b** and **2** filled in these cells are also shown (right).

As far as the author knows, for mesomorphic ion-conductive materials, no anisotropy of ionic conductivities has until now been presented. Cell A comprises a glass plate with comb-shape gold electrodes of which the thickness is 0.8 μm. The mixtures filled in the cell show homeotropic alignment in the N, S_A, and smectic B (S_B) phases, which is confirmed by polarizing microscope. For example, the orthoscopic and conoscopic images at 120 °C for the mixture of **1b** and **2** reveal that the smectic molecular assemblies align homeotropically on the

glass surface in the S_A phase, as demonstrated in Figure 2–4 (upper right). For cell A filled with oriented samples, the ionic conductivity along with the direction parallel to the smectic layer plane ($\sigma_{\parallel}$) can be measured. Cell B consists of a pair of indium tin oxide (ITO) electrodes. The thickness between the two electrodes is fixed by a Teflon spacer to be 30 μm. As shown in Figure 2–4 (lower right), the mixtures in the liquid crystalline states also form homeotropic alignment on the hydrophobic surface of the ITO electrodes, although no such alignment was observed for the mesogenic molecules containing oligo(ethylene oxide)s.[7] The homeotropic alignment of the mixtures based on the ionic liquid has enabled the author to measure the ionic conductivities along with the direction perpendicular to the smectic layer plane ($\sigma_{\perp}$).

Figure 2–5 shows anisotropic ionic conductivities of the self-organized mixtures as a function of temperature. The ionic conductivities parallel to the smectic layer ($\sigma_{\parallel}$) are higher than those perpendicular to the layer ($\sigma_{\perp}$). The highest conductivity ($\sigma_{\parallel}$) achieved for the mixture of **1a** and **2** is 4.1×10^{-3} S cm^{-1} in the S_A phase at 192 °C. The magnitude of anisotropy ($\sigma_{\parallel}/\sigma_{\perp}$) at this temperature is 2.9×10. The magnitude of maximal anisotropy is about 3.1×10^{3} at 73 °C in the S_B phase. In the S_B phase, ordered packing of the aromatic mesogen may effectively disturb the ion conduction perpendicular to the layer. For the mixture of **1b** and **2**, the highest $\sigma_{\parallel}$ value of 2.8×10^{-3} S cm^{-1} and the $\sigma_{\parallel}/\sigma_{\perp}$ value of 8.2×10 are obtained in the S_A phase at 132 °C. No anisotropy of the ionic conductivities is observed when the liquid crystalline order disappears at the isotropization temperatures. The formation of the smectic layered structures through the nanophase segregation between **1** and **2** results in the spontaneous formation of anisotropic ion-conductive pathways with long-range order, as illustrated in Figure 2–6.

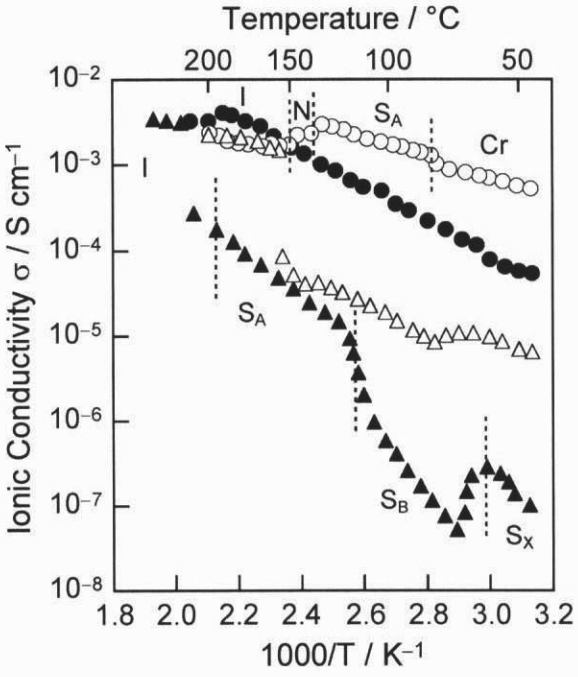

Figure 2–5. Anisotropic ionic conductivities of the homeotropically aligned smectic liquid crystalline complexes composed of equimolar amounts of **1** and **2**: (●) parallel and (▲) perpendicular to the smectic layer plane for **1a** and **2**; (○) parallel and (△) perpendicular to the smectic layer plane for **1b** and **2**.

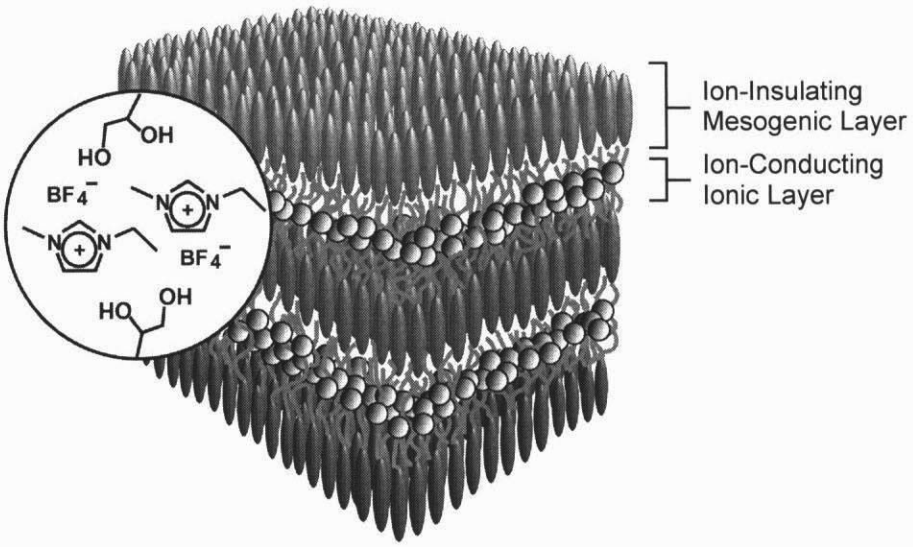

Figure 2–6. Illustration of nanophase-segregated layered structures composed of **1a** and **2**.

It was reported that the ionic conductivities of isotropic ionic liquids alone gradually increase with the increase in temperature.[18] In contrast, for the anisotropic self-organized materials in the present study, the discontinuous changes of ionic conductivities are seen at the phase transition temperatures. For example, the $\sigma_{\parallel}$ values for the self-organized mixture based on **1b** increase at 78 °C and decrease at 138 and 148 °C. These temperatures correspond to the crystalline–S_A, S_A–N, and N–isotropic transitions, respectively.

The activation energy for the ion-conductive process in the S_A phase can be estimated from the slope of the ionic conductivities ($\sigma_{\parallel}$) in Figure 2–5 using the following Arrhenius equation (1):

$$\sigma = \sigma_0 \exp [-(Ea/RT)] \qquad (1)$$

where Ea is the activation energy for the ion conduction process, σ_0 and R are the pre-exponential factor and the gas constant, respectively. The energies required for the mixture of **1a** and **2** and the mixture of **1b** and **2** are 38 and 20 kJ mol^{-1}, respectively. The ionic conductivities along with the direction parallel to the smectic layer depend on the number of hydroxyl groups of the mesogenic molecule in the mixture. It is assumed that the increase of the intermolecular interactions between the hydroxyl groups and ionic liquids results in the lowering of the mobility of the ionic liquids alone. The activation energy for **1b** and **2** is equal to that for **2** alone (20 kJ mol^{-1}). It is found that the high mobility of the ionic liquid is kept in the phase-segregated layered structure formed by compound **1b**.

2.2.2. Improvement of 2D Ion-Conductive Properties

To obtain the liquid crystalline materials showing high ionic conductivities and high anisotropy, the complexes composed of two-ring mesogenic molecule **3** and ionic liquid **2** have been prepared (Figure 2–7). The author expected that ionic conductivity may be improved by reducing the volume of insulating mesogenic part in the materials. Moreover, the use of the mesogenic molecules with lower clearing points can facilitate the alignment control of the assembled materials at ambient temperature. The liquid crystalline properties and the ionic conductivities of the mixtures of **2** and **3** have been examined. These materials have been found to exhibit two-dimensionally ionic conductivities with high anisotropy at room temperature.

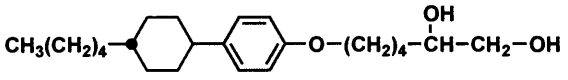

3

Figure 2–7. Molecular structure of a two-ring mesogenic molecule with hydroxyl groups.

Liquid Crystalline Properties

Compound **3** alone shows a S_B phase from 28 to 64 °C on heating and a subsequent S_A phase up to 147 °C. This molecule is miscible with **2** up to the mole fraction of 0.6 for **2** in the mixture. Incorporating the fluid ionic liquid reduced the crystallization temperature of the mixtures. Similar thermal stabilization of the liquid crystalline phase by the introduction of **2** is observed for the assembled materials composed of three-ring mesogenic molecule **1a** and **2**, wherein the material is vitrified without crystallizing. The formation of S_A phases for such mixtures was also observed for imidazoles and hydroxyl mesogenic compounds.[29]

X-ray diffraction measurements of the mixture of **2** and **3** have been carried out to examine the mesomorphic phase structures. For compound **3**, a set of Bragg peaks at

scattering angles with a ratio of 1:1/2:1/3 is observed, which indicates the formation of a well-organized layer of the S_A phase. The layer spacing is 4.37 nm at 100 °C. The length of the mesogenic molecule in the extended conformation is estimated to be 2.3 nm by molecular modeling. The layer spacing (4.37 nm) of **3** indicates the formation of a bilayer molecular packing through hydrogen bonding between the hydroxyl moieties. For the mixture, the similar diffraction pattern to that of **3** is observed at the same temperature and the layer spacing is 4.41 nm. The layer spacing is slightly extended for the mixture due to the incorporation of the ionic layer. The ionic liquid is stabilized and located in the polar environment yielded by self-association of hydroxyl moieties. The formation of such phase-segregated layer structure on the nanometer scale plays a key role for anisotropic ion conduction.

Anisotropic Ionic Conductivities

The anisotropic ionic conductivities of the self-assembled mixture of **2** and **3** have been measured by an alternating current impedance method on heating. Two types of the cells shown in Figure 2–4 were used for the anisotropic measurements of ionic conductivities. The mixtures filled in the cell show homeotropic alignment in the smectic phases. Figure 2–8 shows the anisotropic ionic conductivities of the self-assembled mixture of **2** and **3** in the molar ratio of 8:2 as a function of temperature. The ionic conductivity parallel to the smectic layer ($\sigma_{\parallel}$) is higher than that perpendicular to the layer ($\sigma_{\perp}$). The highest value of $\sigma_{\parallel}$ is 4.8×10^{-4} S cm^{-1} in the S_A phase at 122 °C. The magnitude of anisotropy at the same temperature is 5.0. The magnitude of maximal anisotropy is 2.6×10^3 in the S_B phase at 37 °C. The anisotropy of the ion conduction in the S_B phase is higher than that in the S_A phase. In the S_B phase, the hexagonal ordered packing of the mesogen may effectively disturb the ion conduction perpendicular to the layer. No anisotropy of the ionic conductivity is observed

when the liquid crystalline order disappears at the isotropization temperature on heating. The formation of the smectic layered structure through the nanophase segregation between **2** and **3** results in the spontaneous formation of an anisotropic ion-conductive pathway with long-range order.

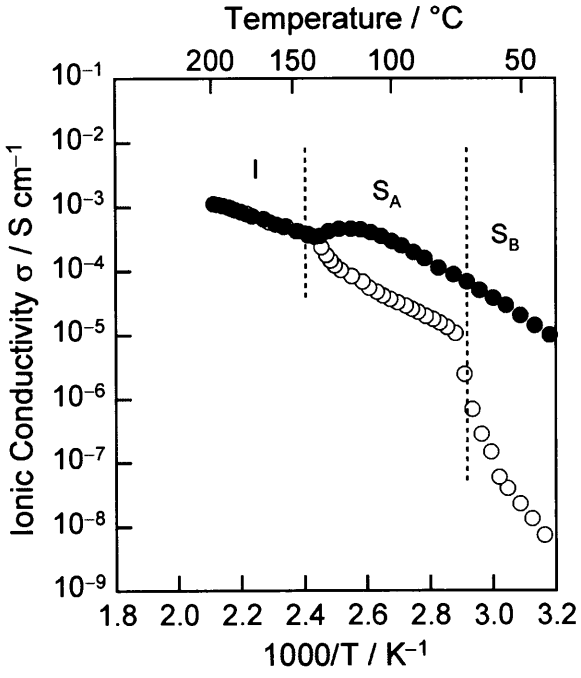

Figure 2–8. Anisotropic ionic conductivities of the homeotropically aligned smectic liquid crystalline complexes composed of equimolar amounts of **2** and **3**: (●) parallel and (○) perpendicular to the smectic layer plane.

In order to obtain high ion-conductive liquid crystalline materials, the concentration of **2** in the assembled materials is increased. The ionic conductivities ($\sigma_{\parallel}$) for the oriented mixtures of **3** and **2** in the molar ratio of 7:3 (▲), 8:2 (●), and 9:1 (■) are shown in Figure 2–9. The increase of the mole fraction of **2** in the mixture results in the increase of ionic conductivities of the materials. It is assumed that the increase of the mobile ions without anchoring from mesogenic molecules enhances the ion conduction in layered nanostructures.

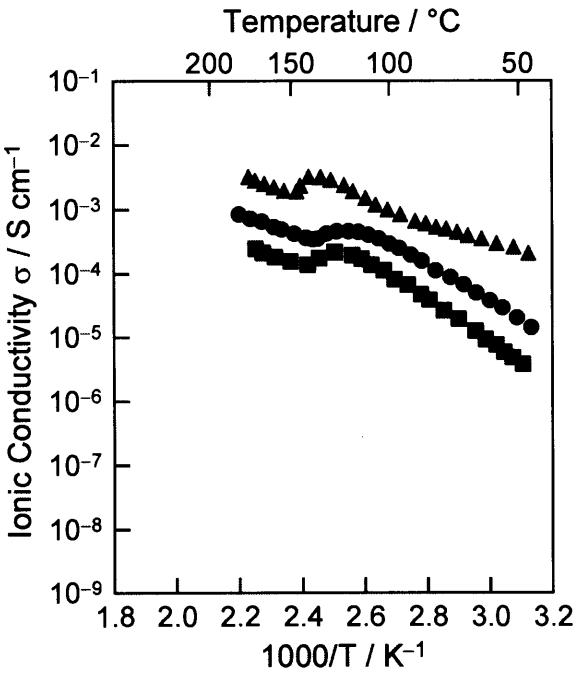

Figure 2–9. Ionic conductivities parallel to the smectic layer of the homeotropically aligned mixtures of **2** and **3** in the molar ratio of 7:3 (▲), 8:2 (●), and 9:1 (■).

2.2.3. One-Dimensional Ion Conductors

In the former chapters 2.2.1 and 2.2.2, the author demonstrated that the smectic liquid crystalline assemblies consisting of rod-like mesogenic molecules with hydroxyl groups and an ionic liquid, 1-ethyl-3-methylimidazolium tetrafluoroborate, exhibit two-dimensionally anisotropic ion conduction. It was found that the formation of hydrogen bonding between the hydroxyl groups and the imidazolium cations would play a key role in the formation of the phase-segregated layered structures. Then, for further functionalization of anisotropic ion conductors, the author developed one-dimensionally ion-conductive columnar liquid crystals by using the self-assembly of ionic liquids and hydroxyl-functionalized mesogenic molecules.

Until now, columnar liquid crystals containing a crown ethers and oligo(ethylene

oxide)s as ion-conductive parts have been designed by Percec Nolte, Meijer, Beginn, and so on.[30–33] However, no ionic conductivities were measured for columnar liquid crystals except for few examples: Percec reported that the columnar liquid crystalline complex consisting of a crown ether derivative and lithium triflate exhibits the ionic conductivity of 5.6×10^{-10} S cm^{-1} at 40 °C for a non-oriented sample.[30]

In this chapter, the author focused on the preparation of columnar liquid crystals containing ionic liquids, in which ions move in the center of columns. A fan-shaped molecule **4** having hydroxyl groups is designed (Figure 2–10). The influence of the species of imidazolium salts **2**, **5**, and **6** on the mesomorphic behavior was examined.

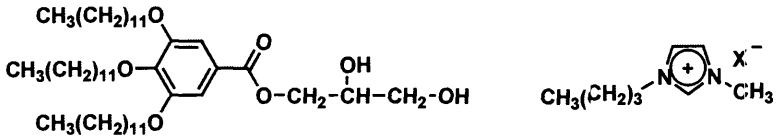

4

5: X = Br
6: X = BF_4

Figure 2–10. Molecular structures of a fan-shaped molecule **4** and ionic liquids **5** and **6**.

Phase Transition Behavior

Compound **4** forms a cubic phase, which is optically isotropic phase under the polarizing microscope, ranging from 68 to 20 °C on cooling. The formation of a hexagonal columnar phase by self-assembly of **4** and ionic liquid **5** was at first confirmed by means of miscibility experiments. Mesogenic molecule **4** and ionic liquid **5** with Br^- are miscible and the mixture can form hexagonal columnar phases (Col_h), while phase separation was observed for the mixtures of **4** and ionic liquids **2** or **6** containing BF_4^-. Figure 2–11 shows the polarizing optical microscopic image of the contact region between the cubic phase of **4** and the isotropic liquid phase of **5**. A hexagonal columnar phase is induced in the contact region.

The observed miscibility of **4** in ionic liquids **5** and **6** is attributable to the difference

of the strength of hydrogen bonding between anions and hydroxyl groups. Rogers et al. reported that ionic liquids containing Br^- and Cl^-, which are strong hydrogen bond acceptors, can dissolve cellulose, while hydrophobic ionic liquids incorporating BF_4^- and PF_6^- can not solvate it.[34] In the present study, it is considered that ionic liquid **5** is stabilized into the center of columns through the formation hydrogen bonding from hydroxyl groups to the bromide anion.

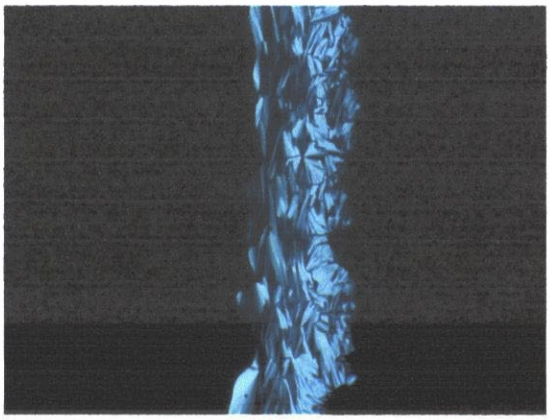

Figure 2–11. Polarized optical micrograph of the Col_h phase induced in the contact region between the isotropic liquid phase of ionic liquid **5** (optically isotropic region at the left-hand side) and the micellar cubic phase of compound **4** (right-hand side) at room temperature.

The detailed phase diagram for the mixtures of mesogenic molecule **4** and ionic liquid **5** as a function of the mole fraction of **5** in the mixture is shown in Figure 2–12. Compounds **4** and **5** are miscible up to the mole fraction of 0.5 for **5** in the mixture. For 0.6 mole fraction of **5** in the mixture, excess ionic liquid that is not assembled into columns is observed as isotropic droplets under polarizing microscope. The formation of columnar phases is observed for 0.2 mole fraction of **5** in the mixture. The isotropization temperatures increase with the increase of the concentration of the ionic liquid. For example, the equimolar mixture of **4** and **5** shows the Col_h phase from 117 to 15 °C on cooling. Interestingly, the

mixture of **4** and **5** in the molar ratio of 8:2 forms a cubic phase from 81 to 26 °C and a subsequent Col_h phase from 26 to 14 °C on cooling. This kind of dynamic materials that can respond to external stimuli and environmental changes would have potential as device materials capable of switching ion conduction.

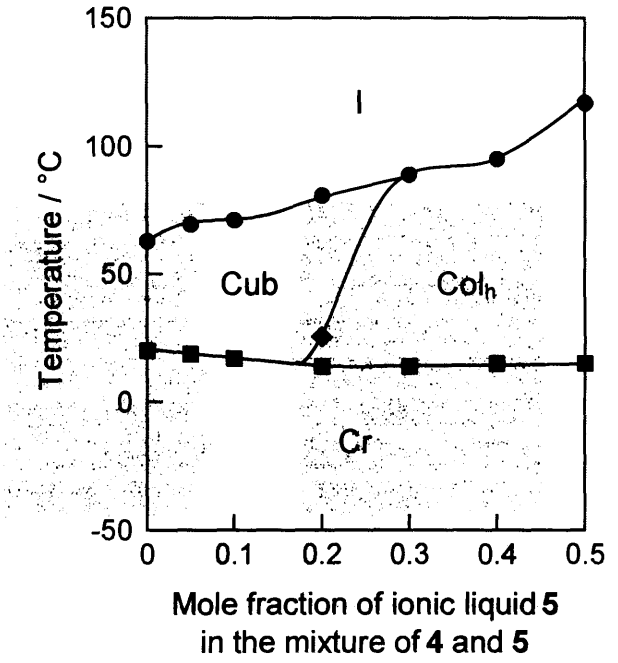

Figure 2–12. Phase transition behavior for the mixtures of mesogenic molecule **4** and ionic liquid **5** on cooling. Col_h: hexagonal columnar, Cr: crystalline, Cub: cubic, I: isotropic.

X-ray Study

X-ray diffraction measurements have been carried out to examine the cubic and columnar structures of the assemblies consisting of **4** and **5**. The X-ray diffraction pattern of the cubic phase for the mixture of **4** and **5** in the molar ratio of 8:2 can be indexed on the basis of a primitive cubic lattice (*Pm3n*) in Figure 2–13a. The lattice parameter (a) and spherical diameter (d) are calculated to be 8.4 and 5.2 nm with the following equations (2) and (3), respectively.[35,36]

$$a = (\sqrt{2}d_{110} + \sqrt{5}d_{210} + \sqrt{6}d_{210})/3 \qquad (2)$$

$$d = 8\sqrt{(3a^3/32\pi)} \qquad (3)$$

On the other hand, the columnar phase observed for the equimolar mixture of **4** and **5** displays a characteristic set of *d*-spacings in the diffraction spectrum with the ratio of 1: $1/\sqrt{3}$: 1/2 (Figure 2–13b), indicating the formation of a hexagonal columnar structure. The intercolumnar distance (a) is calculated to be 4.9 nm with the following equation (4).[35,36]

$$a = 2\langle d_{110}\rangle/\sqrt{3},\ \langle d_{110}\rangle = (d_{100} + \sqrt{3}d_{110} + \sqrt{4}d_{200})/3 \qquad (4)$$

Assuming a density of ρ = 1 g cm^{-3}, the number n of molecules arranged side by side in a single slice of the columns with a thickness (h) of 0.45 nm (the X-ray diffraction from the molten alkyl chains was used) was estimated according to the equation (5)[35,36]:

$$n = \sqrt{3}N_A a^2 h\rho/(2M) \qquad (5)$$

where N_A is the Avogadro's number (6.02×10^{23} mol^{-1}) and M is the molecular weight (968.27 g mol^{-1} for the mixture of **4** and **5**). The estimated value of n is about 6. A schematic illustration of the self-assembled structure is shown in Figure 2–14. In the hexagonal columnar phase, the imidazolium salts might be stabilized into the center of columns, which consists of hydrogen bonding networks surrounded by the molten alkyl chains.

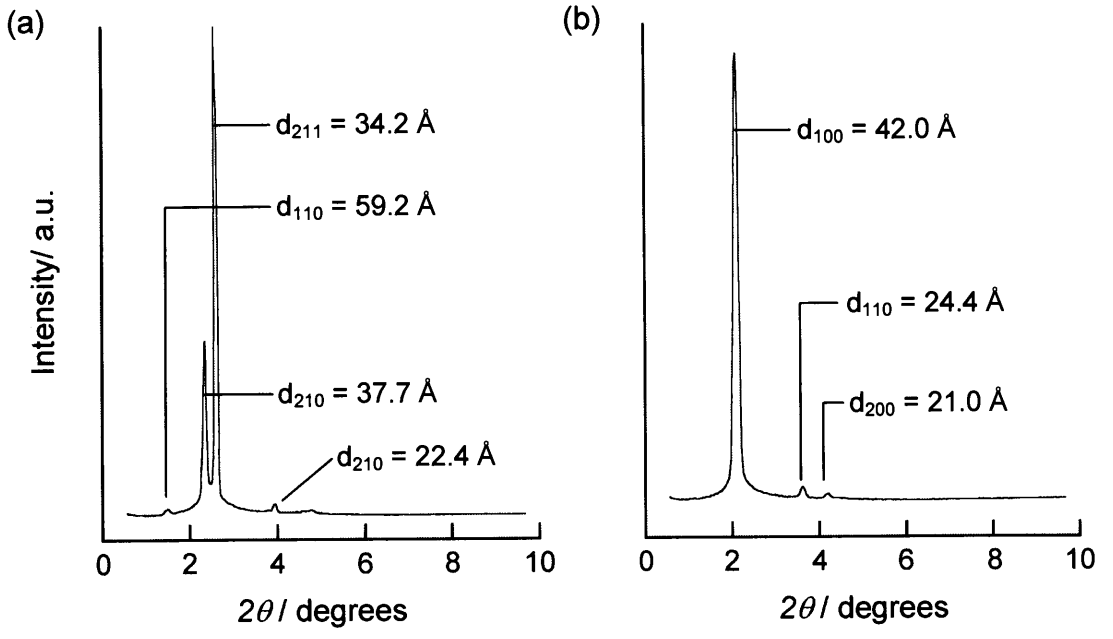

Figure 2–13. X-ray diffraction patterns of (a) the mixture of **4** and **5** (8:2 molar ratio) at 50 °C and (b) the equimolar mixture of **4** and **5** at 50 °C.

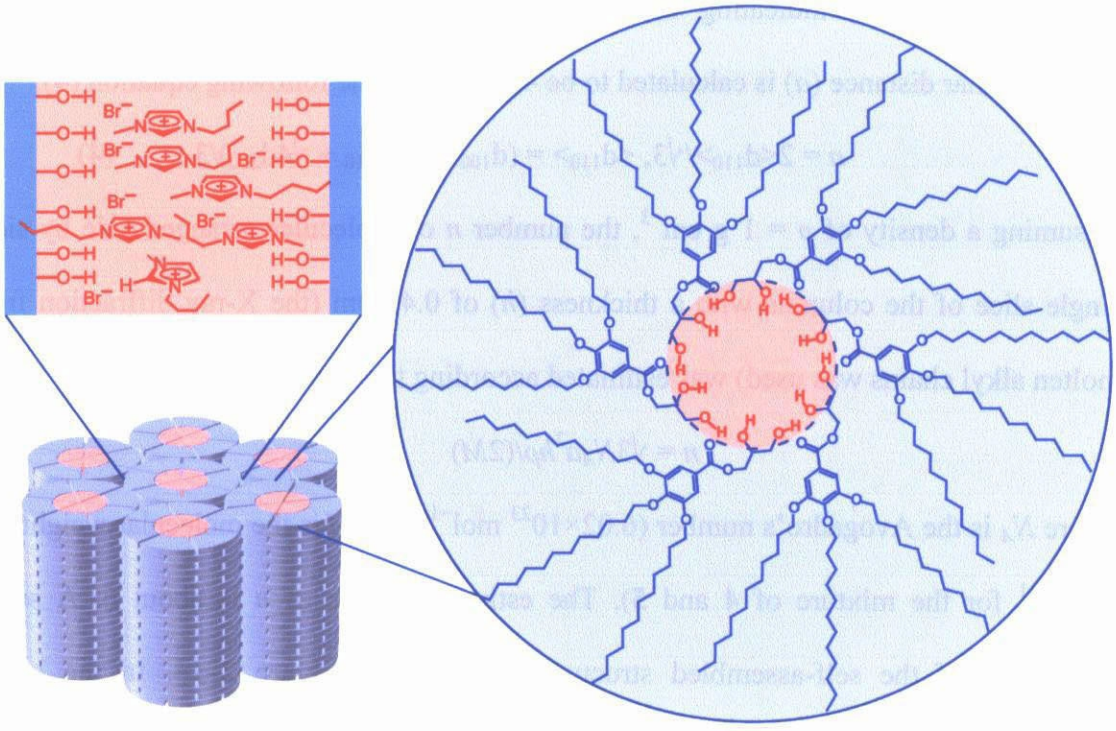

Figure 2–14. Illustration of the formation of self-assembled columnar structure.

IR Study

Infrared measurements were performed to examine the interactions between the ionic liquid and the hydroxyl-functionalized mesogenic molecule. In the IR spectrum of **4** alone in the cubic phase, a broad hydroxyl band is seen at 3424 cm^{-1}. As for the equimolar mixture of **4** and **5** in the columnar phase, the band is observed at 3330 cm^{-1}. This change may be caused by the formation of hydrogen bond between hydroxyl groups and the ionic liquid. On the other hand, for the C=O band of the ester group, no peak shift is observed upon the addition of the ionic liquid, suggesting that the ester group does not interact with the ionic liquid.

NMR Study

In the ^{1}H NMR spectrum of **4** (Figure 2–15), the signals of hydroxyl proton are clearly seen at 2.63 ppm (d, ^3J(H, H) = 5 Hz) and 2.18 ppm (t, ^3J(H, H) = 6 Hz), which is supposed by the result that the peak disappears by the addition of small amount of D_2O in the $CDCl_3$ solution of **4** (10 mM). In order to obtain the information of the interactions between **4** and **5**, ^{1}H NMR titration experiments are performed in $CDCl_3$ at 20 °C. Remarkable changes in the chemical shifts were observed for the hydroxyl groups and the imidazolium ring protons as the composition of **4** and **5** in the mixtures (**4**/**5**, mole %) changes, as shown in Figure 2–16. The hydroxyl protons H^a and H^b are shifted down field in the presence of the salt. Also, the imidazolium ring proton H^2 is shifted down field in the presence of the mesogenic molecule, while the protons H^4 and H^5 are shifted less (the data is not shown here). These changes in the chemical shift are indicative of the formation of hydrogen bonds between the H^2 on the imidazolium ring and hydroxyl groups.

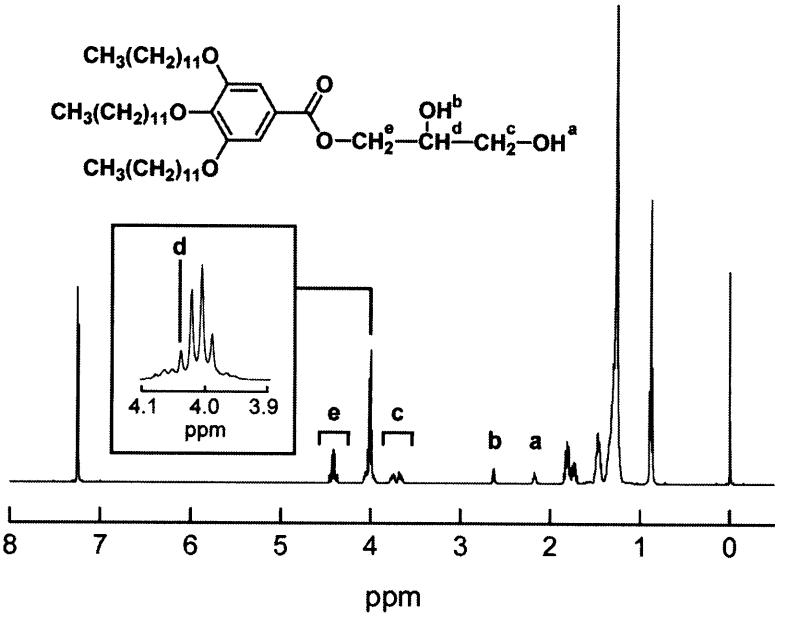

Figure 2–15. ^{1}H NMR spectrum of **4** in $CDCl_3$ at 20 °C.

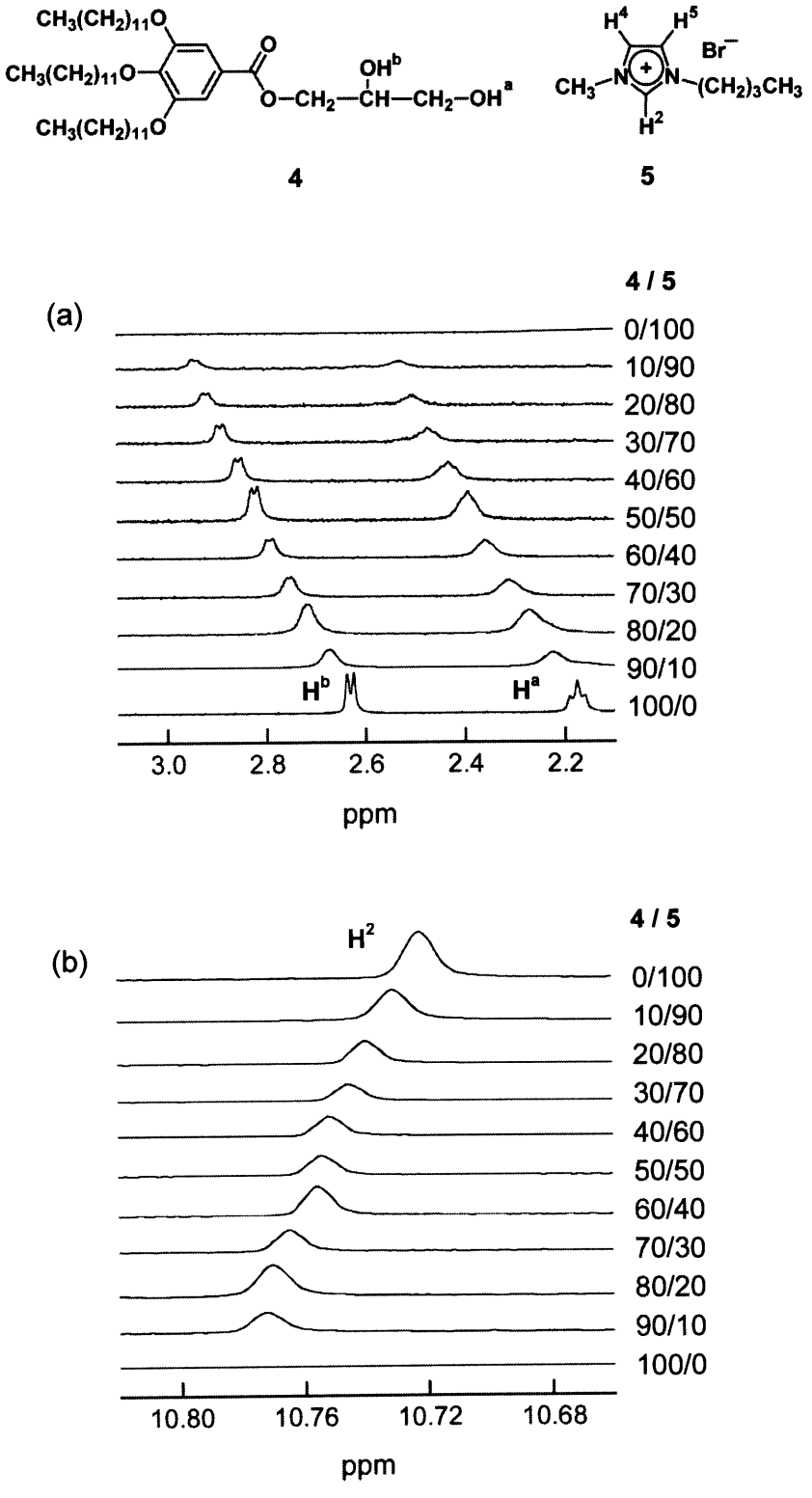

Figure 2–16. ^{1}H NMR spectra of the mixtures of **4** and **5** in $CDCl_3$ (10 mM) at 20 °C: (a) hydroxyl proton resonances and (b) the resonance of proton H^2 on the imidazolium ring.

Moreover, a Job's plot[37,38] was performed in order to estimate the stoichiometry of the assemblies consisting of **4** and **5**. The plot is obtained by plotting the values of [**5**] • $\Delta\delta$, $\Delta\delta = (\delta - \delta_4)$ against the mole faction of **5** in Figure 2–17 (where [**5**] is the mole concentration of **5**, δ is observed chemical shift of **4**, and δ_4 is chemical shift of **4** (2.18 ppm for H^a, 2.63 ppm for H^b) in the absence of **5**). The maximum of this plot occurs at 0.5 for compound **5**. This clearly indicates the formation of a 1:1 complex.

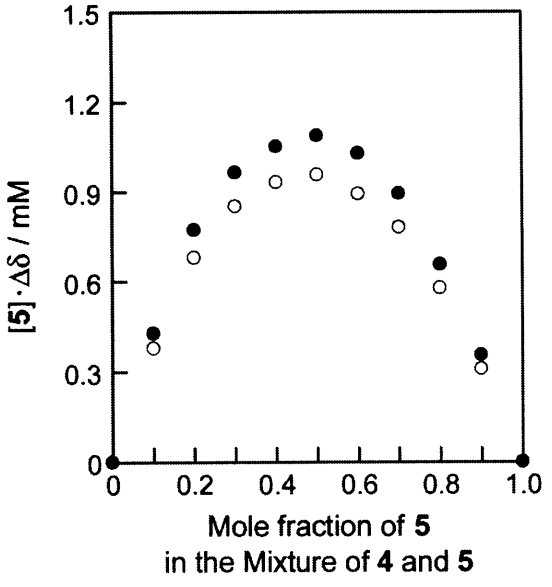

Figure 2–17. Job's plot determined by ^{1}H NMR spectroscopy indicating the 1:1 stoichiometry of the complex formed between **4** and **5**. (•): $\Delta\delta$ for the H^a resonance of **4** induced by the addition of **5** and (○): $\Delta\delta$ for the H^b resonance of **4** induced by the addition of **5**. Total concentration of **4** and **5** is maintained at 10 mM.

The 1:1 stoichiometry of the complex formed in a solution state is related to the result that the equimolar mixture of **4** and **5** forms the most stable columnar liquid crystalline phase, as shown in Figure 2–12. In the NMR study, it turned out that the hydrogen bonding between the ionic liquid and hydroxyl compound is formed even in the solution state.

Furthermore, the existence of such hydrogen bonding was clarified by the X-ray crystallographic studies of the imidazolium salt with a hydroxyl group by Rogers et al.[39] In

the literature, it was reported that the racemic 1-(2-hydroxypropyl)-3-methylimidazolium tetraphenylborate formed a hydrogen-bonded dimer (Figure 2–18), connected by two strong almost linear hydrogen bonds from the acidic imidazolium-ring C(2)-hydrogens to the oxygen atoms of the opposing cation.

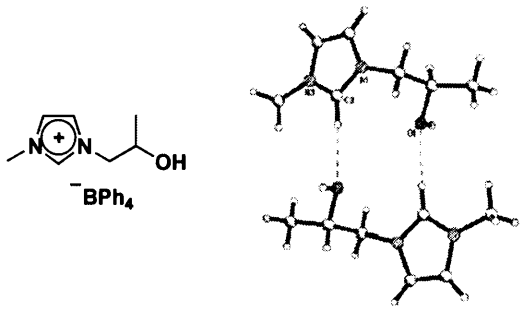

Figure 2–18. Molecular structures and crystal structure of imidazolium salt reported by Rogers.[39] The hydrogen-bonded dimmer formed by R/S-pairs of the 1-(2-hydroxypropyl)-3-methylimidazolium cations.

Macroscopic Orientation of Columns

It is important to control orientation of self-organized columns to achieve anisotropic one-dimensional ion conduction. Self-organized columns prefer to form random orientation on the surface of glass and ITO substrates when the mixture is cooled down from the isotropic liquid state to the hexagonal columnar phase. To align the columns uniaxially, a shear stress was applied at 100 °C to the columnar material with the polydomain structures, which is sandwiched in glass substrates without rubbing treatment. Figure 2–19 shows polarized optical micrographs of the columnar phase of the mixture at room temperature (a) before shearing and (b) after shearing for the material. No boundary of the columnar domains was observed after shearing the material. The periodic change in the pattern was observed for the sheared sample under polarizing microscope. No birefringence was seen under the crossed Nicols condition when the shearing direction is along the polarizer or analyzer axis. The highest brightness was observed when the oriented sample is in a 45° angle. This indicates

that the direction of the long axis of columns corresponds to the shearing direction. Macroscopically homogeneous orientation of the columnar structure is easily achieved by shearing the materials.

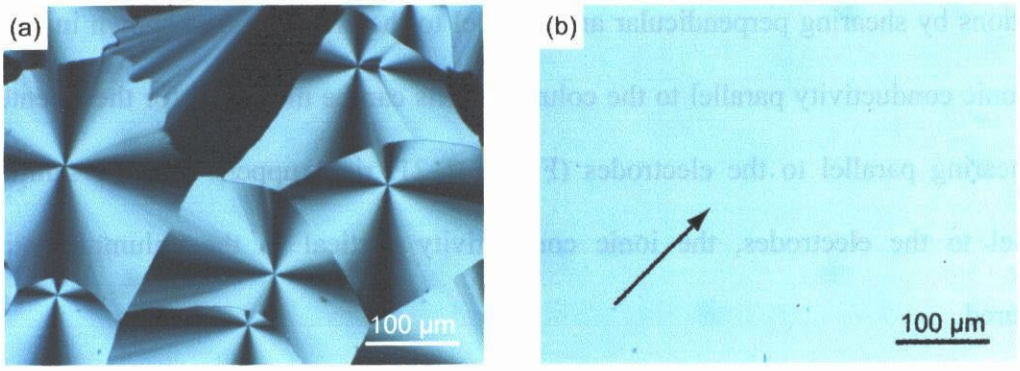

Figure 2–19. Polarized optical micrographs of the equimolar mixture of **4** and **5** in the Col_h phase at room temperature: (a) before shearing; (b) after shearing the materials. The arrow shows the direction of shearing.

Furthermore, the macroscopic orientation of columns was confirmed by two-dimensional small-angle X-ray scattering measurements. As shown in Figure 2–20a, a split diffraction pattern was observed for the sheared sample, indicating a uniaxial orientation of columns along the direction of shearing.

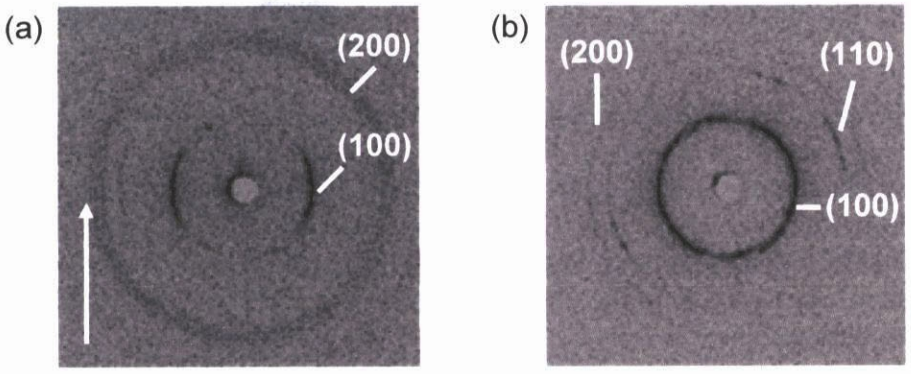

Figure 2–20. Two-dimensional X-ray scattering images of the mixture of **4** and **5** in the hexagonal columnar phase: (a) oriented sample of the mixture by shearing and (b) non-oriented sample of the mixture. The arrow shows the direction of shearing.

Anisotropic Ionic Conductivities

One-dimensional ionic conductivities have been measured by using the glassy cells with comb-shaped gold electrodes. The self-organized columns have been aligned in two directions by shearing perpendicular and parallel to the electrodes, as shown in Figure 2–20. The ionic conductivity parallel to the columnar axis can be measured for the oriented sample by shearing parallel to the electrodes (Figure 2–21, right upper). For the sample aligned parallel to the electrodes, the ionic conductivity vertical to the columnar axis can be measured.

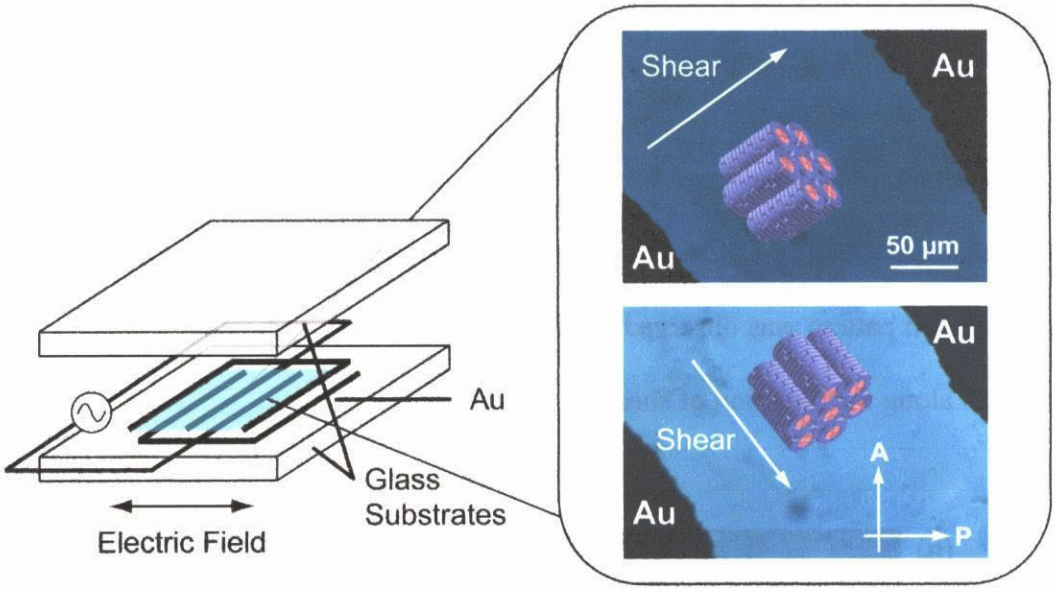

Figure 2–21. Schematic illustration of a glassy cell with comb-shaped gold electrodes with thickness of 0.8 μm for the anisotropic ion-conduction measurements (left). The columnar liquid crystal is filled between electrodes and aligned in two directions by shearing perpendicular and parallel to the electrodes. Polarized optical micrographs and illustrations of the oriented sample in the Col_h state at 50 °C. Directions of A: analyzer and P: polarizer.

Figure 2–22 shows the temperature dependence of ionic conductivities for the columnar liquid crystal composed of equimolar amount of **4** and **5** and ionic liquid **5** alone. The ionic conductivities parallel to the columnar axis ($\sigma_{||}$) is higher than that perpendicular to

the columnar axis ($\sigma_{\perp}$). The anisotropy ($\sigma_{\parallel}/\sigma_{\perp}$) of ionic conductivities was observed to be a constant value of about 53. No anisotropy was observed when the material is in the isotropic liquid state. These results indicate that long-range one-dimensional ion-conductive pathways are formed in the columnar liquid crystalline phase. The ionic conductivity of the ionic liquid alone is of the order of 10^{-2} S cm^{-1}, which is higher than that of 1-ethyl-3methylimidazolium halides containing bromide and iodide anions. These imidazolium salts were reported to exhibit fast-ion conduction in the solid states due to cation diffusion and vacancy diffusion.[40]

The activation energy for the ion conduction in the columnar phase was estimated to be 51 kJ mol^{-1} from the Arrhenius fit of the ionic conductivities parallel to the columnar axis in Figure 2–22. This value is about three times greater than that of ionic liquid **5** alone (16 kJ mol^{-1}). It is considered that the formation of hydrogen bonds between hydroxyl groups and the ionic liquid results in the enhancement of the activation barrier for the ion conduction.

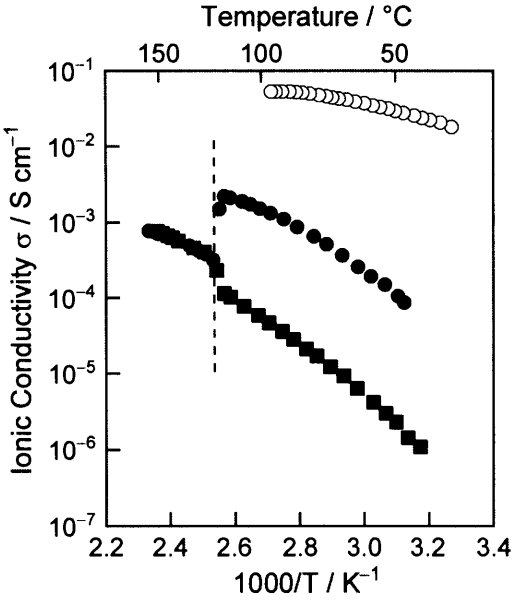

Figure 2–22. Temperature dependence of ionic conductivities for ionic liquid **5** alone (○) and the columnar liquid crystal composed of equimolar amount of **4** and **5** ((■) parallel and (●) perpendicular to the columnar axis).

2.3. Conclusions

The use of interactions between conventional ionic liquids and hydroxyl-functionalized mesogenic compounds leads to the formation of new self-organized anisotropic ion-conductive materials. For the first time, two- and one-dimensionally anisotropic ion conductions have been achieved for macroscopically oriented smectic and columnar liquid crystalline materials, respectively. These ion-transporting materials should be useful for new device systems with nanoscale order.

2.4. Experimental

General Method. All starting materials were purchased from commercial suppliers and were used without purification. Analytical thin layer chromatography (TLC) was performed on silica gel plates of E. Merck (Silica Gel F254). Flash chromatography was carried out with silica gel 60 (spherical 40-50 μm). Recycling preparative GPC was carried out with a Japan Analytical Industry LC-908 chromatograph. ^{1}H NMR and ^{13}C NMR spectra were obtained using a JEOL JNM-LA400 at 400 and 100 MHz, respectively. Chemical shifts of ^{1}H and ^{13}C NMR signals were quoted to $(CH_3)_4Si$ (δ = 0.00) and $CDCl_3$ (δ = 77.0) as internal standards, respectively, and expressed by chemical shifts in ppm (δ), multiplicity, coupling constant (Hz), and relative intensity. IR measurements were conducted on a JASCO FT/IR-660 Plus on KBr plates at room temperature. Elemental analyses were carried out on a Perkin-Elmer CHNS/O 2400 apparatus.

Characterization of Phase Transition Behavior. Differential scanning calorimetry (DSC) measurements were performed with a Mettler DSC 30 at a scanning rate of 20 °C min^{-1}. A polarizing optical microscope Olympus BH-2 equipped with a Mettler FP82 HT hot-stage was used for visual observation. Wide-angle X-ray diffraction (WAXD) patterns were obtained using a Rigaku RINT-2100 system with monochromated CuKα radiation.

Job's Plot. The stoichiometry of the complexes between **4** and **5** was determined by the continuous variation plot. Stock solutions of **4** (10mM) and **5** (10mM) in $CDCl_3$ were prepared. In ten NMR tubes, portion of the **4** and **5** solutions were added in such a way that their ratio changed from 0 to 1, keeping the total volume to be 1.0 mL. The NMR spectra for each sample were taken at 20 °C.

Measurements of Ionic Conductivities. Ionic conductivities were measured by the alternating current impedance method using a Schlumberger Solartron 1260 impedance analyzer (frequency range: 10 Hz–10 MHz, applied voltage: 0.3 V) and a temperature controller. The heating rate of the measurements was fixed to 3 °C min^{-1}. Ionic conductivities were calibrated with a KCl aqueous solution (1.00 mmol L^{-1}) as a standard conductive solution.

Synthesis of the Mesogen. A fluorophenol derivative (**13**) used as the common mesogenic core of compound **1a–c** was obtained by the palladium-catalyzed cross coupling reaction[41] from **9** and **11**, followed by the ether cleavage, through the route shown in scheme 2–1.

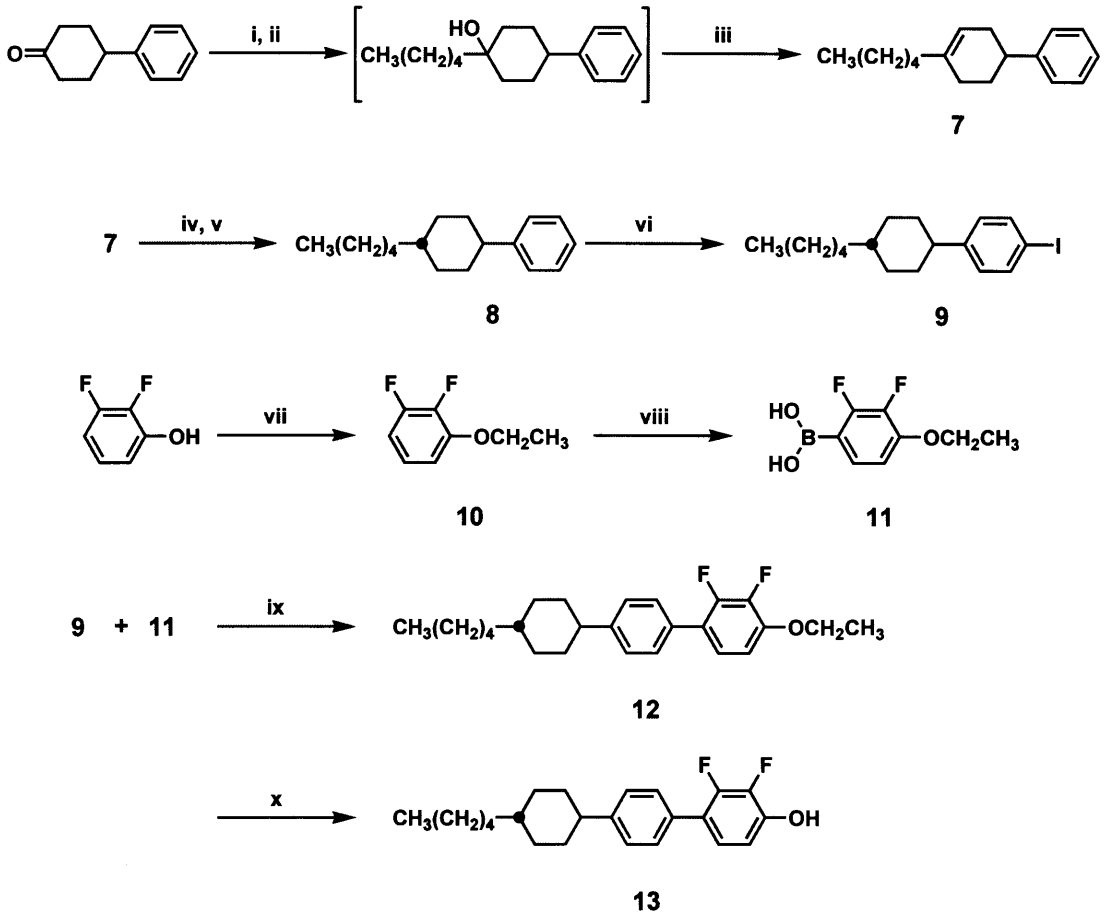

Scheme 2–1. Synthetic procedure of a laterally fluorinated mesogen.
i) $CH_3(CH_2)_4MgBr$, THF, reflux; ii) HCl aq., rt; iii) $TsOH{\cdot}H_2O$, Toluene, reflux; iv) H_2, Pd/C, EtOH, rt; v) *tert*-BuOK, DMF, rt; vi) $HIO_4{\cdot}2H_2O$, I_2, $CH_3COOH/H_2SO_4/H_2O$, 80 °C; vii) CH_3CH_2I, K_2CO_3, Acetone, reflux; viii) n-BuLi, $B(OCH_3)_3$, THF, −78 °C; ix) HCl aq., rt.; x) $[Pd(PPh_3)_4]$, Na_2CO_3, benzene/EtOH/H_2O, reflux; xi) BBr_3, CH_2Cl_2, 0 °C.

4-(4-penthyl-3-cyclohexenyl)benzene (7). To a 50 mL flame-dried, two necked flask containing magnesium (0.85 g, 34.6 mmol), dry THF (2 mL) was introduced to cover the magnesium. About 1.0 mL of a THF (5 mL) solution of 1-bromopentane (5.20 g, 34.4 mmol) was slowly added dropwise to the vigorously stirred mixture. Once the reaction started, the rest of the solution of 1-bromopentane was diluted with THF (10 mL), and the resulting solution was added dropwise and the reaction mixture was stirred under the refluxed condition for 3 h. After cooling the reaction vessel to room temperature, a solution of 4-pentylcyclohexanone (5.00 g, 28.7 mmol) in THF (20 mL) was added dropwise to a stirring solution of the Grignard reagent. Then, the resulting mixture was further stirred for 5 h at 80 °C. The solution was poured into water and the product was extracted with hexane and EtOAc. The combined organic extracts were washed with brine, died over $MgSO_4$, filtered through a pad of Celite, and concentrated *in vacuo*. The crude products containing 4-(4-hydroxy-4-pentylcyclohexyl)benzene (7.07 g) were obtained as a viscous colorless liquid. Then, a solution of the crude products and *p*-toluenesulfonic acid monohydrate (0.14 g, 0.74 mmol) in toluene (200 mL) was refluxed for 10 h with azeotropic removal of water using a Dean-Stark tube. After evaporating the toluene solution under reduced pressure, the residue was purified by flash column chromatography on silica gel (eluent: hexane) to give **7** (2.85 g, 12.5 mmol) in a yield of 44 % as a colorless liquid. ^{1}H NMR (400 MHz, $CDCl_3$): δ = 7.36–7.22 (m, 5H), 5.53 (d, J = 4.4 Hz, 1H), 2.85–2.74 (m, 1H), 2.41–1.23 (m, 14H), 0.89 (t, J = 6.8 Hz, 3H); ^{13}C NMR (100 MHz, $CDCl_3$): δ = 147.8 (s), 138.0 (s), 128.3 (s), 126.9 (s), 125.9 (s), 120.2 (s), 40.3 (s), 37.6 (s), 33.6 (s), 31.7 (s), 30.1 (s), 28.9 (s), 27.5 (s), 22.6 (s), 14.1 (s).

4-(*trans*-4-pentylcyclohexyl)benzene (8).[42] A suspension of **7** (2.85 g, 12.5 mmol) and 10 % Pd/C (0.29 g) in EtOH (20 mL) was vigorously stirred for 4 h at room temperature under a hydrogen atomosphere with a slightly positive pressure. The resulting mixture was filtered through a pad of Celite, and the filtrate was concentrated *in vacuo*. The obtained *cis–trans* mixture was dissolved in DMF (10 mL) containing potassium *tert*-butoxide (7.29 g, 65.0 mmol) and the solution was stirred for 2.5 h at room temperature. The resulting solution was diluted with EtOAc and then poured into a saturated NH_4Cl aqueous solution. The organic phase was separated and the aqueous phase was extracted with EtOAc. The combined organic extracts were washed with brine, dried over anhydrous $MgSO_4$, filtered through a pad of Celite, and concentrated under reduced pressure. The residue was purified by flash column chromatography on silica gel (eluent: hexane) followed by GPC to yield *trans* isomer **8** (2.05 g, 8.90 mmol) in a yield of 71 % as a colorless liquid. ^{1}H NMR (400 MHz, $CDCl_3$): δ = 7.27–7.09 (m, 5H), 2.47–2.41 (m, 1H), 1.86–0.94 (m, 17H), 0.89 (t, J = 6.8 Hz, 3H); ^{13}C NMR (100 MHz, $CDCl_3$): δ = 147.8 (s), 128.2 (s), 126.8 (s), 125.8 (s), 44.7 (s), 37.4 (s), 37.3 (s), 34.4 (s), 33.6 (s), 32.3 (s), 26.7 (s), 22.8 (s), 14.2 (s).

1-Iodo-4-(*trans*-4-pentylcyclohexyl)benzene (9). A mixture of compound **8** (20.2 g, 87.5 mmol), iodine (8.88 g, 17.5 mmol), and $KIO_4{\cdot}2H_2O$ (3.99 g, 17.5 mmol) was added in a solution of acetic acid (100 mL), water (20 mL), and H_2SO_4 (3.0 mL). The reaction solution was stirred for 10 h at 80 °C and then cooled to room temperature. The mixture was poured into water (500 mL), neutralized with NaOH, and extracted with hexane 4 times. The combined organic extracts were washed with brine. The resulting organic phase was dried over anhydrous $MgSO_4$, filtered through a pad of Celite, and concentrated under reduced pressure. The viscous liquid was recrystallized from ethanol twice to produce **9** (27.8 g, 77.8

mmol) in a yield of 89 % as a colorless crystal. ^{1}H NMR (400 MHz, $CDCl_3$): δ = 7.59 (d, J = 8.3 Hz, 2H), 6.96 (d, J = 8.3 Hz, 2H), 2.44–2.36 (m, 1H), 1.86–1.84 (m, 4H), 1.44–0.97 (m, 13H), 0.89 (t, J = 6.8 Hz, 3H); ^{13}C NMR (100 MHz, $CDCl_3$): δ = 147.5 (s), 137.2 (s), 129.0 (s), 90.7 (s), 44.2 (s), 37.3 (s), 37.2 (s), 34.2 (s), 33.4 (s), 32.2 (s), 26.6 (s), 22.7 (s), 14.1 (s). IR (KBr): 2920, 2850, 1484, 1464, 1399, 1370, 1064, 1004, 970, 896, 825, 803, 770, 724, 709, 661 cm^{-1}.

1-Ethoxy-2,3-difluorobenzene (10). A DMF (5 mL) suspension of 2,3-difluorophenol (0.747 g, 5.75 mmol), ethyl bromide (1.88 g, 17.2 mmol), and K_2CO_3 (2.76 g, 20.0 mmol) was vigorously stirred for 3 h at 60 °C. The reaction mixture was poured into a sat. NH_4Cl aqueous solution and extracted with hexane three times. The combined organic extracts were washed with brine. The resulting organic phase was dried over anhydrous $MgSO_4$, filtered through a pad of Celite, and concentrated under reduced pressure. The residue was purified by flash column chromatography on silica gel (eluent: hexane/EtOAc = 10/1) to give **10** (0.59 g, 3.73 mmol) in a yield of 65 % as a colorless liquid. ^{1}H NMR (400 MHz, $CDCl_3$): δ = 6.99–6.93 (m, 1H), 6.77–6.70 (m, 2H), 4.10 (q, J = 6.8 Hz, 2H), 1.45 (t, J = 6.8 Hz, 1H); ^{13}C NMR (100 MHz, $CDCl_3$): δ = 151.4 (dd, J = 245, 11 Hz), 148.6 (dd, J = 7, 3 Hz), 141.3 (dd, J = 245, 14 Hz), 123.1 (dd, J = 5, 9 Hz), 109.6 (d, J = 3 Hz), 108.8 (d, J = 17 Hz), 65.2 (s), 14.6 (s). IR (KBr): 2990, 2593, 1517, 1474, 1074, 766 cm^{-1}.

4-Ethoxy-2,3-difluorophenylboronic acid (11). A flame-dried two neck flask containing **10** (9.66 g, 61.1 mmol) dissolved in dry THF (100 mL) was cooled to −78 °C using an acetone-dry ice bath under an argon atmosphere. To the solution, a hexane solution of n-butyl lithium (1.54 mol L^{-1}, 48 mL, 74 mmol) was slowly added dropwise over 20 min at

−78 °C. After stirring the mixture for 3 h at the same temperature, trimethyl borate ($B(OCH_3)_3$) (13.7 mL, 122 mmol) was added dropwise at −78 °C. The reaction mixture was warm to room temperature and stirred for 5 h. To the resulting suspension, an aqueous 10 % HCl (100 mL) was added and the colorless solution was stirred at room temperature for 3 h. The organic phase was separated, and the aqueous phase was extracted with diethyl ether three times. The combined organic extracts were washed with water and a sat. NaCl aq. solution, dried over $MgSO_4$, and filtered. The solvent was removed *in vacuo*, and the residue was purified by flash column chromatography (eluent: hexane/EtOAc = 3/1) to give **11** (10.7 g, 53.0 mmol) in a yield of 87 % as a white solid. ^{1}H NMR (400 MHz, $CDCl_3$/DMSO-d_6 = 10/1 vol.): δ = 7.45–7.40 (m, 1H), 6.78–6.74 (m, 1H), 4.14 (q, J = 6.8 Hz, 2H), 1.45 (t, J = 7.6 Hz, 3H); ^{13}C NMR (100 MHz, $CDCl_3$): δ = 154.3 (dd, J = 245, 10Hz), 149.3 (dd, J = 8, 4 Hz), 141.0 (s), 138.4 (d, J = 16 Hz), 129.3 (dd, J = 10, 5 Hz), 108.3 (d, J = 3 Hz), 64.2 (s), 13.9 (s). IR (KBr): 3323, 2990, 2593, 1624, 1520, 1469, 1358, 1300, 1223, 1110, 1077, 1038, 1003, 904, 813, 789, 745, 789, 662 cm^{-1}.

1-Ethoxy-2,3-difluoro-4-[4-(*trans*-4-pentylcyclohexyl)phenyl]benzene (12). A mixture of **9** (2.00 g, 5.61 mmol) and **11** (1.25 g, 6.19 mmol), Na_2CO_3 (3.00 g, 28.3 mmol), and tetrakis(triphenylphosphine)palladium, $Pd(PPh_3)_4$ (0.65 g, 0.56 mmol) were added to a heterogeneous mixture of benzene (20 mL), ethanol (20 mL), and water (20 mL). The mixture was vigorously stirred and refluxed under an Ar atmosphere for 3 h. After cooling to room temperature, the organic layer was separated and the aqueous solution was extracted with ethyl acetate. The combined organic solution was washed with a $NaHSO_3$ aqueous solution and brine. The resulting organic phase was dried over anhydrous $MgSO_4$, filtered and the solvent was removed under reduced pressure. The residue was recrystallized from ethanol and

purified by column chromatography (eluent: hexane/EtOAc = 10/1) to give **12** (2.03 g, 5.25 mmol) in a yield of 94 % as a colorless solid. ^{1}H NMR (400 MHz, $CDCl_3$): δ = 7.43 (dd, *J* = 8.2, 2.0 Hz, 2H), 7.28 (d, *J* = 8.4 Hz, 2H), 7.05–7.10 (m, 1H), 6.77–6.82 (m, 1H), 4.56–4.62 (m, 1H), 2.47–2.52 (m, 1H), 1.01–1.95 (m, 23H), 0.90 (t, *J* = 7.1 Hz, 3H).

2,3-Difluoro-4-[4-(*trans*-4-pentylcyclohexyl)phenyl]phenol (13). To the solution of **12** (2.23 g, 5.57 mmol) in CH_2Cl_2 (200 mL) at 0 °C, 8.0 mL (8.0 mmol) of 1.0 M solution of BBr_3 in CH_2Cl_2 was slowly added. After 5 min, the solution was warmed to room temperature and stirred for additional 30 min. The solution was quenched with 2-propanol and water. The organic layer was separated and the aqueous solution was extracted with chloroform. The combined organic solution was washed with brine and dried over $MgSO_4$. The solvent was removed under reduced pressure and the residue was purified by using flash column chromatography (eluent: hexane/EtOAc = 5/1) and recrystallization from hexane to give **13** (1.76 g, 4.91 mmol) in a yield of 88 % as colorless needles. ^{1}H NMR (400 MHz, $CDCl_3$): δ = 7.42 (dd, *J* = 8.2, 2.0 Hz, 2H), 7.28 (d, *J* = 8.4 Hz, 2H), 7.04–7.11 (m, 1H), 6.80–6.87 (m, 1H), 5.22 (d, *J* = 4.0 Hz, 1H), 2.45–2.56 (m, 1H), 1.86–1.95 (m, 4H), 1.04–1.45 (m, 13H), 0.90 (t, *J* = 7.1 Hz, 3H). IR (KBr): 3433, 2917, 2848, 1636, 1497, 1476, 1446, 1331, 1204, 1091, 1023, 894, 834, 813, 726, 680 cm^{-1}.

Syntheses of Compounds 1a–c. Racemic comound **1a** was obtained by the Mitsunobu etherification[43] of **13** with **14**, followed by cleavage of the acetonide protecting group by acidic hydrolysis. To produce **1b** or **1c**, compound **13** was etherified with 6-chlorohexane-1-ol or 1-bromohexane in the presence of potassium carbonate, as shown in scheme 2–2.

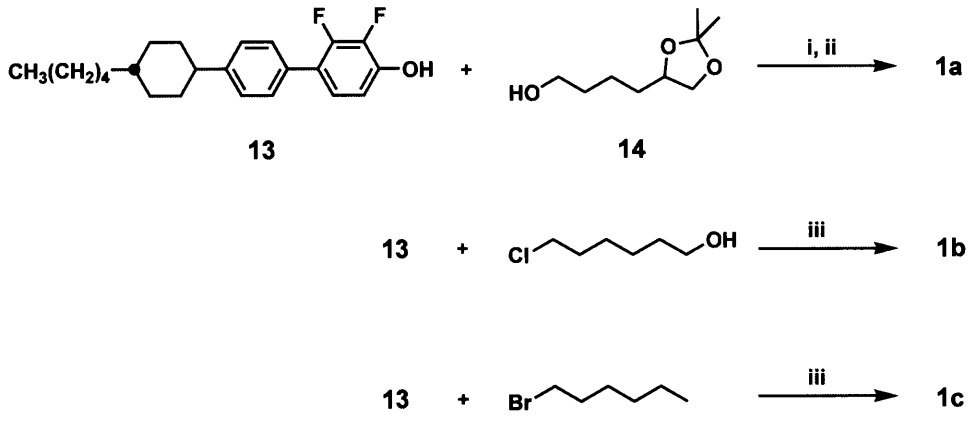

Scheme 2–2. Synthesis of mesogenic molecules **1a–c**.
i) PPh_3, DEAD, toluene, 0°C-rt.; ii) *p*-toluenesulfonic acid monohydrate, EtOH, reflux; iii) K_2CO_3, tetrabutylammnonium iodide, DMF, 70 °C.

2,2-Dimethyl-4-(4-hydoroxybutyl)dioxolane (14). To a solution of 1,2,6-hexanetriol (8.00 g, 59.6 mmol) in acetone (100 mL), *p*-toluenesulfonic acid monohydrate (0.88 g, 5.1 mmol) was added and the reaction mixture was stirred for 24 h at room temperature. After removal of the solvent, the residue was purified by flash chromatography (eluent: $CHCl_3$/MeOH = 10/1) to produce racemic **16** (9.82 g, 56.3 mmol) in a yield of 94 % as a colorless liquid. ^{1}H NMR (400 MHz, $CDCl_3$): δ = 4.14–4.02 (m, 2H), 3.61 (t, J = 6.8 Hz, 2H), 3.51 (t, J = 7.2 Hz, 1H), 3.21 (s, 1H), 1.71–1.44 (m, 6H), 1.40 (s, 3H), 1.35 (s, 3H); ^{13}C NMR (100 MHz, $CDCl_3$): δ = 108.4, 75.8, 69.1, 61.9, 33.0, 32.3, 26.6, 25.4, 21.8.

6-{2,3-Difluoro-4-[4-(*trans*-4-pentylcyclohexyl)phenyl]phenyloxy}hexane-1,2-diol (1a). To a solution of **13** (0.250 g, 0.701 mmol), **14** (0.159 g, 0.918 mmol), and triphenylphosphine (PPh_3) (0.258 g, 0.982 mmol) in dry toluene (10 mL), a 40 % toluene solution of diethylazodicarboxylate (DEAD) (0.64 mL, 1.40 mmol) was added dropwise over 15 min to the stirred mixture at 0 °C, and the reaction mixture was stirred for an additional 10 h at room temperature. Then the solvent was evaporated and the residue was dissolved in hexane. An insoluble triphenylphosphine oxide was filtered off through a pad of Celite and the solvent was evaporated. The residue was dissolved in the mixture of EtOH (50 mL), water (2 mL), and *p*-toluenesulfonic acid monohydrate (1.00 g, 5.26 mmol). The solution was refluxed for 3 h. After removal of the solvent under reduced pressure, the residue was dissolved in $CHCl_3$ (50 mL) and washed with brine. The resulting organic phase was dried over anhydrous Na_2SO_4, filtered, and evaporated under reduced pressure. The residue was purified by flash column chromatography on silica gel (eluent: $CHCl_3$/MeOH = 50/1) and recrystallization from hexane/EtOAc to give **1a** (0.296 g, 0.624 mmol) in a yield of 89 % as a white needles. Phase transition temperature/°C Cr 79 Col 210 I; ^{1}H NMR (400 MHz, $CDCl_3$) δ = 7.43 (d, J = 7 Hz, 2H), 7.28 (d, J = 8 Hz, 2H), 7.06–7.11 (m, 1H), 6.76–6.80 (m, 1H), 4.09 (t, J = 6 Hz, 2H), 3.77 (m, 1H), 3.68 (m, 1H), 3.48 (m, 1H), 2.50 (tt, J = 3, 12 Hz, 1H), 0.94–1.94 (m, 27H), 0.87 (t, J = 7 Hz, 3H). ^{13}C NMR (100 MHz, $CDCl_3$): δ = 148.8 (dd, J = 247, 11 Hz), 147.4 (s), 147.4 (dd, J = 8, 3 Hz), 141.7 (dd, J = 245, 15 Hz), 132.2 (s), 128.5 (d, J = 3 Hz), 127.0 (s), 123.5 (dd, J = 4, 4 Hz), 123.1 (d, J = 11 Hz), 109.4 (d, J = 3 Hz), 72.1 (s), 69.6 (s), 66.7 (s), 44.3 (s), 37.4 (s), 37.3 (s), 34.3 (s), 33.6 (s), 32.7 (s), 32.2 (s), 29.1 (s), 26.6 (s), 22.7 (s), 22.1 (s), 14.1 (s). IR (KBr): 3338, 2921, 2848, 1633, 1508, 1471, 1317, 1200, 1105, 1078, 895, 804 cm^{-1}. Elemental Analysis Calcd. for $C_{29}H_{40}F_2O_3$: C, 73.39; H, 8.49 %. Found: C, 72.99, H, 8.49 %.

6-{2,3-difluoro-4-[4-(*trans*-4-pentylcyclohexyl)phenyl]phenyloxy}hexane-1-ol (1b). A DMF (5 mL) suspension of **13** (0.500 g, 1.40 mmol), 6-chlorohexane-1-ol (0.248 g, 1.81 mmol), tetrabutylammonium iodide (0.067 g, 0.181 mmol), and K_2CO_3 (0.96 g, 6.97 mmol) was vigorously stirred for 5 h at 70 °C. The reaction mixture was poured into a sat. NH_4Cl aqueous solution and extracted with EtOAc three times. The combined organic extracts were washed with brine. The resulting organic phase was dried over anhydrous $MgSO_4$, filtered through a pad of Celite, and concentrated under reduced pressure. The residue was purified by flash column chromatography on silica gel (eluent: CH_2Cl_2/MeOH = 10/1) and recrystallization from hexane to give **1b** (0.634 g, 1.38 mmol) in a yield of 99 % as a colorless solid. Phase transition temperature/°C Cr 79 S_A 149 N 159 I; ^{1}H NMR (400 MHz, $CDCl_3$) δ = 7.43 (d, *J* = 7 Hz, 2H), 7.28 (d, *J* = 8 Hz, 2H), 7.06-7.11 (m, 1H), 6.76–6.80 (m, 1H), 4.09 (t, *J* = 6 Hz, 2H), 3.77 (m, 1H), 3.68 (m, 1H), 3.48 (m, 1H), 2.50 (tt, *J* = 12, 3 Hz, 1H), 0.94-1.94 (m, 27H), 0.87 (t, *J* = 7 Hz, 3H). ^{13}C NMR (100 MHz, $CDCl_3$): δ = 148.8 (dd, *J* = 247, 11 Hz), 147.4 (dd, *J* = 8, 3 Hz), 147.3 (s), 141.7 (dd, *J* = 245, 15 Hz), 132.2 (s), 128.5 (d, *J* = 3 Hz), 127.0 (s), 123.4 (dd, *J* = 4, 4 Hz), 122.9 (d, *J* = 11 Hz), 109.4 (d, *J* = 3 Hz), 69.7 (s), 62.9 (s), 44.3 (s), 37.4 (s), 37.3 (s), 34.3 (s), 33.6 (s), 32.6 (s), 32.2 (s), 29.1 (s), 26.6 (s), 25.7 (s), 25.5 (s), 22.7 (s), 14.1 (s). IR (KBr): 3338, 2921, 2853, 1636, 1508, 1470, 1320, 1199, 1106, 1089, 894, 803 cm^{-1}. Elemental Analysis Calcd. for $C_{29}H_{40}F_2O_2$: C, 75.95; H, 8.79. Found: C, 75.37, H, 8.72.

6-{2,3-difluoro-1-hexyloxy-4-[4-(*trans*-4-pentylcyclohexyl)phenyl]benzene (1c). A DMF (5 mL) suspension of **13** (0.200 g, 0.558 mmol), 1-bromohexane (0.111 g, 0.670 mmol), tetrabutylammonium iodide (0.025 g, 0.068 mmol), and K_2CO_3 (0.386 g, 2.79 mmol) was vigorously stirred for 5 h at 70 °C. The reaction mixture was poured into a sat. NH_4Cl

aqueous solution and extracted with EtOAc three times. The combined organic extracts were washed with brine. The resulting organic phase was dried over anhydrous $MgSO_4$, filtered through a pad of Celite, and concentrated under reduced pressure. The residue was purified by flash column chromatography on silica gel (eluent: hexane/EtOAc = 10/1) and recrystallization from hexane to give **1c** (0.247 g, 0.558 mmol) in a quantitative yield as a colorless needles. Phase transition temperature/°C Cr 10 S_C 43 S_A 119 N 144 I; ^{1}H NMR (400 MHz, $CDCl_3$) δ = 7.43 (d, *J* = 7 Hz, 2H), 7.28 (d, *J* = 8 Hz, 2H), 7.06–7.11 (m, 1H), 6.76–6.80 (m, 1H), 4.09 (t, *J* = 6 Hz, 2H), 2.50 (tt, *J* = 3, 12 Hz, 1H), 0.88–1.96 (m, 22H). ^{13}C NMR (100 MHz, $CDCl_3$): δ = 148.8 (dd, *J* = 248, 11 Hz), 147.6 (dd, *J* = 8, 3 Hz), 147.3 (s), 141.7 (dd, *J* = 245, 15 Hz), 132.3 (s), 128.6 (d, *J* = 3 Hz), 127.0 (s), 123.4 (dd, *J* = 4, 4 Hz), 122.9 (d, *J* = 11 Hz), 109.4 (d, *J* = 2 Hz), 69.9 (s), 44.3 (s), 37.4 (s), 37.3 (s), 34.3 (s), 33.6 (s), 32.2 (s), 31.5 (s), 29.1 (s), 26.6 (s), 25.5 (s), 22.7 (s), 22.6 (s), 14.1 (s), 14.0 (s). IR (KBr): 2924, 2853, 1634, 1506, 1470, 1313, 1298, 1200, 1106, 1077, 894, 803 cm^{-1}. Elemental Analysis Calcd. for $C_{29}H_{40}F_2O$: C, 78.69; H, 9.11. Found: C, 78.91, H, 9.19.

1-Ethyl-3-methylimidazolium tetrafluoroborate (2). Ionic liquid **2** was synthesized according to the reported procedure.[44,45] A solution of fleshly distilled *N*-methylimidazole (3.16 g, 38.5 mmol) and iodoethane (6.01 g, 38.5 mmol) in toluene (10 mL) was stirred for 3 h at 80 °C and cooled to room temperature. The resulting crystal was washed with Et_2O (20 mL, 10 times) and dried in vacuo to give 1-ethyl-3-methlimidazolium iodide (9.09 g, 38.2 mmol) in a yield of 99 % as a precursor of the tetrafluoroborate salt. Tetrafluoroboric acid (5.50 mL, 21.5 mmol, 48 % aqueous solution) was added slowly to a vigorously stirred suspension of silver (I) oxide (Ag_2O) (2.32 g, 10.0 mol) in water (15 mL) at room temperature. The reaction mixture was covered with aluminium foil to prevent photodegradation and

stirred for a further 2 h until the Ag_2O had completely reacted to give a colorless solution. A solution of the iodide salt (5.00 g, 21.0 mmol) in water (5 mL) was added to the reaction mixture and stirred at room temperature for 3 h. The resulting yellow-green precipitate of silver iodide was removed by filtration with Celite and the solvent was evaporated under reduced pressure. The residue was washed with Et_2O (20 mL, 5 times) and purified by using flash column chromatography (eluent: CH_2Cl_2/MeOH = 10/1) to give the tetrafluoroborate salt (3.95 g, 20.0 mmol) as a colorless liquid in a yield of 95 %. ^{1}H NMR (400 MHz, $CDCl_3$/DMSO-d_6 = 10/1 vol.): δ = 8.79 (s, 1H), 7.48 (s, 1H), 7.44 (s, 1H), 4.24 (q, J = 7.6 Hz, 2H), 3.92 (s, 1H), 1.52 (t, J = 7.2 Hz, 3H); ^{13}C NMR (100 MHz, $CDCl_3$/DMSO-d_6 = 10/1 vol.): δ = 135.3, 123.2, 121.5, 44.5, 35.5, 14.6. Elemental analysis calcd. for $C_6H_{11}BF_4N_2$: C, 36.40; H, 5.60; N, 14.15 %. Found: C, 36.53; H, 5.81; N: 13.94 %.

6-[4-(*trans*-4-Pentylcyclohexyl)phenoxy]hexane-1,2-diol (3).

4-(*trans*-4-Pentylcyclohexyl)phenol (2.00g, 8.12 mmol) and PPh_3 (3.20 g, 12.2 mmol) were dissolved in dry THF (20 mL). After addition of 1,2-*O*-isopropylidenehexane-1,2,6-triol (1.74 g, 10.0 mmol), the mixture was cooled to 0 °C. At this temperature, DEAD (2.09 g, 12.0 mmol) was added dropwise over 10 min to the stirred mixture, and the solution was stirred for an additional 10 h at room temperature. Then the solvent was evaporated and the residue was dissolved in hexane. An insoluble triphenylphosphine oxide was filtered off through a pad of Celite and the solvent was evaporated. The residue was dissolved in wet EtOH (50 mL, containing 5 % water). After addition of *p*-TsOH·H_2O (1.72 g, 10.0 mmol), the solution was refluxed for 3 h. Removal of the solvent *in vacuo* gave a residue, which was dissolved in EtOAc (50 mL) and washed with water and brine successively. The resulting organic phase was dried over sodium sulfonate, filtered, and evaporated under reduced pressure. The residue

was purified by flash column chromatography on silica gel (eluent: $CHCl_3$/MeOH = 20/1) and recrystallization from hexane to give **3** (2.09 g, 5.77 mmol) in a yield of 71 %. ^{1}H NMR (400 MHz, $CDCl_3$): δ = 7.11 (d, J = 9 Hz, 2H), 6.81 (d, J = 9 Hz, 2H), 3.94 (t, J = 6 Hz, 2H), 3.74 (m, 1H), 3.66 (m, 1H), 3.45 (m, 1H), 2.40 (tt, J = 12, 4 Hz, 1H), 1.01–2.05 (m, 17 H), 0.89 (t, J = 7 Hz, 3H); ^{13}C NMR (100 MHz, $CDCl_3$): δ = 157.0, 140.1, 127.6, 114.2, 72.1, 67.6, 66.7, 43.7, 37.4, 37.3, 34.5, 33.6, 32.8, 32.2, 29.2, 26.6, 22.7, 22.2, 14.1. Elemental analysis calcd. for $C_{23}H_{38}O_3$: C, 76.20; H, 10.56 %. Found: C, 75.88; H, 10.43 %.

3-(3,4,5-Tridodecyloxybenzoyloxy)propane-1,2-diol (4). A solution of 3,4,5-tridodecyloxybenzoic acid (2.50 g, 3.70 mmol), 2,2-dimethyl-1,3-dioxolan-4-methanol (0.53 g, 4.01 mmol), 1-ethyl-3-(3-dimethylaminopropyl)carbodiimide hydrochloride (EDC) (0.769 g, 4.01 mmol), and 4-dimethylaminopyridine (DMAP) (5 mg, 0.04 mmol) in dry CH_2Cl_2 (10 mL) was stirred for 3 h at room temperature. The reaction mixture was poured into a sat. NH_4Cl aqueous solution and the products were extracted with EtOAc. The solvent was evaporated. The residue was dissolved in wet EtOH (50 mL, containing 5 % water). After addition of *p*-TsOH·H_2O (1.72 g, 10.0 mmol), the solution was refluxed for 3 h. After removal of the solvent under reduced pressure, the residue was dissolved in EtOAc (50 mL) and washed with water and brine, successively. The resulting organic phase was dried over sodium sulfonate, filtered, and evaporated *in vacuo*. The residue was purified by flash column chromatography on silica gel (eluent: $CHCl_3$/MeOH = 20/1) and recrystallization from hexane to give **4** (1.81 g, 2.41 mmol) in a yield of 65 %. Phase transition temperature/°C: Cr_1 42 Cr_2 48 Cub 69 I (first heating on DSC); ^{1}H NMR (400 MHz, $CDCl_3$): δ = 7.25 (s, 2 H), 4.47–4.36 (m, 2 H), 4.13–3.93 (m, 7 H), 3.80–3.72 (m, 1 H), 3.71–3.63 (m, 1 H), 2.80 (d, J = 4.9 Hz, 1 H), 2.35 (t, J = 6.3 Hz, 1 H), 1.87–1.70 (m, 6 H), 1.56–1.20 (m, 54 H), 0.88 (t, J = 6.8 Hz,

9H); ^{13}C NMR (100 MHz, $CDCl_3$): δ = 166.9, 152.8, 142.7, 123.9, 108.1, 73.5, 70.3, 69.2, 65.7, 63.3, 31.89, 31.88, 30.3, 29.71, 29.68, 29.67, 29.65, 29.63, 29.60, 29.5, 29.37, 29.36, 29.33, 29.26, 26.05, 26.00, 22.65, 14.1. IR (KBr): 3394, 2919, 2850, 1712, 1587, 1503, 1469, 1431, 1389, 1338, 1254, 1220, 1120, 859, 762, 721 cm^{-1}. Elemental analysis calcd. for $C_{46}H_{84}O_7$: C, 73.75; H, 11.30 %. Found: C, 74.09; H, 11.20 %.

1-Butyl-3-methylimidazolium bromide (5). A solution of fleshly distilled *N*-methylimidazole (8.04 g, 97.9 mmol) and 1-bromobutane (13.5 g, 98.5 mmol) in toluene (10 mL) was vigorously stirred for 3 h at 80 °C and cooled to room temperature. The resulting crystal was washed with Et_2O (20 mL, 10 times). A pure compound **5** as a white crystal (20.5 g, 93.6 mmol) was obtained by recrystallization from acetone three times in a yield of 96 %. This salt becomes a viscous supercooled liquid on cooling from the isotropic melt. mp = 81 °C. ^{1}H NMR (400 MHz, $CDCl_3$): δ = 10.40 (s, 1 H), 7.62 (s, 1 H), 7.61 (s, 1H), 4.35 (t, *J* = 7.2 Hz, 2H), 4.14 (s, 3H), 1.96–1.88 (m, 2H), 1.44–1.35 (m, 2H), 0.97 (t, *J* = 8.0 Hz, 3H); ^{13}C NMR (100 MHz, $CDCl_3$): δ = 137.2, 123.6, 121.9, 49.7, 36.6, 32.0, 19.3, 13.3. IR (KBr): 3080, 2961, 1572, 1465, 1170, 849, 754, 623 cm^{-1}. Elemental analysis calcd. for $C_8H_{15}BrN_2$: C, 43.85; H, 6.90 %. Found: C, 43.65; H, 6.89 %.

1-Butyl-3-methylimidazolium tetrafluoroborate (6). Ionic liquid **6** was synthesized according to the reported procedure.[46] To a stirred solution of **5** (3.23 g, 14.7 mmol) in MeOH (20 mL), tetrafluoroboric acid (2.86 g, 14.7 mmol) was slowly added at room temperature. The reaction mixture was stirred for 3 h. After removal of the solvent under reduced pressure, the residue was dried at 50 °C *in vacuo*. The residue was purified by flash column chromatography on silica gel (eluent: $CHCl_3$/MeOH = 50/1) to give **6** (2.64 g, 11.7 mmol) as

a colorless liquid in a yield of 80 %. mp = 15 °C. ^{1}H NMR (400 MHz, $CDCl_3$/DMSO-d_6 = 10/1 vol.): δ = 9.27 (s, 1 H), 8.12 (s, 1 H), 7.75 (s, 1H), 4.25 (t, J = 7.2 Hz, 2H), 3.97 (s, 3H), 1.88–1.84 (m, 2H), 1.39–1.34 (m, 2H), 0.98 (t, J = 8.0 Hz, 3H); ^{13}C NMR (100 MHz, $CDCl_3$/DMSO-d_6 = 10/1 vol.): δ = 136.2, 123.4, 122.2, 48.7, 35.7, 31.5, 18.8, 13.1.

Preparation of Ionic Liquid Mixtures. A $CHCl_3$ solution of ionic liquids was added to a requisite amount of a $CHCl_3$ solution of mesogenic molecules. The solvent was removed by slow evaporation, and the resultant mixture was dried under reduced pressure at 25 °C for 5 h.

2.5. References

1. D. Demus, J. W. Goodby, G. W. Gray, H.-W. Spiess, V. Vill, eds., *Handbook of Liquid Crystals*, Wiley-VCH, Weinheim **1998**.
2. P. V. Wright, Y. Zheng, in *Functional Organic and Polymeric Materials* (Eds.: T. H. Richardson), John Wiley & Sons Ltd, Chichester **2000**, Ch.9.
3. G. Ungar, S. V. Batty, V. Percec, J. Heck, G. Johansson, *Adv. Mater. Opt. Electron.* **1994**, *4*, 303.
4. V. Percec, G. Johansson, J. Heck, G. Ungar, S. V. Batty, *J. Chem. Soc., Perkin Trans. 1* **1993**, 1411.
5. U. Beginn, G. Zipp, M. Möller, *Adv. Mater.* **2000**, *12*, 510.
6. L. Brunsveld, J. A. J. M. Vekemans, H. M. Janssen, E. W. Meijer, *Mol. Cryst. Liq. Cryst.* **1999**, *331*, 449.
7. T. Ohtake, M. Ogasawara, K. Ito-Akita, N. Nishina, S. Ujiie, H. Ohno, T. Kato, *Chem. Mater.* **2000**, *12*, 782.
8. C. T. Imrie, M. D. Ingram, G. S. McHattie, *Adv. Mater.* **1999**, *11*, 832.
9. N. Boden, R. J. Bushby, J. Clements, *J. Chem. Phys.* **1993**, *98*, 5920.
10. D. Adam, P. Schuhmacher, J. Simmerer, L. Häussling, K. Siemensmeyer, K. H. Etzbach, H. Ringsdorf, D. Haarer, *Nature* **1994**, *371*, 141.
11. C. F. van Nostrum, R. J. M. Nolte, *Chem. Commun.* **1996**, 2385.
12. M. Funahashi, J. Hanna, *Phys. Rev. Lett.* **1997**, *78*, 2184.
13. T. Welton, *Chem. Rev.* **1999**, *99*, 2071.
14. P. Wasserscheid, W. Keim, *Angew. Chem. Int. Ed.* **2000**, *39*, 3772.
15. L. A. Blanchard, D. Hancu, E. J. Beckman, J. F. Brennecke, *Nature* **1999**, *399*, 28.
16. P. Bonhôte, A.-P. Dias, N. Papageorgiou, K. Kalyanasundaram, M. Grätzel, *Inorg.*

Chem. **1996**, *35*, 1168

17. J. Fuller, R. T. Carlin, R. A. Osteryoung, *J. Electrochem. Soc.* **1997**, *144*, 3881.
18. A. B. McEwen, H. L. Ngo, K. LeCompte, J. L. Goldman, *J. Electrochem. Soc.* **1999**, *146*, 1687.
19. C. J. Bowlas, D. W. Bruce, K. R. Seddon, *Chem. Commun.* **1996**, 1625.
20. K. M. Lee, C. K. Lee, I. J. B. Lin, *Chem. Commun.* **1997**, 899.
21. J. D. Holbrey, K. R. Seddon, *J. Chem. Soc., Dalton Trans.* **1999**, 2133.
22. F. Neve, O. Francescangeli, A. Crispini, J. Charmant, *Chem. Mater.* **2001**, *13*, 2032.
23. J. S. Wilkes, M. J. Zaworotko, *J. Chem. Soc., Chem. Commun.* **1992**, 965.
24. R. Hagiwara, Y. Ito, *J. Fluorine Chem.* **2000**, *105*, 221.
25. T. Nishida, Y. Tashiro, M. Yamamoto, *J. Fluorine Chem.* **2003**, *120*, 135.
26. B. Neumann, C. Sauer, S. Diele, C. Tschierske, *J. Mater. Chem.* **1996**, *6*, 1087.
27. M. Kölbel, T. Beyersdorff, C. Tschierske, S. Diele, J. Kain, *Chem. Eur. J.* **2000**, *6*, 3821.
28. T. Kato, *Struct. Bonding* **2000**, *96*, 95.
29. T. Kato, T. Kawakami, *Chem. Lett.* **1997**, 211.
30. (a) V. Percec, G. Johansson, J. Heck, G. Ungar, S. V. Batty, *J. Chem. Soc., Perkin Trans. 1* **1993**, 1411.
31. C. F. van Nostrum, R. J. M. Nolte, *Chem. Commun.* **1996**, 2385.
32. L. Brunsveld, J. A. J. M. Vekemans, H. M. Janssen, E. W. Meijer, *Mol. Cryst. Liq. Cryst.* **1999**, *331*, 449.
33. U. Beginn, G. Zipp, M. Möller, *Adv. Mater.* **2000**, *12*, 510.
34. R. P. Swatloski, S. K. Spear, J. H. Holbrey, R. D. Rogers, *J. Am. Chem. Soc.* **2002**, *124*, 4974.

35. V. Percec, M. N. Holerca, S. Uchida, W.-D. Cho, G. Ungar, Y. Lee, D. J. P. Yeardley, *Chem. Eur. J.* **2002**, *8*, 1106.

36. K. Borisch, S. Diele, P. Göring, H. Kresse, C. Tschierske, *J. Mater. Chem.* **1998**, *8*, 529.

37. K. Hirose, *J. Inc. Phenom. Macrocyclic Chem.* **2001**, *39*, 193.

38. L. Fielding, *Tetrahedron* **2000**, *56*, 6151.

39. J. D. Holbrey, M. B. Turner, W. M. Reichert, R. D. Rogers, *Green Chem.* **2003**, *5*, 731.

40. H. A. Every, A. G. Bishop, D. R. MacFarlane, G. Orädd, M. Forsyth, *J. Mater. Chem.* **2001**, *11*, 3031.

41. M. Hird, G. W. Gray, K. J. Toyne, *Mol. Cryst. Liq. Cryst.* **1991**, *206*, 187.

42. R. Eidenschink, D. Erdmann, J. Krause, L. Pohl, *Angew. Chem. Int. Ed. Engl.* **1977**, *16*, 100.

43. D. L. Hughes, *Org. React.* **1992**, *42*, 335.

44. A. G. Avent, P. A. Chaloner, M. P. Day, K. R. Seddon, T. Welton, *J. Chem. Soc., Dalton Trans.* **1994**, 3405.

45. J. Fuller, R. T. Carlin, H. C. De Long, D. Haworth, *J. Chem. Soc., Chem. Commun.* **1994**, 299.

46. T. Nishida, Y. Tashiro, M. Yamamoto, *J. Fluorine Chem.* **2003**, *120*, 135.

Chapter 3

One-Dimensional Ion Conduction in Self-Organized Columnar Ionic Liquids

Abstract: New fan-shaped ionic liquids forming columnar liquid crystalline phases have been prepared to obtain one-dimensional ion-transporting materials. The ionic liquids consist of incompatible two parts: an imidazolium-based ionic part as an ion-conducting part and tris(alkyloxy)phenyl parts as insulating parts. Self-assembly of these materials leads to the formation of thermotropic hexagonal columnar liquid crystalline states at room temperature. Anisotropic one-dimensional ionic conductivities have been successfully measured by using the cell having comb-shaped gold electrodes. The self-organized columns have been aligned macroscopically in two directions by shearing perpendicular and parallel to the electrodes. The ionic conductivities parallel to the column axis are higher than those perpendicular to the axis. The incorporation of lithium salts in these columnar materials leads to the enhancement of the ionic conductivities and their anisotropy. Fan-shaped ionic liquids with a different anion size are synthesized. The conductivities increase with the increase in the anion size. These materials would be useful for anisotropic transportation of ions in nanometer scale.

3.1. Introduction

Columnar liquid crystals can be used for one-dimensional transportation of charge, ion, and energy.[1–3] For such functionalization, it is important to control orientation, supramolecular association, and phase-segregation for the columnar assemblies ranging from molecular to macroscopic scales.[1–6] In particular, the formation of self-organized monodomain in macroscopic scale plays key roles for the enhancement of properties. For example, fast charge (electron and hole) transports through columns were achieved for π-conjugated discotic molecules. As for ion-conductive liquid crystals, crown-ethers[2a–c] and oligo(ethylene oxide)s (PEO)[2d] were incorporated into mesogenic molecules to form columnar structures. However, no one-dimensional ionic conductivities in a macroscopic monodomain had been measured for columnar liquid crystalline phases although two-dimensional macroscopic alignment of PEO-containing molecules leads to high two-dimensional ion conduction.[7] Ionic liquids are functional isotropic liquids exhibiting high ionic conductivities.[8] For example, *N,N'*-dialkylimidazolium salts containing perfluoro anions are one of common ionic liquids.[9] Such materials have considerable potentials as electrolytes for batteries and capacitors. Recently, the author has prepared two-dimensional ion-conductive materials formed by self-organization of dihydroxy-functional rodlike molecules and ionic liquids.[10] The design strategy here is to modify ionic liquids to prepare simpler columnar assemblies that exhibit fluid ordered states, maintaining both of high ionic conductivities and liquid crystalline states at room temperature ranges.

Here the author reports a new class of ionic liquids exhibiting fluid self-organized structures. For the first time, one-dimensional ion conduction has been achieved for columnar liquid crystalline materials, which are oriented uniaxially.

3.2. Results and Discussion

3.2.1. Liquid Crystalline Properties

The author has designed fan-shaped imidazolium salts **1a–h** shown in Figure 3–1. These molecules consist of incompatible two parts: an ionic part as an ion-conducting part and a tris(alkyloxy)phenyl part as an insulating and self-organizing part.

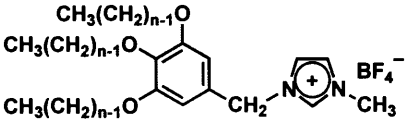

1a: n = 2 **1e:** n = 12
1b: n = 6 **1f:** n = 14
1c: n = 8 **1g:** n = 16
1d: n = 10 **1h:** n = 18

Figure 3–1. Molecular structures of imidazolium tetrafluoroborate salts.

Phase transition behavior of compounds **1a–h** was determined by differential scanning calorimetry (DSC), polarized optical microscopy, and X-ray measurements. Thermal properties of compounds **1a–h** are summarized in Table 3–1. On heating the crystal of **1a** obtained by recrystallization from ethyl acetate solution, it melts at 140 °C to transform into an isotropic liquid. On cooling the **1a** melt, it is vitrified at −10 °C without crystallizing. On the second heating, the amorphous glass changes into the isotropic liquid at −5 °C, the liquid crystallizes at 57 °C, and eventually changes into the isotropic liquid at 140 °C. In contrast, compounds **1b–h** having the longer alkyl chains were found to exhibit enantiotropic hexagonal columnar phases over wide temperature ranges. Interestingly, compounds **1b,c** form glassy columnar liquid crystalline phases below −30 °C. This tendency to form a glassy phase was also observed for conventional ionic liquids. The formation of glassy columnar phases for **1b,c** suggest that the ionic moieties are fluid state like ionic liquids in the liquid crystalline states. These materials are promising candidates as fast ion conductors. The DSC

thermograms of compounds **1b** and **1c**, as representative compounds forming a glassy and crystalline phases below room temperature, are displayed in Figure 3–2.

Table 3–1. Thermal Properties of Compounds **1a–h**.

Compound	Phase transition behavior [a]						
1a (n = 2)	G	−5	I	57 (36.2)	Cr	140 (36.2)	I
1b (n = 6)	G	−35	Col_h	32 (0.4)			I
1c (n = 8)	G	−29	Col_h	133 (1.0)			I
1d (n = 10)	Cr	−10 (6.1)	Col_h	162 (1.2)			I
1e (n = 12)	Cr	17 (29.3)	Col_h	183 (1.3)			I
1f (n = 14)	Cr	82 (61.8)	Col_h	185 (0.9)			I
1g (n = 16)	Cr	74 (42.1)	Col_h	177 (1.5)			I
1h (n = 18)	Cr	88 (87.4)	Col_h	148 (1.1)			I

[a] Transition temperatures (°C) and enthalpies of transition (kJ mol^{-1}, in parentheses) determined by DSC (second heating scan, 10 °C min^{-1}). Col_h: hexagonal columnar; Cr: crystalline; G: glassy; I: isotropic.

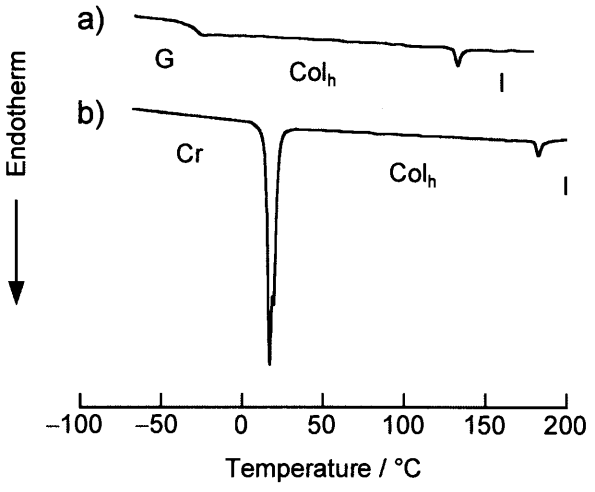

Figure 3–2. DSC thermograms of a) **1c** and b) **1e** on the second heating at a scanning rate of 10 °C min^{-1}. Col_h: hexagonal columnar; Cr: crystalline; G: glassy; I: isotropic.

The X-ray diffraction profiles observed for **1b–h** display a characteristic set of *d*-spacings that match the expected ration of $1:1/\sqrt{3}:1/\sqrt{4}$ (the d_{100}, d_{110}, and d_{200} diffraction planes) for two-dimensional hexagonal array of cylinders. For examples, the X-ray diffraction patterns are shown in Figure 3–3. The intercolumnar distance (a) is calculated to be 3.5 for **1c** and 3.8 nm for **1e** by using the following equation:

$$a = 2\langle d_{110}\rangle/\sqrt{3},\ \langle d_{110}\rangle = (d_{100} + \sqrt{3}d_{110} + \sqrt{4}d_{200})/3$$

The intercolumnar distances increase with the increase in the length of alkyl chains.

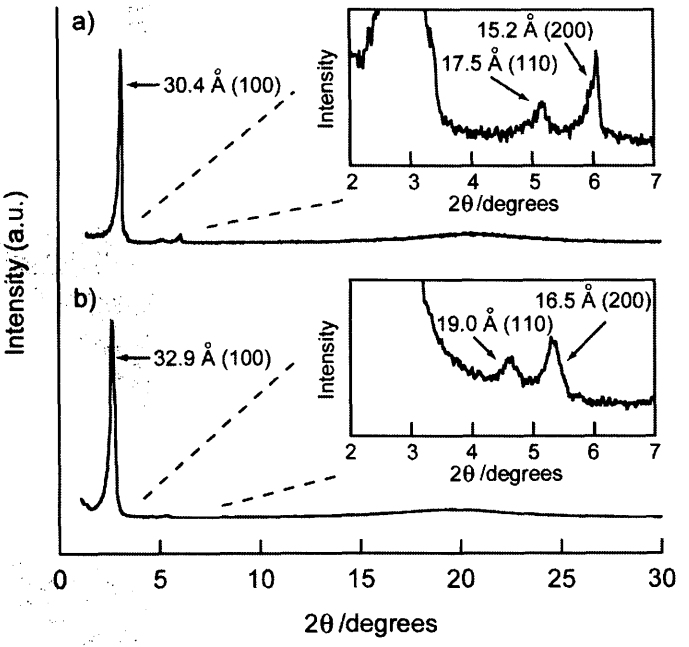

Figure 3–3. WAXD patterns of the Col_h phases of a) **1c** and b) **1e** at 25 °C. Insets indicate the enlarged views of the small-angle region.

3.2.2. Orientation of Columns

Macroscopically homogeneous alignment of the columnar structure is easily achieved by shearing these self-assembled materials. Figure 3–4 shows polarizing microscope images of **1e** in the columnar phases before and after shearing. The formation of monodomain of the column is achieved after the polydomain of the columnar phase is sheared in the sandwiched glasses without rubbing treatment. The oriented structure is uniform over

millimeters. The direction of the long axis of columns corresponds to the shearing direction, which is confirmed by the periodic change in the pattern with the sample's rotation for the polarizing microscopic observation. No birefringence is seen under the crossed Nicols condition when the shearing direction is along the polarizer or analyzer axis. The highest brightness is observed when the oriented sample is in a 45° angle.

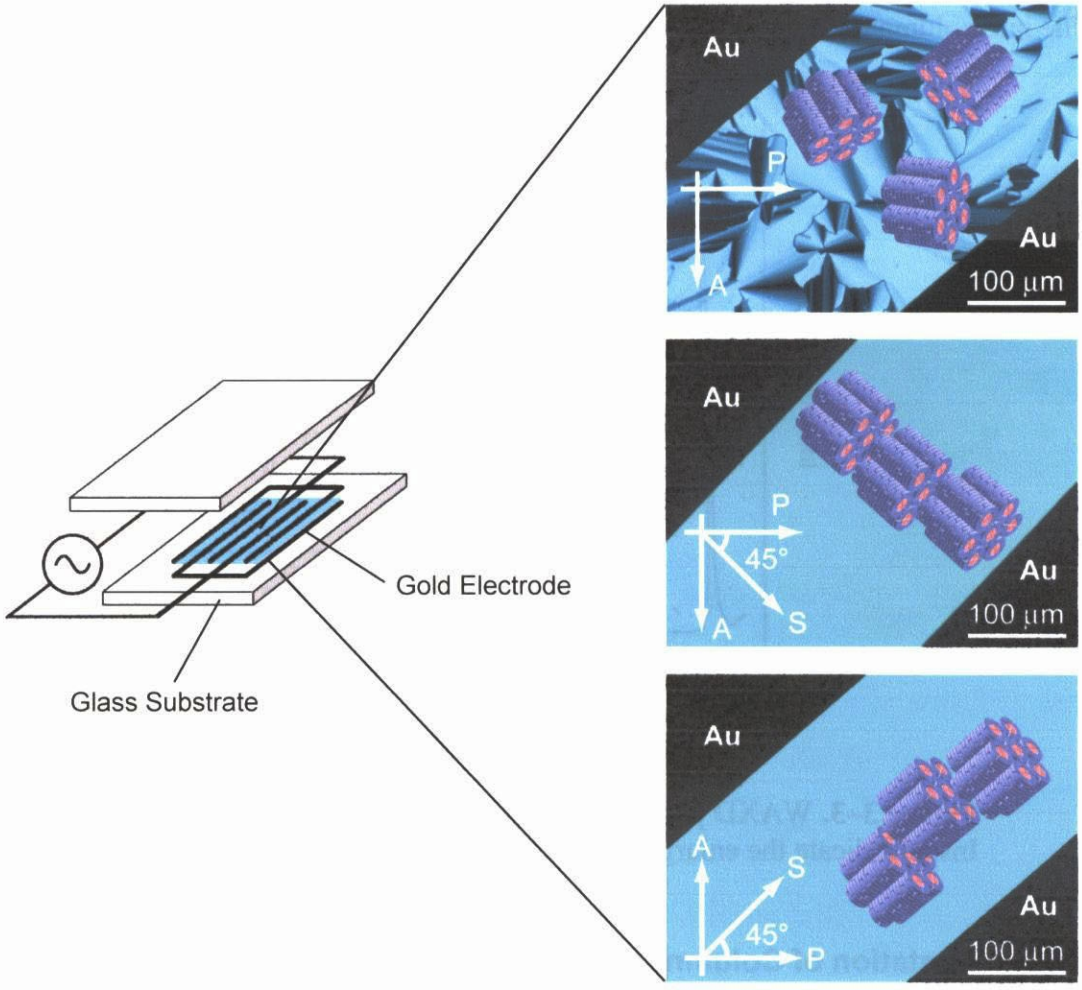

Figure 3–4. Schematic illustration of a glassy cell with comb-shaped gold electrodes with thickness of 0.8 μm for the anisotropic ion-conduction measurements (left). The samples forming the Col_h phases are filled between electrodes. Polarizing optical microscopic images and illustrations of the oriented and self-assembled structures of **1e** in the Col_h state at 25 °C (right). Directions of A: analyzer; P: polarizer; S: shearing.

In addition, the uniaxial orientation of columns by shearing is confirmed by the small-angle X-ray scattering measurements (Figure 3–5).

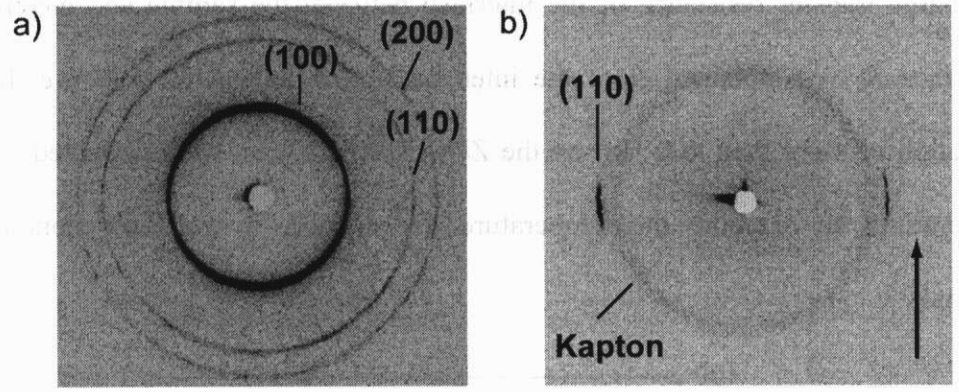

Figure 3–5. 2D SAXS patterns of **1c** in the Col_h state at 25 °C: a) unoriented **1c** and b) oriented **1c** by shearing. An arrow indicates the shearing direction. A halo shown in the figure b) originates from the X-ray scattering from a Kapton film. (100) and (200) diffraction arcs are not observed.

3.2.3. Ion-Conductive Properties

One-dimensional ionic conductivities have been successfully measured with the complex impedance method by the cells having gold comb-like electrodes.[11] The self-organized columns have been aligned in two directions by shearing perpendicular and parallel to the electrodes.

Ionic conductivities (σ) can be obtained from the following equation: $\sigma = d / (R_b A)$, where R_b, d, and A are the bulk resistance, the sample thickness, and the cross sectional area of the electrode, respectively. Ionic conductivities were practically calculated to be the product of $1/R_b$ (Ω^{-1}) times cell constants (cm^{-1}) for comb-shaped gold electrodes, which were calibrated with KCl aqueous solution (1.00 mmol L^{-1}) as a standard conductive solution. The impedance data (Z) were modeled as a connection of two RC circuits in series (R: resistance, C: capacitance) and was divided into real (Z') and imaginary (Z''). A representative example of an impedance spectrum exhibited by **1c** at 100 °C is displayed in

Figure 3–6. The impedance plot shows two distinct processes, a high frequency relaxation attributed to the bulk resistance and an incomplete low frequency relaxation associated with the charge transfer resistance of the interface between the sample and electrode. The bulk resistance R_b was obtained from the intercept of the left semi-circle (*i.e.* high frequency relaxation of more than 400 Hz) on the Z' axis. These data were collected over a range of temperatures to examine the temperature dependence of the ionic conductivity of the materials.

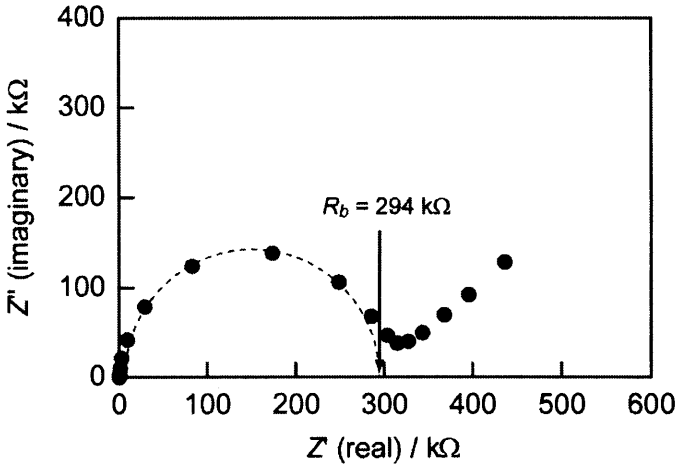

Figure 3–6. Impedance spectrum for **1c** aligned perpendicular to the comb-shaped gold electrode in the columnar state at 100 °C. The cell constant is 47.6 cm^{-1}. The bulk resistance R_b was obtained from the intercept of the left semi-circle on the Z' axis.

Figure 3–7 shows anisotropic ionic conductivities of the self-organized materials of **1c** and **1e** forming monodomains as a function of temperature. Anisotropic one-dimensional ionic conductivities have been successfully measured for supramolecular liquid crystalline materials. The ionic conductivities parallel to the columnar axis ($\sigma_{||}$) for **1c** and **1e** are higher than those perpendicular to the axis ($\sigma_{\perp}$) because the alkyloxyphenyl parts function as insulating parts. The $\sigma_{||}$ values for **1c** are higher than those of **1e** because the conductivities are calculated based on the whole cross section area of the materials and the area fraction of the

insulating part of **1c** should be smaller than **1e**. The highest conductivity of 4.8×10^{-4} S cm^{-1} ($\sigma_{\parallel}$) is achieved for **1c** at 130 °C in the columnar phase. The anisotropy ($\sigma_{\parallel}/\sigma_{\perp}$) of ionic conductivities is observed to be a constant value of ca. 10 for **1c** in the columnar phase. No anisotropy is observed when the materials form isotropic liquid phases. The ionic conductivities of polydomain samples as a function of temperature are also measured for **1c** and **1e** (Figure 3–8). For compound **1e**, the values of 2.5×10^{-6} S cm^{-1} and 3.1×10^{-5} S cm^{-1} obtained in the polydomain at 100 and 150 °C, respectively, are between the values of $\sigma_{\parallel}$ and $\sigma_{\perp}$ of the oriented samples at the same temperatures.

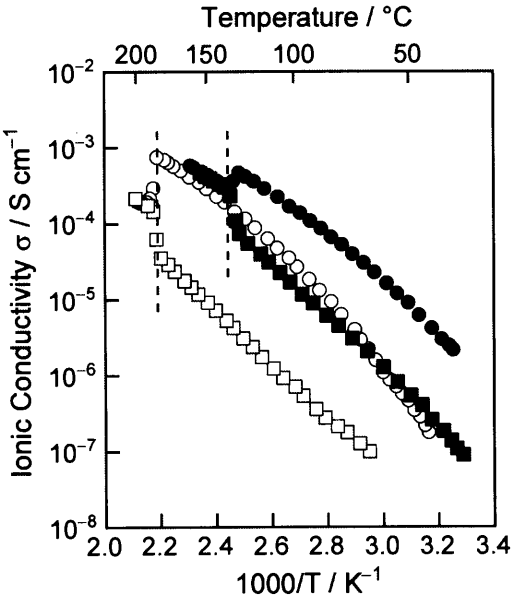

Figure 3–7. Anisotropic ionic conductivities of **1c** and **1e** as a function of temperature: (●) parallel and (■) perpendicular to the columnar axis for **1c**; (○) parallel and (□) perpendicular to the columnar axis for **1e**. The broken lines denote the Col_h–I phase transition temperatures

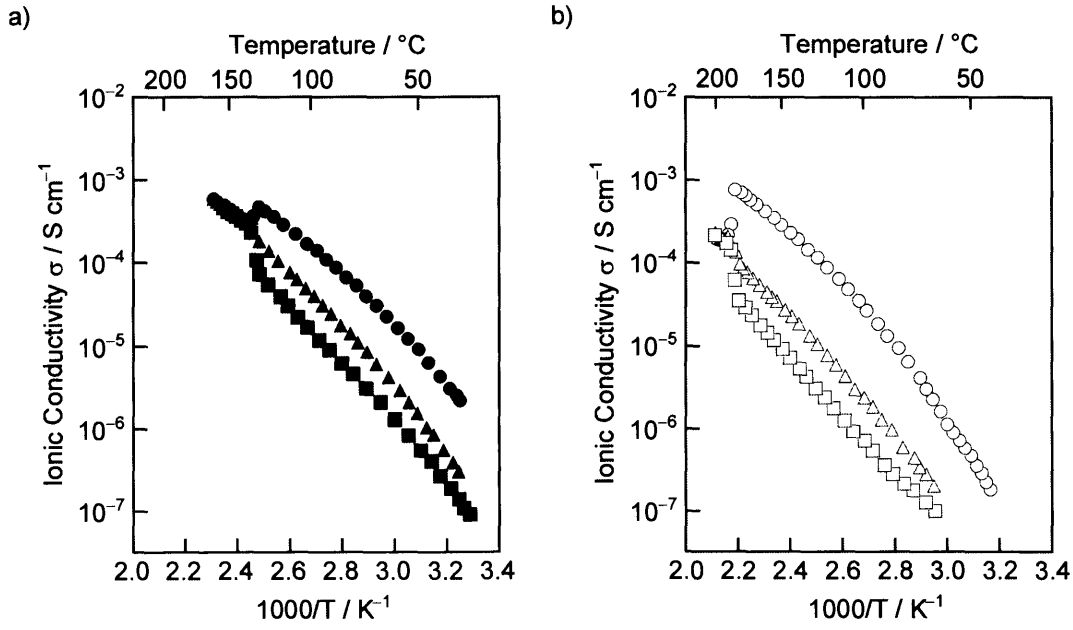

Figure 3–8. Anisotropic ionic conductivities of a) **1c** and b) **1e** as a function of temperature: (●) parallel and (■) perpendicular to the columnar axis for oriented **1c**; (▲) for unoriented sample of **1c**; (○) parallel and (□) perpendicular to the columnar axis for oriented **1e**; (Δ) for unoriented sample of **1e**.

These self-organized columnar ionic liquids can also function as self-organized electrolytes, which dissolve a variety of ionic species. The incorporation of the lithium salts in these columnar materials leads to the enhancement of the ionic conductivities and their anisotropy. For example, columnar material **1e** containing $LiBF_4$ (molar ratio of $LiBF_4$ to **1e**: 0.25) shows the conductivities of 7.5×10^{-5} S cm^{-1} ($\sigma_{\parallel}$), 8.0×10^{-7} S cm^{-1} ($\sigma_{\perp}$), and $\sigma_{\parallel}/\sigma_{\perp}$ of 94 at 100 °C respectively (Figure 3–9), while those of **1e** alone are 3.1×10^{-5} S cm^{-1} ($\sigma_{\parallel}$), 7.5×10^{-7} S cm^{-1} ($\sigma_{\perp}$), and $\sigma_{\parallel}/\sigma_{\perp}$ of 41 at 100 °C, respectively. The existence of the lithium salts increases only the conductivity along the columnar axis ($\sigma_{\parallel}$), which leads to the enhancement of anisotropy. These results suggest that the ions are incorporated in the central ionic part of the column. This approach would enable us to make a variety of ion conductors based on these materials. It should be noted that the addition of the lithium salt enhances the liquid

crystallinity. Phase transition temperatures of the mixtures of **1e** with lithium salt are plotted as a function of mole fraction of the lithium salt in the mixture (Figure 3–10). For example, **1e** incorporating $LiBF_4$ (molar ratio of $LiBF_4$ to **1e**: 0.25) shows the columnar phase from 17 to 193 °C, while for the single component of **1e**, the columnar phase is observed from 17 to 183 °C. The ionic columnar core in the liquid crystalline phase is stabilized by the existence of the metal salt.

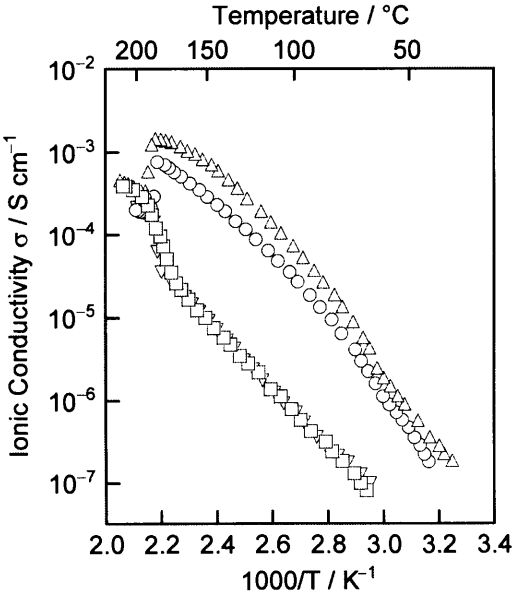

Figure 3–9. Anisotropic ionic conductivities of **1e** alone and complex of **1e** and $LiBF_4$ (molar ratio of $LiBF_4$ to **1e**: 0.25): (△) parallel and (▽) perpendicular to the columnar axis for the oriented complex.

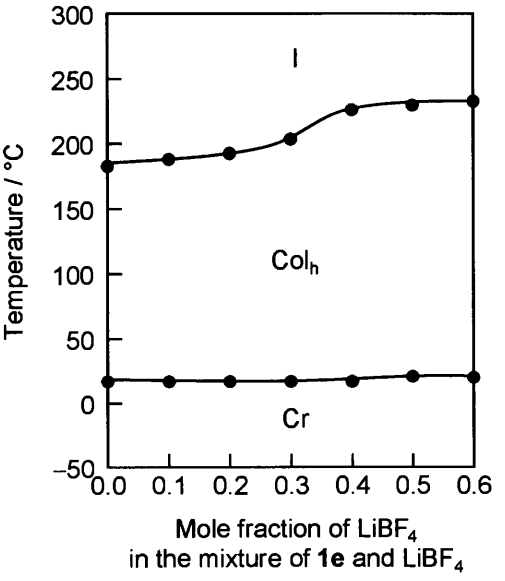

Figure 3–10. Phase transition behavior for a mixture of **1e** and $LiBF_4$. Compound **1e** and $LiBF_4$ are miscible up to the mole fraction of 0.6 for $LiBF_4$ in the mixture.

3.2.4. Effects of Anion Species on Ionic Conductivities

In the former section, the author designed new imidazolium salts that self-assemble into columnar structures. In this system, only anion can migrate in the center of columns because the cation is immobilized on the insulating part. It is considered that ionic conductivities can be improved by changing the anion species. To examine the effects of

anion species on ionic conductivities, the author prepared fan-shaped imidazolium salts **IL(X^-)** containing a hexafluorophosphate anion [PF_6^-], trifluoromethanesulfonate anion [$CF_3SO_3^-$], and bis(trifluoromethanesulfonyl)imide anion [$(CF_3SO_2)_2N^-$] as shown in Figure 3–11. These fluorinated anions are used for the preparation of ionic liquids with low viscosity and high ionic conductivity.

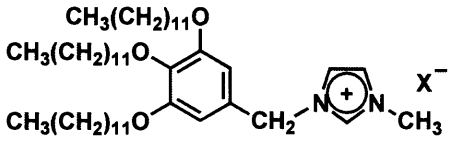

IL(X^-)

X^- = BF_4^-, PF_6^-, $CF_3SO_3^-$, $(CF_3SO_2)_2N^-$

Figure 3–11. Molecular structures of fan-shaped imidazolium salts containing fluorinated anions.

Table 3–2. Phase transition behavior of compounds **IL(X^-)**.

Compound	Anion radius (nm)	Phase transition temperature /°C [c]				
IL(BF_4^-)	0.205 [a]	I	183	Col_h	8	Cr
IL(PF_6^-)	0.242 [a]	I	146	Col_h	3	Cr
IL($CF_3SO_3^-$)	0.267 [b]	I	73	Col_h [d]	10	Cr
IL($(CF_3SO_2)_2N^-$)	0.327 [b]	I	–	–	12	Cr

[a]Ref. 38; [b]Ref. 39, van der Waals radius obtained from MM2 and ab initio molecular orbital caluculations. [c]Transition temperatures were determined by DSC measurement on cooling at a scanning rate of 10 °C min^{-1}. [d]Monotropic liquid crystalline phase. Col_h: hexagonal columnar; Cr: crystalline; I: isotropic liquid phase.

Phase transition temperatures of **IL(X^-)** and the anion radius are listed in Table 3–2. Compounds **IL(PF_6^-)** and **IL($CF_3SO_3^-$)** are found to show hexagonal columnar liquid crystalline phases by the X-ray measurements and polarized optical microscope observation (Figure 3–12). For **IL($CF_3SO_3^-$)**, the columnar phase is formed only on cooling. It is difficult to achieve macroscopic orientation of the columns by shearing. On the other hand, no mesomorphic behavior is observed for **IL($(CF_3SO_2)_2N^-$)**. The isotropization temperatures decrease with increase in the size of anion. This can be explained in terms of decreasing of

electrostatic interaction with increasing anion radius and losing a volume balance between ionic and non-ionic parts. For common salts like NaCl, the melting point is dictated by the electrostatic potential which exists between its cations and anions. This electrostatic potential is expressed as their lattice energy $E = kQ_1Q_2/d$. In this equation, k is the Madelung constant, Q_1 and Q_2 are the charges on the ions, and d is the interionic separation. With large ions, d is effectively larger, resulting in a smaller lattice energy and lower melting point.

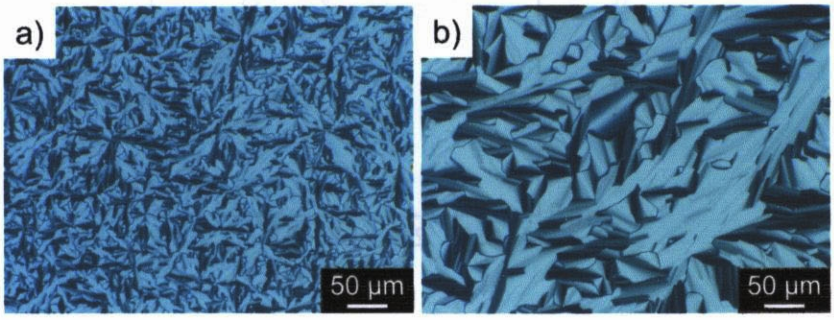

Figure 3–12. Polarized optical micrographs of (a) **IL($CF_3SO_3^-$)** and (b) **IL(PF_6^-)** in the hexagonal columnar phases at 50 °C.

Next, the ionic conductivities of compounds **IL(X^-)** have been measured as a function of temperature (Figure 3–13). As for both compounds **IL(PF_6^-)** and **IL(BF_4^-)**, macroscopic homogeneous orientation is achieved by shearing the material. The conductivities parallel to the columnar axis are shown for these compounds.

The conductivities increase with the increase in the cation size because of easy dissociation of the salts with larger anion. This tendency was also observed for conventional isotropic ionic liquids. It is found that the conductivities for these liquid crystalline salts are affected by changing anion species.

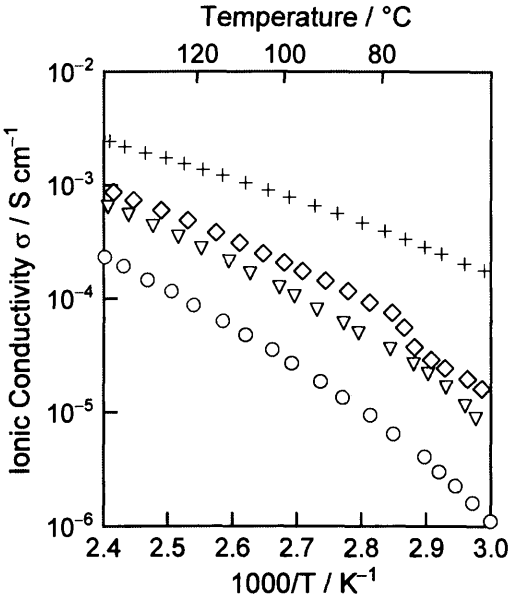

Figure 3–13. Ionic conductivities of **IL(X^-)** as a function of temperature: (+) for **IL($(CF_3SO_2)_2N^-$)**, (◇) for **IL($CF_3SO_3^-$)**, (▽) for **IL(PF_6^-)**, (○) for **IL(BF_4^-)**.

3.3. Conclusions

A family of columnar ionic liquid crystals has been obtained by the chemical derivation of an imidazolium salt forming ionic liquids. Homogeneous alignment of columnar structures is achieved by the application of a shearing force to the materials. These materials showed higher conductivities along the direction of the columnar axis. In addition, the conductivities are improved by changing anion species of the materials. These materials would be useful for transportation of ion, energy, and information in nanometer level.

3.4. Experimental

General Procedures and Materials. Reagents and solvents were obtained from commercial suppliers and were used without further purification unless otherwise specified. ^{1}H NMR and ^{13}C NMR spectra were obtained using a JEOL JNM-LA400 at 400 and 100 MHz in $CDCl_3$, respectively. Chemical shifts of ^{1}H and ^{13}C NMR signals were quoted to internal standard Me_4Si and expressed by chemical shifts in ppm (δ), multiplicity, coupling constant (Hz), and relative intensity. Elemental analyses were carried out on a Perkin-Elmer CHNS/O 2400 apparatus. Liquid crystalline phases were observed with an Olympus BH-2 optical polarizing microscope equipped with a Mettler FP82 HT hot-stage. Thermal characterization was conducted with a Mettler DSC 30 system at a scanning rate of 10 °C min^{-1}. Wide-angle X-ray diffraction (WAXD) patterns were obtained using a Rigaku RINT-2100 system with monochromated CuKα radiation. Two-dimensional small-angle X-ray scattering (2D SAXS) patterns of aligned samples were also recorded using an image plate detector (R-AXIS DS3C).

Synthesis of 1-methyl-3-[3,4,5-tris(alkyloxy)benzyl]imidazolium tetrafluoroborates (1a–h). The synthetic pathways used to obtain compounds **1a–h** are shown in scheme 3–1. Ethyl-3,4,5-trihydroxybenzoate was etherified with 1-bromoalkane ($CH_3(CH_2)_{n-1}Br$, n: carbon number of alkyl chain) in the presence of potassium carbonate (K_2CO_3) in *N*,*N*-dimethylformamide (DMF) to yield ethyl-3,4,5-tris(alkyloxy)benzoates (**2a–h**). After reduction of the esters (**2a–h**) with lithium aluminium hydride ($LiAlH_4$) in tetrahydrofuran (THF), the resulting benzyl alcohols (**3a–h**) were converted to 3,4,5-tris(alkyloxy)benzyl chlorides (**4a–h**) with thionyl chloride ($SOCl_2$) in dichloromethane (CH_2Cl_2). Subsequent quarternalization reaction of 1-methylimidazole with compounds **4a–h**

in toluene gave imidazolium chlorides (**5a–h**). Finally, imidazolium tetrafluoroborates (**1a–h**) were prepared by the metathesis reaction of the corresponding imidazolium chlorides with silver tetrafluoroborate ($AgBF_4$) in methanol (MeOH). One example for **1b** (n = 12) is given below.

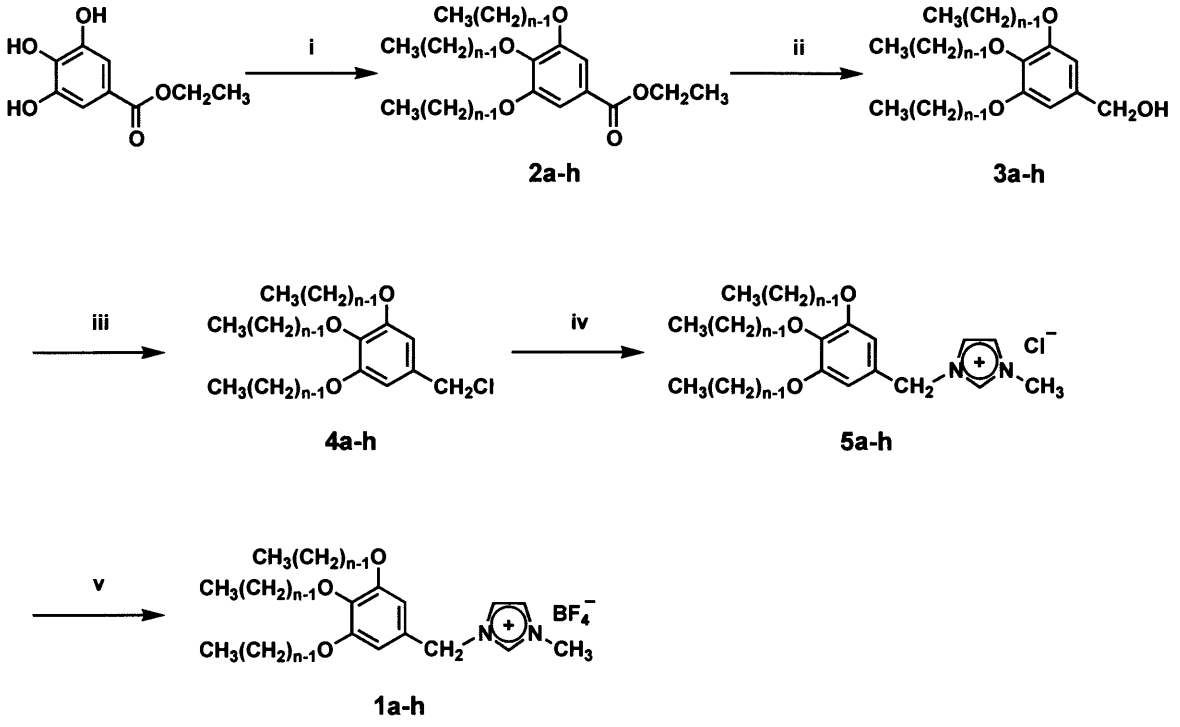

Scheme 3–1. Synthesis of imidazolium tetrafluoroborate salts **1a–h**.
i) $CH_3(CH_2)_{n-1}Br$, K_2CO_3, DMF, 70 °C; ii) $LiAlH_4$, THF, rt.; iii) $SOCl_2$, CH_2Cl_2, rt.; iv) imidazole, toluene, 80 °C; v) $AgBF_4$, MeOH, rt..

Ethyl-3,4,5-tris(dodecyloxy)benzoate (2e). A DMF (20 mL) suspension of ethyl-3,4,5-trihydroxybenzoate (3.30g, 16.7 mmol), 1-bromododecane (14.9 g, 59.8 mmol), and K_2CO_3 (13.9 g, 10.1 mmol) in a round-bottomed flask (200 mL) equipped with a stirring bar was deaerated under reduced pressure, and the flask was filled with argon. The deaeration was repeated three times to remove oxygen in the flask, thoroughly. After the resulting mixture was heated at 70 °C for 6 h with vigorous stirring, the mixture was poured into a

mixture of ethyl acetate (EtOAc) and water (150 mL of each). The organic phase was separated, and the aqueous phase was extracted with EtOAc three times. The combined organic extracts were washed with water, saturated NH_4Cl aqueous solution, and sat. NaCl aq., successively. The resulting organic phase was dried over anhydrous $MgSO_4$, filtered through a pad of Celite, and concentrated under reduced pressure. The residue was recrystallized from ethanol to give 11.2 g (95 %) of a white solid. ^{1}H NMR (400 MHz, $CDCl_3$) δ = 0.88 (t, J = 6.8 Hz, 9H), 1.23–1.51 (m, 54H), 1.61 (s, 3H), 1.71–1.85 (m, 6H), 4.01 (t, J = 6.4 Hz, 6H), 4.35 (q, J = 7.2 Hz, 2H), 7.25 (s, 2H). ^{13}C NMR (100 MHz, $CDCl_3$): δ = 14.11, 14.38, 22.68, 26.04, 26.06, 29.28, 29.36, 29.38, 29.56, 29.62, 29.65, 29.69, 29.71, 29.72, 29.74, 30.30, 31.91, 31.93, 60.95, 69.10, 73.45, 107.86, 125.00, 142.19, 152.75, 166.47.

3,4,5-Tris(dodecyloxy)benzyl alcohol (3e). To a stirred suspension of $LiAlH_4$ (0.683 g, 18.0 mmol) in THF (5 mL) was added a solution of **2e** (10.0 g, 14.2 mmol) in THF (10 mL) at 0 °C over a period of 10 min. The mixture was stirred at room temperature for 3 h, quenched by slow addition of isopropyl alcohol (3 mL), water (10 mL), and 30 % aq. NaOH (2 mL), successively. The reaction mixture was extracted with EtOAc (50 mL, 3 times). The insoluble materials were filtered off through a pad of Celite by using a suction funnel. The filtrate was dried over anhydrous $MgSO_4$, filtered, and concentrated by using a rotary evaporator. The crude product was recrystallized from EtOAc to give 8.94 g (95 %) of a white solid. Spectral data were consistent with those reported in the literature.[1]

3,4,5-Tris(dodecyloxy)benzyl chloride (4e). To a solution of **3e** (8.51 g, 12.9 mmol) in CH_2Cl_2 (50 mL) under argon was added $SOCl_2$ (3.0 mL, 41 mmol) with stirring at 0 °C. The mixture was stirred at room temperature for 2 h and slowly quenched with sat. $NaHCO_3$ aq.

solution. The reaction mixture was extracted with CH_2Cl_2 and washed with sat. NaCl aq. solution. The resulting organic phase was dried over anhydrous $MgSO_4$, filtered through a pad of Celite, concentrated, and dried in vacuo. The crude solid was purified by silica gel flash-column chromatography eluting with $CHCl_3$ to give 8.32 g (95 %) of the pure product as a white solid. Spectral data agreed with that reported in the literature.[1]

1-Methyl-3-[3,4,5-tris(dodecyloxy)benzyl]imidazolium chloride (5e). A toluene (2 mL) solution of compound **4e** (3.61 g, 5.31 mmol) and distilled 1-methylimidazole (0.872 g, 10.6 mmol) in a pressure tube (100 mL) equipped with a stirring bar was heated at 80 °C for 8 h with vigorous stirring. The solvent was removed in vacuo, and the residue was recrystallized from hexane three times to give 3.59 g (89 %) as a white solid. ^{1}H NMR (400 MHz, $CDCl_3$): δ = 0.88 (t, J = 6.8 Hz, 9H), 1.26–1.49 (m, 54H), 1.69–1.81 (m, 6H), 4.01 (t, J = 6.4 Hz, 6H), 4.08 (s, 3H), 5.44 (s, 2H), 6.66 (s, 2H), 7.22 (s, 1H), 7.32 (s, 1H), 10.61 (s, 1H). ^{13}C NMR (100 MHz, $CDCl_3$): δ = 14.04, 22.61, 26.02, 26.06, 29.29, 29.31, 29.39, 29.53, 29.58, 29.59, 29.61, 29.64, 29.66, 29.68, 30.24, 31.84, 31.85, 36.58, 53.69, 69.32, 73.37, 107.43, 121.31, 122.97, 127.64, 137.96, 138.72, 153.69. Elemental analysis calcd. for $C_{47}H_{85}ClN_2O_3$: C, 74.12; H, 11.25; N, 3.68. Found: C, 74.35; H, 11.13; N, 3.99.

1-Methyl-3-[3,4,5-tris(dodecyloxy)benzyl]imidazolium tetrafluoroborate (1e). To a solution of **5e** (0.697 g, 0.915 mmol) in MeOH (3 mL) under argon was added a solution of $AgBF_4$ (0.178 g, 0.915 mmol) in MeOH (2 mL) with stirring at room temperature. The mixture was stirred at room temperature for 2h. An insoluble AgCl was filtered off through a pad of Celite by using a suction funnel. The filtrate was concentrated by using a rotary evaporator. The crude product was purified by flash-column chromatography on silica gel

(eluent: CH_2Cl_2MeOH = 10 : 1) to give 0.651 g (88 %) of the pure product as a white solid. ^{1}H NMR (400 MHz, $CDCl_3$): δ = 0.89 (t, J = 6.8 Hz, 9H), 1.28–1.51 (m, 54H), 1.71–1.82 (m, 6H), 3.92 (s, 3H), 4.01 (t, J = 6.4 Hz, 6H), 5.19 (s, 2H), 6.63 (s, 2H), 7.21 (s, 1H), 7.24 (s, 1H), 8.81 (s, 1H). ^{13}C NMR (100 MHz, $CDCl_3$): δ = 14.09, 22.66, 26.09, 26.12, 29.36, 29.37, 29.47, 29.60, 29.66, 29.68, 29.71, 29.73, 29.74, 30.32, 31.90, 36.28, 53.78, 69.20, 73.41, 107.30, 121.70, 123.31, 127.44, 136.37, 138.71, 153.78. Elemental analysis calcd. for $C_{47}H_{85}BF_4N_2O_3$: C, 69.44; H, 10.54; N, 3.45. Found: C, 69.44; H, 10.52; N, 3.58.

Synthesis of 1-Methyl-3-[3,4,5-tris(dodecyloxy)benzyl]imidazolium salts having perfluorinated anions. The salts containing Trifluoromethenesulfonate, bis(trifluoromethanesulfonyl)imide, and hexafluoroborate anions were prepared by anion-exchange reactions of the corresponding lithium salts and **5e**.

Sample Preparation for 2D SAXS Measurements. Unoriented samples with polydomain structures were obtained when the materials filled in aluminum holders were slowly cooled from the isotropic states to the columnar liquid crystalline states. Oriented samples were prepared by shearing polydomain samples in sandwiched polyimide film (Kapton) without rubbing treatment.

Measurements of Ionic Conductivities. Dynamic ionic conductivities were measured by the complex impedance method using a Schlumberger Solartron 1260 impedance analyzer (frequency range: 10 Hz–10 MHz, applied voltage: 0.3 V) and a temperature controller. The heating rate of ionic conductivity measurements was fixed to 3 °C min^{-1} from 30 to 200 °C.

3.5. References

1. R. J. Bushby, O. R. Lozman, *Curr. Opin. Solid State Mater. Sci.* **2002**, *6*, 569.
2. M. Sawamura, K. Kawai, Y. Matsuo, K. Kanie, T. Kato, E. Nakamura, *Nature* **2002**, *419*, 702.
3. R. C. Smith, W. M. Fischer, D. L. Gin, *J. Am. Chem. Soc.* **1997**, *119*, 4092.
4. V. Percec, M. Glodde, T. K. Bera, Y. Miura, I. Shiyanovskaya, K. D. Singer, V. S. K. Balagurusamy, P. A. Heiney, I. Schnell, A. Rapp, H.-W. Spiess, S. D. Hudson, H. Duan, *Nature* **2002**, *419*, 384.
5. A. Sautter, C. Thalacker, F. Würthner, *Angew. Chem. Int. Ed.* **2001**, *40*, 4425.
6. N. Mizoshita, H. Monobe, M. Inoue, M. Ukon, T. Watanabe, Y. Shimizu, K. Hanabusa, T. Kato, *Chem. Commun.* **2002**, 428.
7. M. L. Bushey, A. Hwang, P. W. Stephens, C. Nuckolls, *Angew. Chem. Int. Ed.* **2002**, *41*, 2828.
8. S. T. Trzaska, T. M. Swager, *Chem. Mater.* **1998**, *10*, 438.
9. R. Zniber, R. Achour, M. Z. Cherkaoui, B. Donnio, L. Gehringer, D. Guillon, *J. Mater. Chem.* **2002**, *12*, 2208.
10. A. M. van de Craats, J. M. Warman, A. Fechtenkötter, J. D. Brand, M. A. Harbison, K. Müllen, *Adv. Mater.* **1999**, *11*, 1469.
11. A. M. van de Craats, J. M. Warman, K. Müllen, Y. Geerts, J. D. Brand, *Adv. Mater.* **1998**, *10*, 36.
12. J. F. Hulvat, S. I. Stupp, *Angew. Chem. Int. Ed.* **2003**, *42*, 778.
13. D. Adam, P. Schuhmacher, J. Simmerer, L. Häussling, K. Siemensmeyer, K. H. Etzbach, H. Ringsdorf, D. Haarer, *Nature* **1994**, *371*, 141.
14. N. Boden, R. J. Bushby, J. Clements, *J. Chem. Phys.* **1993**, *98*, 5920.

15. A. Tracz, J. K. Jeszka, M. D. Watson, W. Pisula, K. Müllen, T. Pakula, *J. Am. Chem. Soc.* **2003**, *125*, 1682.

16. C. F. van Nostrum, R. J. M. Nolte, *Chem. Commun.* **1996**, 2385.

17. V. Percec, G. Johansson, J. Heck, G. Ungar, S. V. Batty, *J. Chem. Soc., Perkin Trans. 1* **1993**, 1411.

18. U. Beginn, G. Zipp, M. Möller, *Adv. Mater.* **2000**, *12*, 510.

19. V. Percec, J. A. Heck, D. Tomazos, G. Ungar, *J. Chem. Soc., Perkin Trans. 2* **1993**, 2381.

20. T. Kato, *Science* **2002**, *295*, 2414.

21. A. R. A. Palmans, J. A. J. M. Vekemans, R. A. Hikmet, H. Fischer, E. W. Meijer, *Adv. Mater.* **1998**, *10*, 873.

22. T.-Q. Nguyen, M. L. Bushey, L. E. Brus, C. Nuckolls, *J. Am. Chem. Soc.* **2002**, *124*, 15051.

23. T. Kato, N. Mizoshita, *Curr. Opin. Solid State Mater. Sci.* **2002**, *6*, 579.

24. K. Kanie, M. Nishii, T. Yasuda, T. Taki, S. Ujiie, T. Kato, *J. Mater. Chem.* **2001**, *11*, 2875.

25. T. Kato, *Struct. Bonding* **2000**, *96*, 95.

26. C. Tschierske, *J. Mater. Chem.* **2001**, *11*, 2647.

27. T. Kato, *Science* **2002**, *295*, 2414.

28. T. Ohtake, M. Ogasawara, K. Ito-Akita, N. Nishina, S. Ujiie, H. Ohno, T. Kato, *Chem. Mater.* **2000**, *12*, 782.

29. T. Ohtake, Y. Takamitsu, K. Ito-Akita, K. Kanie, M. Yoshizawa, T. Mukai, H. Ohno, T. Kato, *Macromolecules* **2000**, *33*, 8109.

30. K. Kishimoto, M. Yoshio, T. Mukai, M. Yoshizawa, H. Ohno, T. Kato, *J. Am. Chem. Soc.* **2003**, *125*, 3196.

31. P. Bonhôte, A.-P. Dias, N. Papageorgiou, K. Kalyanasundaram, M. Grätzel, *Inorg. Chem.* **1996**, *35*, 1168.

32. H. Every, A. G. Bishop, M. Forsyth, D. R. MacFarlane, *Electrochim. Acta* **2000**, *45*, 1279.

33. K. Ito, N. Nishina, H. Ohno, *Electrochim. Acta* **2000**, *45*, 1295.

34. M. Yoshio, T. Mukai, K. Kanie, M. Yoshizawa, H. Ohno, T. Kato, *Chem. Lett.* **2002**, 320.

35. R. Hagiwara, Y. Ito, *J. Fluorine Chem.* **2000**, *105*, 221.

36. M. Yoshio, T. Mukai, K. Kanie, M. Yoshizawa. H. Ohno, T. Kato, *Adv. Mater.* **2002**, *14*, 351.

37. (a) Macdonald, J. R. *Impedance Spectroscopy Emphasizing Solid Materials and Systems*, John Wiley & Sons, New York, 1987. (b) Tominaga, Y.; Ohno, H. *Electrochim. Acta* **2000**, *45*, 3081.

38. "*Handbook of Chemisty and Physics*", 82nd Edition 2001–2002, CRC Press LLC.

39. (a) M. Ue, A. Murakami, S. Nakamura, *J. Electrochem. Soc.* **2002**, *149*, A1385; (b) H. Tokuda, K. Hayamizu, K. Ishii, M. A. B. H. Susan, M. Watanabe, *J. Phys. Chem. B.* **2004**, *108*, 16593.

40. A. E. Bradley, C. Hardacre, J. D. Holbrey, S. Johnston, S. E. J. McMath, M. Nieuwenhuyzen, *Chem. Mater.* **2002**, *14*, 629.